SCUOLA DI DOTTORATO

UNIVERSITÀ DEGLI STUDI DI MILANO-BICOCCA

Department of Material Science

PhD program Science and Nanotechnology of Materials – Cycle XXX

New strategies for the controlled release of vulcanization curatives in rubber blends

Brazzo Paolo - Registration number 717161

Tutor: Prof. Luca Beverina

Supervisor: Dr.ssa Raffaella Donetti

Coordinatore / Coordinator: Prof. Marco Bernasconi

ANNO ACCADEMICO / ACADEMIC YEAR 2016/2017

Lord, here comes the flood
We'll say goodbye to flesh and blood
If again the seas are silent
In any still alive
It'll be those who gave their island to survive
Drink up, dreamers, you're running dry.
Peter Gabriel – Here comes the flood

E quando poi sparì del tutto
A chi diceva "È stato un male"
A chi diceva "È stato un bene"
Raccomandò "Non vi conviene
Venir con me dovunque vada"
Ma c'è amore un po' per tutti
E tutti quanti hanno un amore
Sulla cattiva strada
Fabrizio De Andrè – La cattiva strada

Forza Panino!
Elio e le Storie Tese - Tapparella

Summary

Overview 7

1. The vulcanization process 9

1.1. Introduction to vulcanization 9

1.2. Characterization of the vulcanization process 11

1.3. Accelerated-Sulfur Vulcanization 14

1.4. Chemistry of the vulcanization process 17

1.5. Diffusion of curatives in rubber blends 19

1.6. Our approach to the problem 22

2. Microencapsulation 25

2.1. Introduction to microencapsulation 25

2.2. Methods of encapsulation 28

2.2.1. Phase separation 28

2.2.2. Interfacial and in-situ polymerization 31

2.2.3. Spray drying 35

2.2.4. Solvent evaporation 37

2.2.5. Coating processes 39

2.3. Microencapsulation and vulcanization technology 41

2.4. Our choice 42

2.5. Cellulose ethers as encapsulants 43

3. Encapsulation of vulcanization accelerators 47

3.1. Reprecipitation technique 48

3.2. Solvent evaporation from emulsion droplets 49

3.3. Encapsulation of TBBS in ZnO 60

3.4. Encapsulation of TBBS in polymethylmethacrylate 62

3.5. Encapsulation of TBBS in polycarbonate 66
3.6. Synthetic process for TBBS encapsulation in EC 69
4. Crosslinking of EC capsules 76
4.1. Epoxy crosslinking 77
4.2. Silane crosslinking 92
4.3. Synthethic attempt for epoxy-crosslinked TEC 100
5. Test of capsules in polymer blends 104
5.1. Blend preparation 104
5.2. Reference test with BR and SBR 106
5.3. Rubber blends 110
5.4. Vulcanization of secondary accelerator-free blends 118
5.5. Crosslinked capsules in polymer blends 121
Recipes for rubber blends preparation 136
6. Functionalization of TBBS 139
6.1. BOC-TBBS design and synthetic attempts 139
6.2. Synthesis of Br-TBBS 141
6.3. Test of BrTBBS in rubber blends 143
7. Conclusion 146
Appendix A – Materials and instruments 149
Appendix B – Synthesis of TBBS derivatives 151
Synthesis of 6-bromobenzo[d]thiazole-2-thiol (BrMBT) 151
Synthesis of S-(6-bromobenzo[d]thiazol-2-yl)-N-(tert-butyl)thiohydroxylamine (BrTBBS) 152
Synthetic attempt for tert-butyl benzo[d]thiazol-2-ylthio(tert-butyl)carbamate 154
Appendix C – Diffusion test in rubber samples 155
Bibliography 161

List of Abbreviations

AcOEt	Ethyl acetate
BIIR	Bromobutyl rubber
BOC	Tert-butyloxycarbonyl
BR	Butadiene rubber
CAB	Cellulose acetate butylate
CBS	N-cyclohexylbenzothiazole-2-sulfenamide
CIIR	Chlorobutyl rubber
CTP	(Cyclohexylthio)phthalimide
DCBS	N-dicyclohexylbenzothiazole-2-sulfenamide
DCM	Dichloromethane
DER 332	Bisphenol A diglycidyl ether
DMAP	Dimethylaminopyridine
DOTG	Di-o-tolylguanidine
DPG	Diphenylguanidine
DS	Degree of substitution
DSC	Differential scanning calorimetry
EC	Ethyl cellulose
EDX	Energy dispersive x-ray analysis
EPDM	Ethylene-propylene diene monomer
FTIR	Fourier transform infrared (spectroscopy)
IIR	Butyl rubber
IR	Synthetic isoprene rubber
MB	Masterbatch
MBS	2-morpholinothiobenzothiazole
MBT	2-mercaptobenzothiazole
MBTS	2,2'-dithiobisbenzothiazole
MESE	Microemulsion solvent evaporation

MF	Melamine-formaldehyde
MRD	Moving die rheometer
MS-TGA	Mass spectroscopy - thermogravimetric analysis
NBR	Nitrile rubber
NMR	Nuclear magnetic resonance (spectroscopy)
NR	Natural rubber
ODR	Oscillating disk rheometer
PC	Polycarbonate
PCM	Phase change material
PHR	Parts per hundred rubber
PMMA	Poly(methylmethacrylate)
PVA	Poly vinyl alcohol
QA	Quinacridone
RPM	Revolutions per minute
SBR	Styrene-butadiene rubber
SDS	Sodium dodecyl sulfate
SEM	Scanning electron microscopy
TBBS	N-tert-butyl-benzothiazole-2-sulfenamide
TEOS	Tetraethyl ortosilicate
TESPD	3-triethoxysilylpropyl)disulfide
TMPG	Trimethylolpropane triglycidyl ether
TMTD	Tetramethylthiuram disulfide
TMTM	Tetramethylthiuram monosulfide
UF	Urea-formaldehyde
UV	Ultraviolet
ZDEC	Zinc diethylcarbamate

Overview

This project represents an innovative approach in the tire industry and it is also at the same time the first incursion into rubber technology of the research group I have been working in. As it frequently happens when a specific problem is faced by researchers not coming from the field, the approach I ended up using had no previous track record in the field, thus making comparisons difficult. First of all, in any case I had to learn the basics of rubber technology and to focus on a very specific and thus far still unresolved issue common to all tire manufacturers in the world. The rubbers employed in tires have to be vulcanized. When working with blends – that is in all practical cases – vulcanization is carried out directly on the complex mixture of different rubbers, fillers, Sulphur and curatives. As the vulcanization kinetics of the different rubbers, as well as the diffusion coefficients of the various components of the vulcanization package, are different, vulcanization is highly inhomogeneous. The most relevant practical consequence of this issue is the fact that the final mechanical proprieties of the tire never reach those expected by the linear combination of the performances of the single constituents.

Instead of going for the extensive screening of all possible vulcanization curatives available on the market, in the hope of finding the almost magical combination that could do the trick for a specific blend, we decided to explore something that is more in the background of the research group: supramolecular chemistry and formulation technology, microencapsulation in particular.

On doing so, we were prepared for the struggle of trying to do something which was largely unprecedented in the tire industry. As it turns out, the results very often were counterintuitive and every once in a while we had to

start from scratches. Also, the project is supported by an industrial partner, and the characterization of rubber blends is performed in industrial laboratories. This means that not all the material that produced in the laboratory can be tested, and only a fraction of what we produced will be effectively tested in the rubber samples. In force of this, only the material we are more confident in can be tested. Also, due to the nature of the industrial equipment we had to deal with, samples had to be in the hundreds of grams scale, which made sometimes progresses very slow due to the intrinsic time consuming encapsulation procedure we ended up using.

The first chapter of this thesis is about the vulcanization process from the historical and technological point of view. At the end of the chapter, the focus is put on the issue that we decided to face and what we proposed to do. The second chapter is a review of the various microencapsulation technology, how they have been used in the field of rubber industry and what kind of approach we decided to follow.

The third chapter is about the optimization of the encapsulation process of a primary accelerator in various materials and the test in rubber blends of a selected class of microcapsules. The fourth chapter will show some crosslink attempts to enhance the thermo-mechanical stability of the capsules, focusing on an original and simple crosslinking method using an epoxy as crosslinker agent. The chapter ends with the description of the effect of the capsule crosslinking on the vulcanization kinetics of the rubber blends and with an attempt to rationalize the observed effect. The last chapter will present a side strategy that we developed to add a tracking moiety on the accelerant that we used to have a better qualitative understanding of its distribution in the rubber blend.

1. The vulcanization process

1.1. Introduction to vulcanization

The vulcanization process is necessary to produce most useful rubber articles, like tires and mechanical goods. Unvulcanized rubber is generally not strong, does not retract essentially to its original shape after a large deformation, and it can be very sticky. In short, unvulcanized rubber can have the same consistency as chewing gum. The first commercial method for vulcanization has been attributed to Charles Goodyear. His process (heating natural rubber with sulfur) was first used in Springfield, Massachusetts, in 1841. Thomas Hancock used essentially the same process about a year later in England. However, Hancock filed his patent on November 21, 1843, eight weeks before Goodyear filed his US Patent on January 30, 1844.

Since those early days, there has been continued progress toward the improvement of the process and in the resulting vulcanized rubber articles. In addition to natural rubber, over the years, many synthetic rubbers have been introduced. Also, in addition to sulfur, other substances have been introduced as components of curing (vulcanization) systems[1].

Vulcanization is a process generally applied to rubbery or elastomeric materials. These materials forcibly retract to their approximately original shape after a rather large mechanically imposed deformation.

Vulcanization can be defined as a process that increases the retractile force and reduces the amount of permanent deformation remaining after removal of the deforming force. Thus, vulcanization increases elasticity while it decreases plasticity. It is generally accomplished by the formation of a crosslinked molecular network (Figure 1).

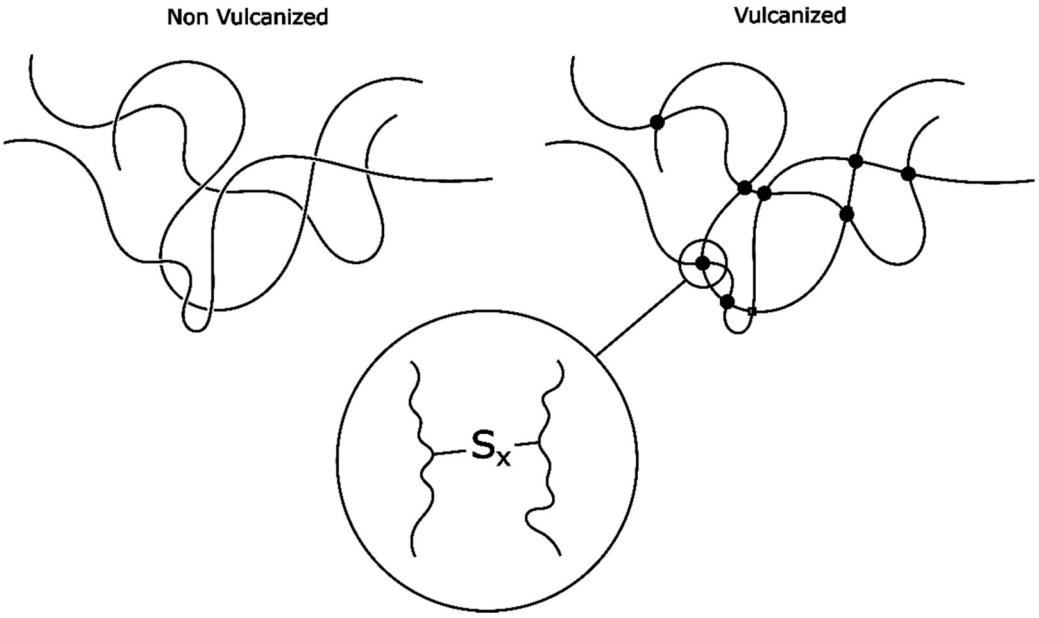

Figure 1 - Network formation by sulfur bridges

In an unvulcanized linear high polymer (above its melting point) only molecular chain entanglements constitute junctures.

Vulcanization, thus, is a process of chemically producing network junctures by the insertion of crosslinks between polymer chains. A crosslink may be a group of sulfur atoms in a short chain, a single sulfur atom, a carbon-to-carbon bond, a polyvalent organic radical, an ionic cluster, or a polyvalent metal ion.

Vulcanization causes highly significant changes at the molecular level[2]. Because of the network formation, the rubber becomes essentially insoluble in any solvent. Moreover, it cannot be processed anymore by any means that require it to flow (like mixing or extruding). Thus, it is essential that vulcanization occurs after the rubber object is in its final form. Vulcanization causes a trade-off of elasticity for viscous or plastic behavior. Properties like tear strength, recovery and hysteresis change dramatically, but their change is not truly a function of the crosslinking degree, since they are affected by numerous factors like the type of crosslink, the type of polymer, the nature and the amount of fillers.

1.2. Characterization of the vulcanization process

Some important characteristics related to the vulcanization process are the time elapsed for the process to start, the rate of vulcanization and the final crosslinking degree. Usually scorch resistance – defined as the delay before the crosslink starts – is measured for the time required and at a specific temperature. The onset of the crosslink formation is indicated by an abrupt viscosity increase. For this purpose, the Mooney viscometer has been extensively used. A sample of fully mixed – but unvulcanized – rubber is put into a heated cylindrical cavity. A disc rotates against the rubber at constant speed, while the torque required to keep that speed constant is measured. A number proportional with the value of this torque is taken as viscosity index (Mooney viscosity) and is reported in arbitrary Mooney units.

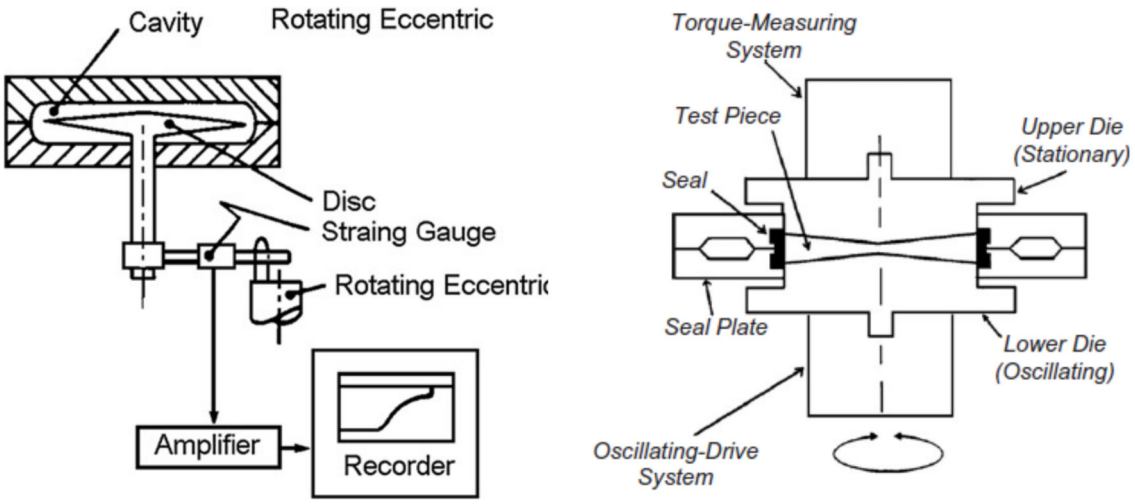

Figure 2- Oscillating disk rheometer schematic diagram

Both the rate of vulcanization after the scorch period and the final extent of vulcanization are now measured by using devices called cure meters[3]. Widely used cure meters are Oscillating Disk Rheometers (ODR, figure 2). The rubber is enclosed in a heated cavity, with a metal disc embedded into that oscillates sinusoidally in its plane about its axis. Vulcanization is measured by the increase in the torque required to maintain a given amplitude (e.g., degrees of arc) of oscillation at a given temperature. The torque is proportional to a low-strain modulus of elasticity. Since this torque is measured at the elevated temperature of vulcanization, the portion of it due to viscous effects is minimal. Thus, it has been assumed that the increase in torque during vulcanization is proportional to the number of crosslinks formed per unit volume of rubber. The torque is automatically plotted against time to give a so-called rheometer chart, rheograph, or cure curve (figure 3). The cure curve gives a complete picture of the overall kinetics of crosslink formation and even crosslink

disappearance (reversion) for a given rubber mix. When the curve reaches a plateau, it is referred as *Normal cure* regime. *Reversion* is a term generally applied to the loss of network structures by non-oxidative thermal aging. It can be the result of too long vulcanization time (overcure) or of hot aging of thick sections. *Marching cure* refers to a regime in which a linear torque increase is observed in the final part of the cure curve[4].

Newer versions of cure meters have smaller cavities and no rotor. Only half of the die oscillates (e.g. the upper half), while the other one is stationary. Those are the so called Moving Die Rheometers (MDR). Because of the smaller sample, the heat transfer is faster. Both with ODR and MDR, the obtained chart is similar to the one reported in figure 3.

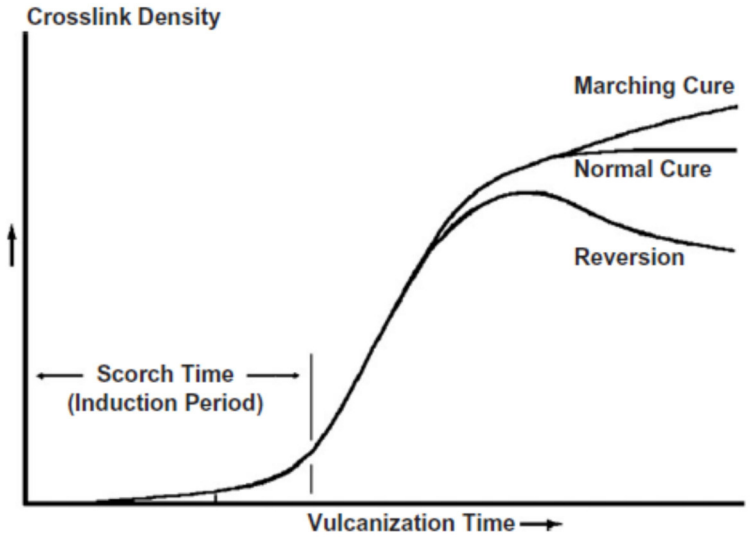

Figure 3- Example of rheometer cure curve.

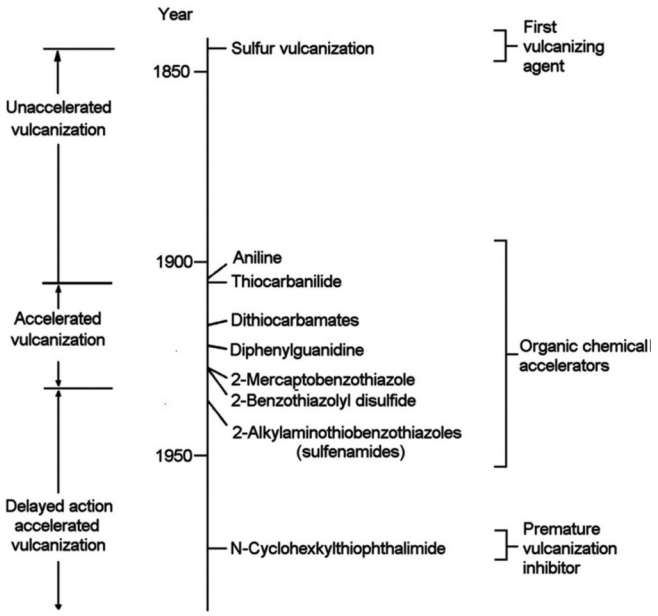

Figure 4 - Milestones of sulfur vulcanization

1.3. Accelerated-Sulfur Vulcanization

Organic-chemical accelerators were not used until 1906 (65 years after the Goodyear-Hancock development of unaccelerated vulcanization; Figure 4), when Oenslager discovered the effect of aniline on sulfur vulcanization[5]. Aniline, however, is too toxic for use in rubber products. Further developments led to guanidine accelerators[6]. Reaction products formed between carbon disulfide and aliphatic amines (dithiocarbamates) were first used as accelerators in 1919. These were and are still the most active accelerators with respect to both crosslinking rate and extent of crosslink formation. However, most of the dithiocarbamate accelerators give little or no scorch resistance and their use is impossible in many factory-processing situations.

Compound	Abbreviation	Structure
Benzothiazoles		
2-Mercaptobenzothiazole	MBT	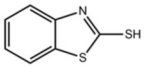
2,2'-Dithiobisbenzothiazole	MBTS	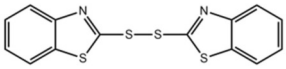
Benzothiazolesulfenamides		
N-Cyclohexylbenzothiazole-2-sulfenamide	CBS	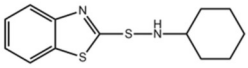
N-tert-butyl-benzothiazole-2-sulfenamide	TBBS	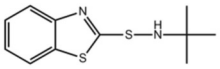
2-Morpholinothiobenzothiazole	MBS	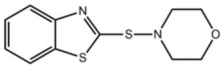
N-Dicyclohexylbenzothiazole-2-sulfenamide	DCBS	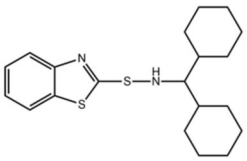
Dithiocarbamates		
Tetramethylthiuram monosulfide	TMTM	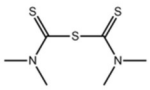
Tetramethylthiuram disulfide	TMTD	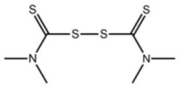
Zinc diethyldithiocarbamate	ZDEC	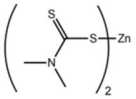
Amines		
Diphenylguanidine	DPG	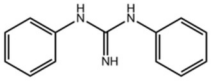
Di-o-tolylguanidine	DOTG	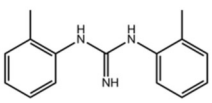

Figure 5 - Most common accelerators for sulfur vulcanization

The first delayed-action accelerators were introduced in 1925 with the development of 2-mercaptobenzothiazole (MBT) and 2-benzothiazole disulfide (or 2,2-dithiobisbenzothiazole) (MBTS)[7].

Even more delayed-action and yet faster curing vulcanization were possible in 1937 with the introduction of the first commercial benzothiazolesulfenamide accelerator[8]. Still more delay became possible in 1968, with the availability of an extremely effective premature vulcanization inhibitor (PVI). This compound was N-(cyclohexylthio)phthalimide (CTP), small concentrations of which were used along with benzothiazolesulfenamide accelerators[9]. Figure 5 summarize the most common used curative agents.

Accelerated-sulfur vulcanization is the most widely used method. For many applications, it is the only rapid crosslinking technique that can, in a practical manner, give the delayed action required for processing, shaping, and forming before the formation of the intractable vulcanized network. It is used to vulcanize natural rubber (NR), synthetic isoprene rubber (IR), styrene-butadiene rubber (SBR), nitrile rubber (NBR), butyl rubber (IIR), chlorobutyl rubber (CIIR), bromobutyl rubber (BIIR), and ethylene-propylenediene- monomer rubber (EPDM)[10]. Typically a recipe for the vulcanization system for one of these elastomer contains 2–10 phr of zinc oxide, 1–4 phr of fatty acid (e.g., stearic), 0.5–4 phr of sulfur, and 0.5–2 phr of accelerator*. Zinc oxide and the fatty acid are vulcanization-

*Phr is a unit of measure used by compounders, which stands for Part per Hundred Rubber. It is the amount of an additive to be added per hundred parts of base polymer in the compounding mixture. As an example, a typical compounding formula can

system activators. The fatty acid with zinc oxide forms a salt, which can form complexes with accelerators and reaction products, formed between accelerators and sulfur[11].

1.4. Chemistry of the vulcanization process

Although its diffusion, there is a lack in the theoretical background basis of the vulcanization process. People agree about the basic steps of the process, while the details are still objects of discussion[12]. The vulcanization reactions can be divided into three sub-categories: (i) accelerator chemistry, which involves the reactions leading to the formation of an active-sulfurating agent; (ii) crosslinking chemistry which includes reactions leading to the formation of crosslinks; and (iii) post-crosslinking chemistry which involves reactions that lead to crosslink shortening and crosslink degradation. Figure 6 summarize the basic reactions that lead to vulcanized rubber. The first step in accelerated sulfur vulcanization is the formation of an active accelerator complex via reaction of the accelerator and the activator, which subsequently reacts with molecular sulfur to form a distribution of sulfurating species.

These activated sulfurating species then react with an unsaturated site, in particular an allylic carbon, on the rubber chain to form crosslink

---

contain 100 phr of polymer, 15 phr of additive A, 3 phr of additive B. The percentage fraction of the i-th ingredient can be calculated as follows:

$$f_i(\%) = \frac{f_i(\text{phr})}{\sum_n f_n(\text{phr})}$$

precursors, which are accelerator-terminated polysulfidic pendant groups attached to the rubber chain. These crosslink precursors subsequently react with additional unsaturated sites on the rubber chain resulting in polysulfidic crosslinks. The polysulfidic crosslinks may eventually (i) desulfurate over longer times to form shorter crosslinks, or (ii) degrade to cyclic sulfides or other main-chain modifications, which can cause the long-term deterioration of vulcanizate properties[13].

The first step in sulfur vulcanization is the formation of an active sulfurating species, which is a prerequisite for the formation of a crosslink precursor. A sulfurating species is a molecule that is able to insert sulfur in the form of crosslinks into the elastomer, where it has been long recognized that accelerator polysulfide complexes are better sulfurating species than molecular sulfur[14]. Heating the accelerator at vulcanization temperature causes its dissociation, liberating free amine and 2-mercaptobenzothiazole (MBT). MBT reacts with another molecule of accelerator, forming the disulfide specie. People still debate on the ionic or radical nature of the mechanism, but they agree on the nature of the species formed at the end of the reaction[15,16]. The disulfide is a key intermediate that reacts with sulfur giving the polysulfidic species.

Crosslink precursors are formed when the accelerator polysulfides react with the rubber chains, resulting in pendant groups attached to the rubber chains. Those precursors evolve into the final polysulfidic crosslinks.

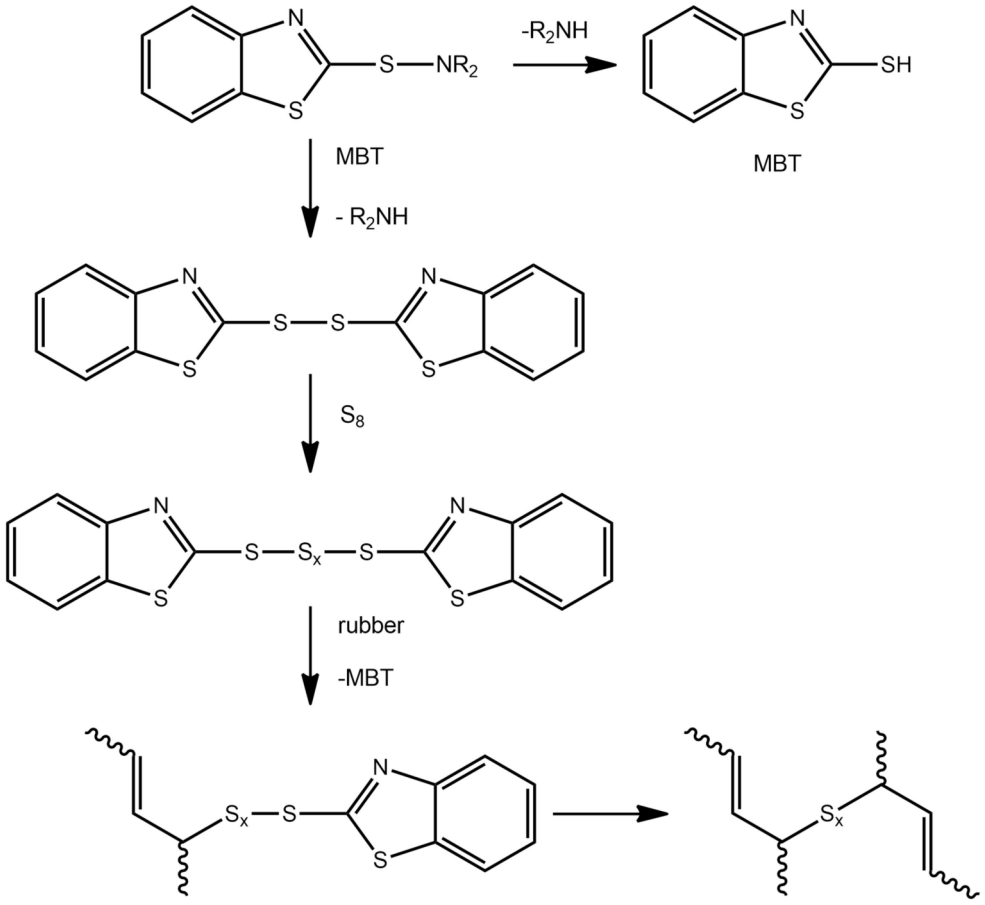

Figure 6 - Overview of the different steps during the vulcanization process using a generic sulfenamide derivative as curing agent (without considering the addition of secondary accelerators or actrivators).

1.5. Diffusion of curatives in rubber blends

The majority of rubber is used in the form of blends, an industrial fact of life, which is sufficient in itself to show the importance of vulcanization of blends. The aim of blending is to combine the desirable features of each component, but often the properties obtained are worse than anticipated from those of the single component rubbers and, generally,

the properties of vulcanized blends cannot be linearly interpolated from those of the individual rubber vulcanized. The following factors arise specifically for blends and determine their properties:

- The rubbers used and their ratio;
- The phase morphology;
- The distribution of filler between the rubber or at the interface;
- The distribution of plasticizer between the rubbers;
- The distribution of crosslinks between the rubbers.

Whilst most of the issues and consequences have been known for many years, it is only in the past decades that techniques have been developed to allow accurate, informed study of the vulcanization of blends[17]. This has led to better control of the two key factors which are peculiar to the vulcanization of blends – distribution of crosslinks between the rubber phases and interfacial crosslinking between the rubbers (figure 7) – and hence to improved physical properties and performances.

A difference in the concentration of the chemicals responsible for crosslink formation can arise through preferential solubility (partition) of the added curatives[18] (figure 8) and/or the vulcanization intermediates. Differences in solubility parameters of the rubbers will cause both, and partition will be further enhanced when there is the possibility of specific interactions, such as hydrogen bonding or dipolar interactions in one of the rubbers. Whilst equilibrium concentrations of curatives in each rubber might be expected to be achieved during mixing of the curatives in a rubber blend, equilibrium is unlikely to be achieved for vulcanization intermediates. Indeed, phase size will dictate whether

migration of intermediates during vulcanization will play a significant role in dictating the eventual crosslink distribution.

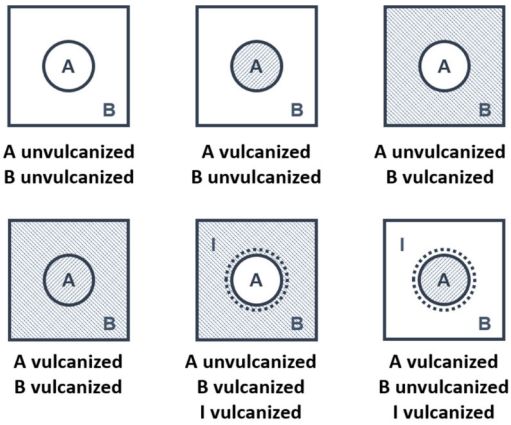

Figure 7 - Scheme of the possible scenario that can verify during rubber blend covulcanization.

a b

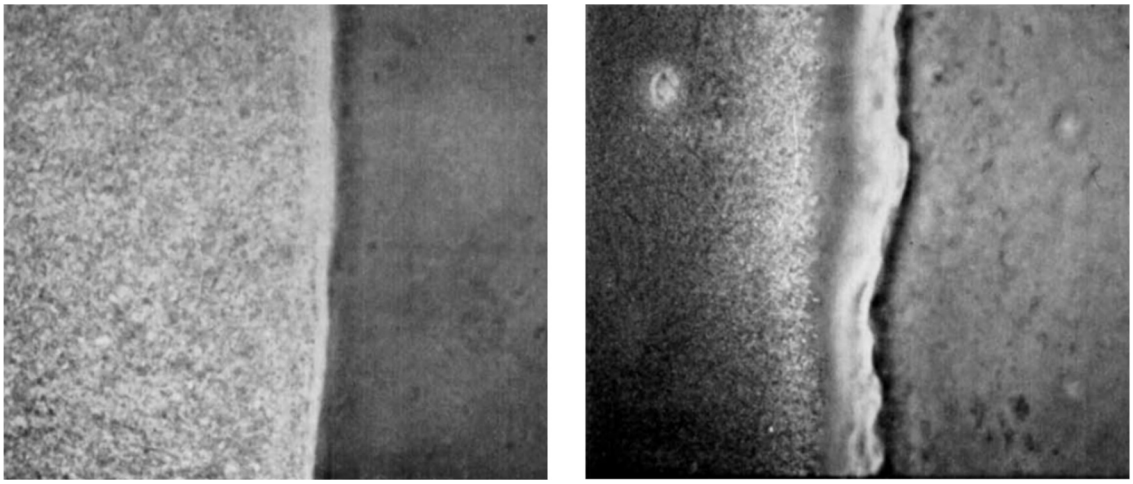

Figure 8 - Chlorobutyl rubber stripe containing 3 phr of tellurium triethyl dithiocarbamate (left phase) pressed against a SBR stripe (right phase); (a) no curative diffusion after 3 s at 100°C; (b) curative diffusion after 60 s at 150°C

The other reactant in crosslinking is the crosslink site, or more commonly sites, on the elastomer. For sulfur vulcanization, these are associated with the unsaturation in the elastomer. Some blends have an obvious

difference in concentration of double bonds within the rubber phases, such as blends of the highly-unsaturated natural rubber (NR) with ethylene-propylene-diene rubber (EPDM). As the curatives or vulcanization intermediates become depleted in the faster reacting rubber phase, diffusion from the slower reacting phase will occur. This will limit the crosslinking in the latter phase and increase it in the former, either throughout when phase sizes are small, or close to the interface when they are large.

Numerous techniques have been employed to obtain the diffusion coefficients of different species (e.g. sulfur, accelerators, plasticizers) into different type of rubber. In one of the most cited literature work on the topic, Gardiner used optical microscopy to determine the solubility of curatives in rubber by looking at the dissolution of the crystals into the rubber matrix[19]. They used also microinterferometry to measure sulfur and MBTS diffusion across interfaces between dissimilar rubbers[20]. Guillaumond demonstrated that when the polymer phase in which the curative will migrate into is saturated (in terms of curative concentration), it is possible to covulcanize rubber blends without curative migration, highlighting the diffusion role during the vulcanization process[21]. However, this process can be used only as a demonstration, being not technically feasible due to the vastly too high concentration of curatives required.

1.6. Our approach to the problem

Before going on with some more background information, it is worthwhile to summarize our approach to the problem. This will in fact justify why the next section is dedicated to microencapsulation.

Early on in the project we started to face the accelerant unbalanced partition between different rubbers by a standard chemical approach: the modification of the accelerant chemical structure. Even though practical considerations essentially forbid the introduction of new accelerants in a real industrial environment (tire technology is highly standardized), the information we obtained from this approach are valuables to better understand some of the effects we observed, we will thus in any case describe the synthesis an behavior of such original accelerants. The way we really wanted to face the issue however was a strictly formulative approach. The advantage of using a formulation strategy is that the composition of the vulcanization package remains the same - thus according to existing industrial recipes – while the delivery method changes.

As it is shown in figure 3 in section 1.2, modern vulcanization only leads to appreciable crosslinking after an often prolonged scorch time of several minutes at 150-170°C, depending on the details of the chemicals employed. On the other hands, the diffusion coefficient at the processing temperature of the small molecules acting as accelerants is so high that when vulcanization starts to take place, the concentration of the curatives in the different phases has already reached equilibrium values. This is for example demonstrated by the master batching experiments described in chapter 5.

Ideally, we would like to be able to distribute the curatives in the different phases according not to the respective partition coefficient but to the specific requirements for optimized vulcanization. To do so, we proposed a microencapsulation strategy. If the key accelerant is introduced in the blend not as the free powder but as a capsule within a material capable of withstanding the mechanical and thermal stress of the mixing process, only to eventually collapse during the scorch phase. In this case the distribution of the curatives in the mixture will remain statistic up to the point of collapse of the capsule. At that point, due to the already high temperature as well as to the high local concentration of curatives, vulcanization will immediately start. The local high crosslinking density will likely reduce the diffusion coefficient thus hindering the equilibration of the curatives concentration due to concomitant densification of the network.

As we have already stated, the idea is unprecedented and the combination of different processes that are required to happens in an orderly and coordinated fashion is large. Thus, this project is an example of high risk/high gain activity, with the notable complication of being industrially funded an thus, since its very beginning, already happening in an industrial environment and according to industrial consuetudes.

The next chapter will thus be devoted to microencapsulation techniques.

2. Microencapsulation

2.1. Introduction to microencapsulation

Encapsulation is defined as a technology of casing solids, liquids, or gaseous materials in miniature sealed capsules (which are commonly micrometer to millimeter range, thus the name microencapsulation) that can release their contents at controlled rates under specific conditions[22]. This technique depends on the physical and chemical properties of the material to be encapsulated[23]. The microencapsulation technology has been employed in a diverse range of industrial applications such as chemicals, cosmetics, food, pharmaceuticals, printing, etc. The development of early encapsulation technology and preparation of microcapsules dates back to 1950s when Green and coworkers produced microencapsulated dyes by complex coacervation of gelatin and gum Arabic, for the manufacture of carbonless copying paper[24].

The capsule has the ability to preserve a substance in the finely divided state and to release it as needed[25]. The size of the capsules may range from submicrometer to several millimeters in size and have a multitude of different shapes, depending on the materials and methods used to prepare them. The encapsulations/entrapment of active ingredients are done for a variety of reasons:

- Protecting the core material from degradation by reducing its reactivity to the outside environment (such as UV light, heat, moisture, air oxidation, chemical attack, acids, bases, etc.).
- Reducing/retarding the evaporation or transfer rate of a volatile active ingredient (the core material) to the outside environment.
- Modifying the physical characteristics of a material, making it easier to handle (e.g., converting liquid into solid form, improving the handling properties of a sticky material, etc.).
- Achieving controlled and/or targeted release of active ingredients. The product can be tailored to either release slowly over time or at a certain point. Improving shelf life by preventing degradative reactions (dehydration, oxidation, etc.).

The morphology of microcapsules depends mainly on the core material, how it is distributed within the system, and the deposition process of the shell. Similarly, the morphology of the internal structure of a microparticle depends largely on the selected shell materials and the microencapsulation methods that are employed. The microcapsules may be categorized into several arbitrary classifications (figure 9) such as:

- Mononuclear (also known as core-shell) – microcapsules that have a shell around the core. These are also called single-core or monocore capsules;
- Polynuclear – capsules that have many cores enclosed within the shell (called also polycore or multicore-type capsules);

- Matrix encapsulated – the core material is distributed homogeneously within the shell material.

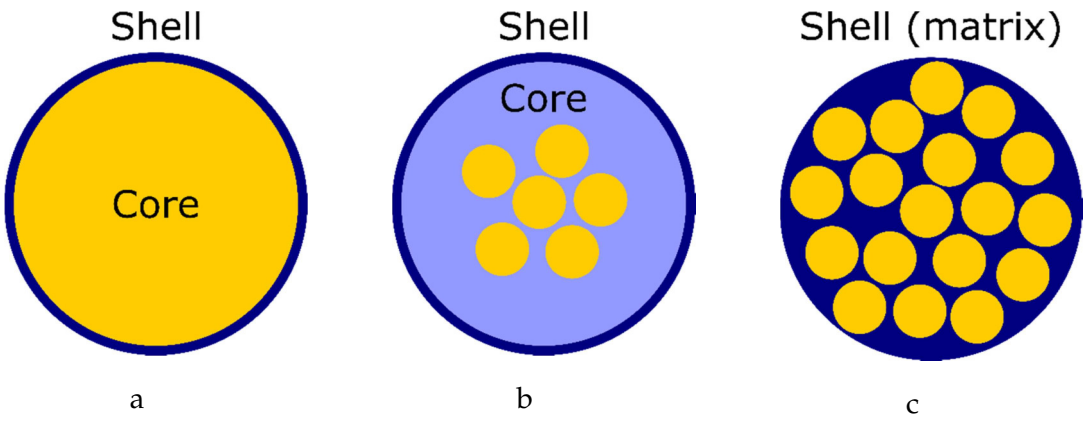

Figure 9 - Scheme of: (a) mononuclear capsule; (b) polynuyclear capsule; (c) matrix-type capsule

Matrix encapsulation is the simplest structure, in which the active ingredient (core) is much more dispersed within the carrier/shell material either in the form of relatively small droplets or more homogenously distributed/embedded in a continuous matrix of wall material. The active ingredients in the matrix type morphology are also present at the surface unless there is additional coating applied.

The selection of the microencapsulation process is determined by the physical and chemical properties of core and shell/coating materials and the intended application. Various technologies and shell materials have been developed to design microcapsules with wide variety of functionalities[26]. By using selective encapsulation techniques and shell materials, designed microcapsules with controlled and/or targeted release of the active encapsulated ingredients (by using triggers, such as

pH change, mechanical stress, temperature, enzymatic activity, time, osmotic force, etc.) can be obtained.

2.2. Methods of encapsulation

2.2.1. Phase separation

Phase separation can be divided into aqueous or organic phase separation, depending on the solubility of the wall material. In phase separation, the core material is first suspended in a solution of the wall material. The wall polymer is induced to separate as a viscous liquid phase (not as a precipitate) by several different methods (e.g., by adding either a nonsolvent for the polymer or salts, by lowering the temperature, or by adding an incompatible polymer). This separation process is known as coacervation. Coacervation is recognized by the appearance of turbidity, droplet formation, or actual separation of liquid layers[27].

Coacervation may be simple or complex. In simple coacervation, addition of a water-miscible nonsolvent (e.g., ethanol) to an aqueous polymer solution causes formation of a separate polymer-rich phase due to a partial miscibility effect. An example of a simple coacervation system consists of water, gelatin, and ethanol. The system is, however, difficult to control, and the core material must be insoluble in both ethanol and water. An example for organic phase separation is the microencapsulation of water-soluble organic compounds which can be finely dispersed in a solution of cellulose acetate butyrate (CAB) in

methylene chloride. Toluene (a nonsolvent for CAB) is slowly added, causing coacervation of the polymer around the emulsified droplets of the aqueous solution of the organic compound as it separates from solution. The capsule walls can then be hardened by addition of an aliphatic hydrocarbon solvent with a low solvent power (e.g., hexane). Spherical microspheres with thin elastic walls are usually obtained[28].

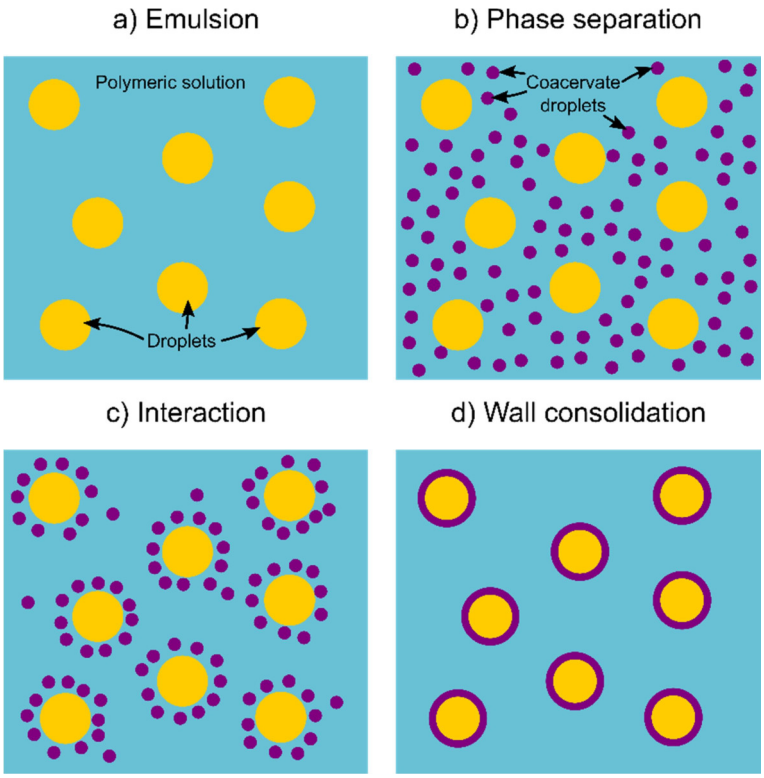

Figure 10 – Microencapsulation by coacervation: a) Droplets of core material dispersed in gelatin – gum Arabic solution; b) onset of coacervation by separation of finely divided microcoacervates from the solution; c) gradual separation of the microcoacervate on to the surface of the core material droplets; d) Coalescence of the microcoacervate into wall material of the droplets.

Complex coacervation results from the mutual neutralization of two or more oppositely charged colloids in aqueous solution. For example, the

positively charged gelatin (pH <8) forms a complex coacervate with negatively charged gum arabic. Complex coacervation is closely related to the precipitation of colloidal material from solution: coacervation immediately precedes precipitation. Microencapsulation by complex coacervation consists of three stages (figure 10):

1. Dispersion of the active component to be encapsulated into an aqueous solution of a polyelectrolyte;
2. Deposition around the core material of the coacervate formed by addition of an aqueous solution of a second electrolyte of opposite charge;
3. Gelation of the coacervate.

Practically, the core material is emulsified with an aqueous solution of gum Arabica (or gelatin); then, an aqueous solution of gelatin (or gum Arabica, depending on the starting solution) is mixed. A ternary phase diagram gelatin/gum/water allows to identify the concentration needed to induce coacervation (at a given pH, which is 4.5 in this case without any external modification)[29]. The actual water concentration is low enough to keep the colloid stable. Adding water will cause the coacervation of the two components. If the pH is higher, dilution is no longer followed by coacervation. However, lowering the pH after dilution set the right conditions for coacervation to happen. Cooling the solution to 0°C causes the coacervate droplets to form a gel and, therefore, the consolidation of the capsules wall[24]. Eventually, the capsules can be hardened by reaction with crosslinkers such as glutaraldehyde[30].

2.2.2. Interfacial and in-situ polymerization

Polymerization plays a key role in chemical microencapsulation. The basic mechanism of this method is to put a polymer wall (can be multilayer) through polymerization on a core material, or to embed the core material in a polymer matrix through polymerization. Interfacial polymerization is one of the most important methods that have been extensively developed and industrialized for microencapsulation[31].

Both interfacial polycondensation and polyaddition involve two reactants dissolved in a pair of immiscible liquids, one of which is preferably water, which is normally the continuous phase, and the other one is the dispersed phase, which is normally called the oil phase. The polymerization takes place at the interface and controlled by reactant diffusion (figure 11)[32]. Researches indicate that the polymer film occurs and grows toward the organic phase[33]. In most cases, oil-in-water systems are employed to make microcapsules, but water-in-oil systems are also common for the encapsulation of hydrophilic compounds[34].

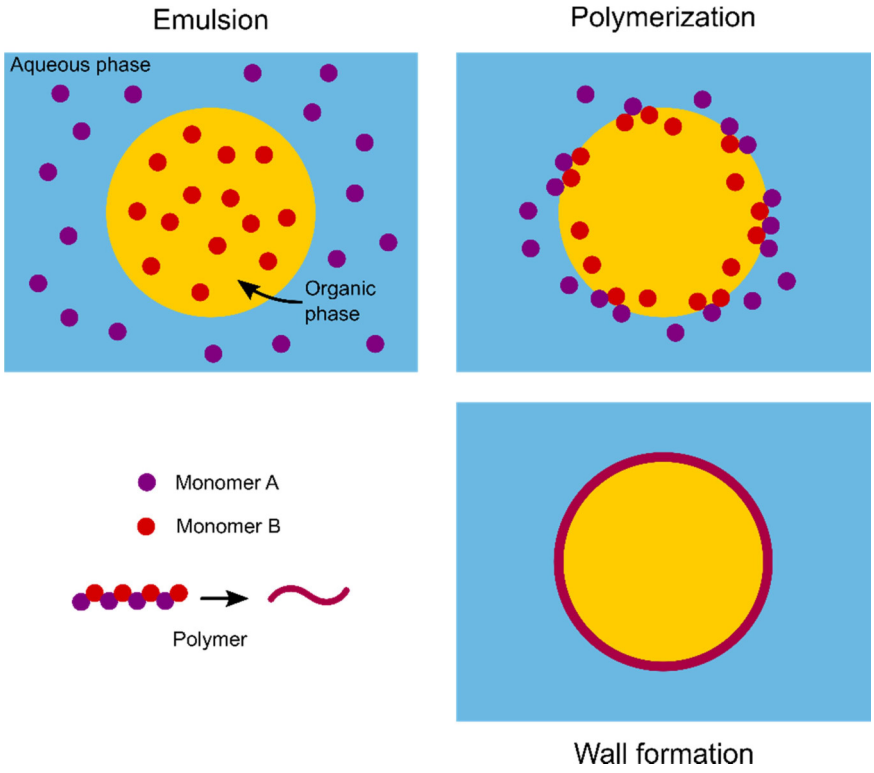

Figure 11 - Schematic representation of encapsulation by emulsion interfacial polymerization

The following equations illustrate the main polymers and reactant systems of microcapsule making through interfacial polycondensation:

- (di or poly)acyl chlorides + (di or poly)amines → polyamides;
- (di or poly)isocyanates + (di or poly)amines → polyureas;
- (di or poly)isocyanates + (di or poly)ols → polyurethane;
- (di or poly)acyl chlorides + (di or poly)ols → polyesters;
- Bischloroformate + (di or poly)amines → polycarbonates

The formation of a microcapsule wall through interfacial polycondensation takes place in two steps. First step is the deposit of the oligomer (initial wall) at the oil droplet, and the second step is the wall

thickness builds up. In order to prepare the microcapsule with expected structure, the chosen polymer wall material should match with the core material. The affinity interaction between the polymer wall and the core material can determine the structure of the microcapsule. Highly cross-linked polyurea and polyurethane can form so-called "compact" capsules with 2-methylbenzothiazole (the core material) homogeneously distributed in the polymer matrix, while in the case of polyamide core-shell structure capsules were found. The "compact" form is due to the high affinity of the core to the polymers, and the core-shell form is resulted from the low affinity[35].

Aliphatic or aromatic structure, as well as liner or branched structure of the reactants, can give the microcapsule shell different porosity and permeability, which can greatly influence the release performances[36]. Multifunctional reactants can help to achieve more thermal mechanical stable microcapsules since the wall is a three-dimensional cross-linked polymer network[37].

The encapsulation of an agrochemical product in polyurea microcapsules is described as an example[38]; the core material is milled to reduce the powder dimension, then it is dispersed in a molten wax (i.e. 10-20°C above the wax melting point) along with an oil dispersant. An isocyanate is dissolved in the organic phase, which is then emulsified with an aqueous PVA solution. An aqueous polyamine solution is added to the emulsion, starting the polymerization process. A microcapsule slurry is obtained, helped also by the cooling of the system, which allows the consolidation of the waxy material.

Compared to interfacial polymerization, in situ polymerization differs in terms of localization of the reagents. While in the interfacial polymerization, the two monomers are dissolved in different phases, in the in situ process the monomers are in the same phase; the formed polymer migrates and deposits on the dispersed phase to generate a solid wall thus forming a microcapsule. Amino resin-based microcapsules are widely produced in this way. Amino resins are thermosetting polymers made by the reaction of an aldehyde with an amino containing compound. Urea-Formaldehyde (UF) and Melamine-Formaldehyde (MF) resins are predominant in this area[39]. The main advantages of this method are as follows: inexpensive and easy-to-get materials, relatively simple and controllable process, highly cross-linked impermeable wall with superior thermal and mechanical properties, high loading core (up to 95%), high resistance to harsh chemical environments (e.g., in detergents, softeners), and easy to large industry scale-up. By this method, many microcapsules with different active core materials such as color precursor, fragrance, phase change material (PCM), insecticide, etc., were prepared[40–43]. However, there are two major disadvantages of this process, which may affect the microcapsule's properties made from and its future development. The first one is the same wall thicknesses apply to all the microcapsules with different sizes in a batch[44]. That means larger microcapsules have thinner wall relative to their sizes and thus are weaker, while smaller microcapsules have thicker wall and stronger. The second disadvantage of this method is this process is formaldehyde involved. For environmental and health considerations, formaldehyde is

regulated[45]. With different starting materials and formulas, the process might be different. However, in general, to encapsulate water-immiscible oil, the key steps should include the following: Disperse oil-in-water phase that contains the reactants (i.e. MF or UF resin prepolymer) and create a stable emulsion with the expected oil droplet size; Polymerize from the water phase and deposit monomer/oligomer on the oil phase; Build wall thickness and cure. Figure 12 illustrates a process of making a MF perfume microcapsule[46].

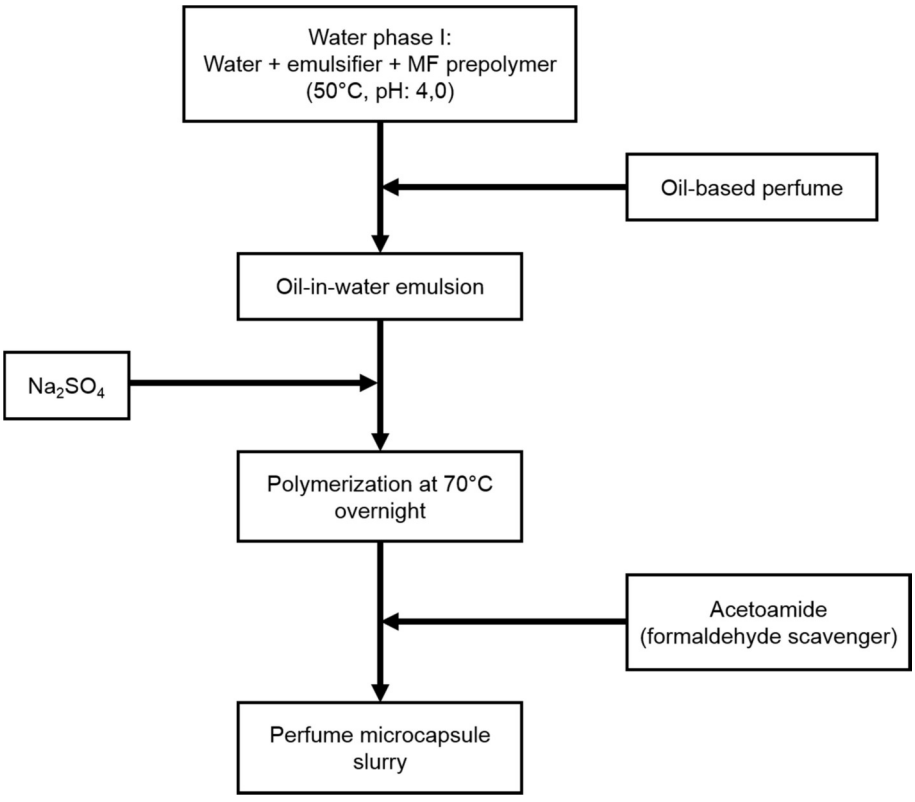

Figure 12 - Example of perfume MF microcapsule making

2.2.3. Spray drying

Microencapsulation by spray-drying is a low-cost commercial process, which is mostly used for the encapsulation of fragrances, oils, and flavors. Spray-drying encapsulation has been used in the food industry since the late 1950s to convert liquids to powders. The process is economical and flexible, in that it offers substantial variation in microencapsulation matrix, and produces particles of good quality.

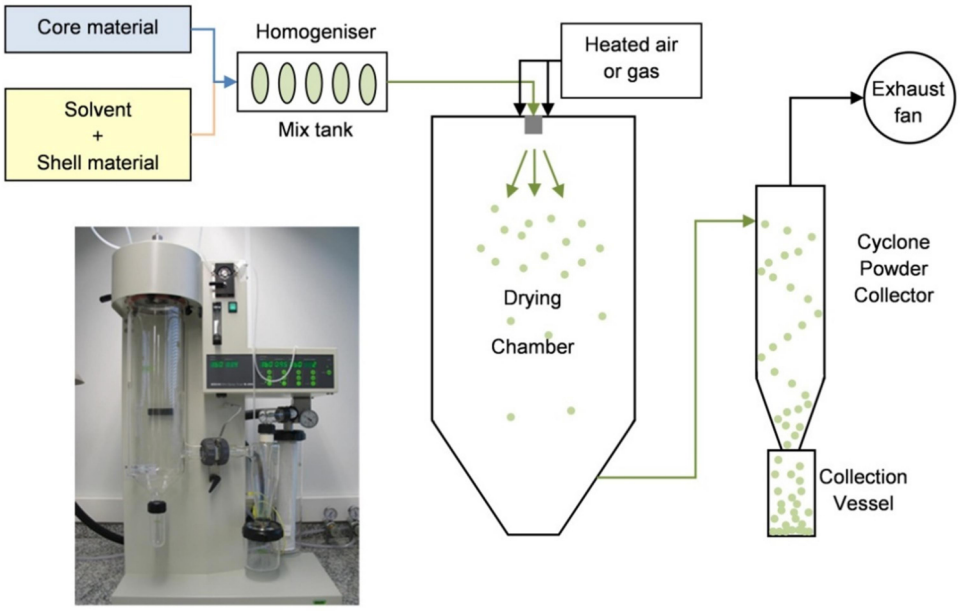

Figure 13 - Operating scheme of a spray-drying apparatus

In the spray drying process (schematized in figure 13), a microparticle powder is formed by spraying (atomizing) a solution/dispersion of active material and the film forming wall material as fine droplets into hot air. The water then evaporates and the dried solid is separated, usually by air separation. An aqueous solution, an organic solution, or a slurry of the material to be coated can be used. Important variables that must be taken into account are the core/wall material ratio, the

concentration, the viscosity and the temperature of the starting solution[47,48].

The technique is extremely suitable for the continuous manufacture of dry solids as either powder, granulates, or agglomerates from liquid feeds. The microcapsules obtained are of polynuclear or matrix type, and the particle dimensions span from 10 to 200 μm.

2.2.4. Solvent evaporation

The solvent evaporation method is a technique widely used for the preparation of biodegradable and nondegradable microspheres[49]. In this method, summarized in figure 14, the active material and the polymer are dispersed in a volatile, water-immiscible organic solvent (e.g. methylene chloride, chloroform, ethyl acetate). This solution – or dispersion – is then emulsified in an external aqueous phase containing an emulsifying agent (e.g. poly vinyl alcohol, poly vinyl pyrrolidone) by using conventional emulsification equipment (e.g. mechanical stirrers, ultrasonicators, homogenizers) to form an o/w-emulsion. After the organic solvent evaporation, microspheres are obtained. For water soluble active compounds, a multiple emulsion – w/o/w method – can be used.

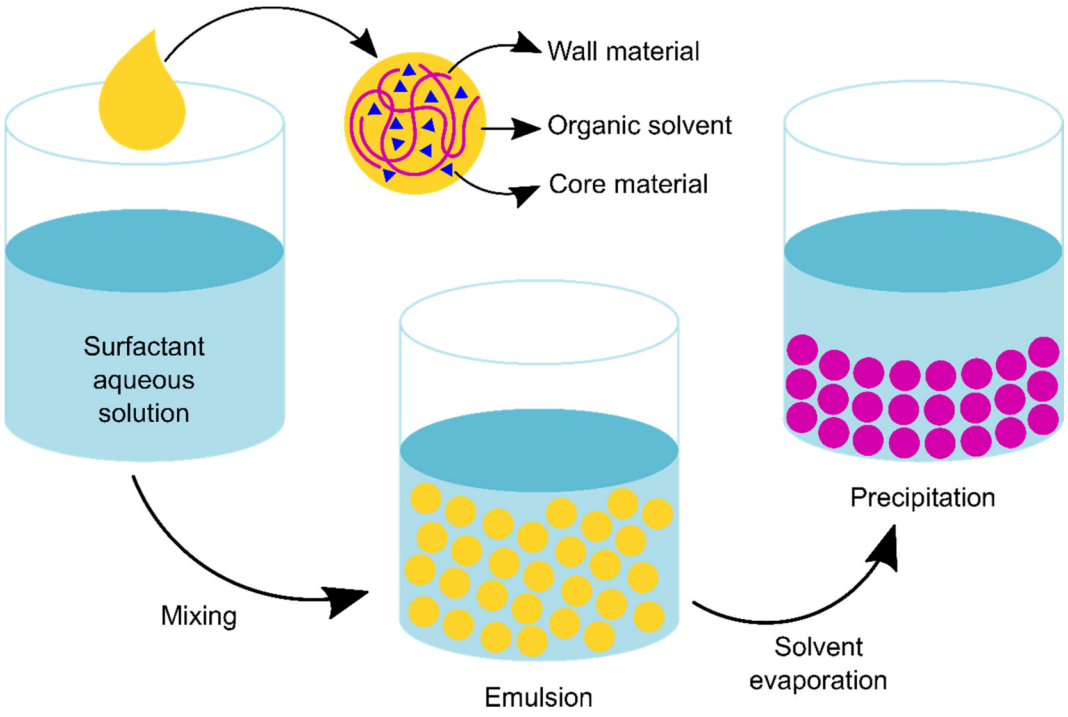

Figure 14 - Schematic representation of encapsulation by solvent evaporation

The droplet formation step determines the size and size distribution of the resulting microspheres. Stirring is the most straightforward method to generate droplets of the core/matrix dispersion in the continuous phase. The simplest approach is the agitation with an impeller; the main parameter for controlling the droplet size is the impeller speed. Increasing the impeller speed generally results in decrease microsphere mean size[50], as it results in stronger shear forces and increased turbulence. Increased viscosity of the organic phase yields larger microparticles because higher shear forces are necessary for droplet disruption[51].

The rate of volatile solvent removal from the solidifying microspheres can be controlled by the temperature of the microsphere dispersion. Higher temperatures will facilitate the evaporation of the solvent from the continuous phase and thereby maintain a high concentration gradient for the solvent between the microspheres and the continuous phase. However, if the temperature is too close to the boiling point of the organic solvent, larger size distribution and less dense particles are obtained, most likely due to the fast solidification of the outer wall.

2.2.5. Coating processes

Small, particulate cores can also be coated by air suspension coating technologies (like fluidized-bed coating ones)[52]. In air suspension techniques, particles are suspended in an upward-moving air stream and are coated by spraying polymer solutions or aqueous colloidal polymer dispersions onto the particles. It is claimed that air control and powder coating systems provide more uniform film coatings on the active materials[53]. This in turn gives reliable reproduction of predetermined release profiles for controlled-release microencapsulation systems.

The most widely used device for this purpose is the Wurster coating chamber (figure 15). The Wurster process is used for pharmaceutical products, food, animal feeds, chemicals, agricultural products and pesticides. It is a reproducible system and can be run on a small as well as on a production-size scale. The operating chamber is designed to induce a smooth cyclic flow of particles past a nozzle which atomizes the

coating solution. The wall material could also be a molten wax (e.g., a fatty material), or dissolved in an aqueous or organic solvent. The coated particles are lifted on the air stream and dried as they rise on the airstream from the nozzle. They then settle out and descend to begin another cycle. The coating film thickness is controlled by the type of coating, the solvent concentration, the air volume and temperature, atomizing conditions, and the number of coating cycles; since many thin coats are applied, the systems can be used with irregularly shaped particles. Because this process uses large volumes of air, the system has a large drying capacity and the particles are separated as they are carried on the air stream. Small particles can thus be coated with good control of agglomeration[54].

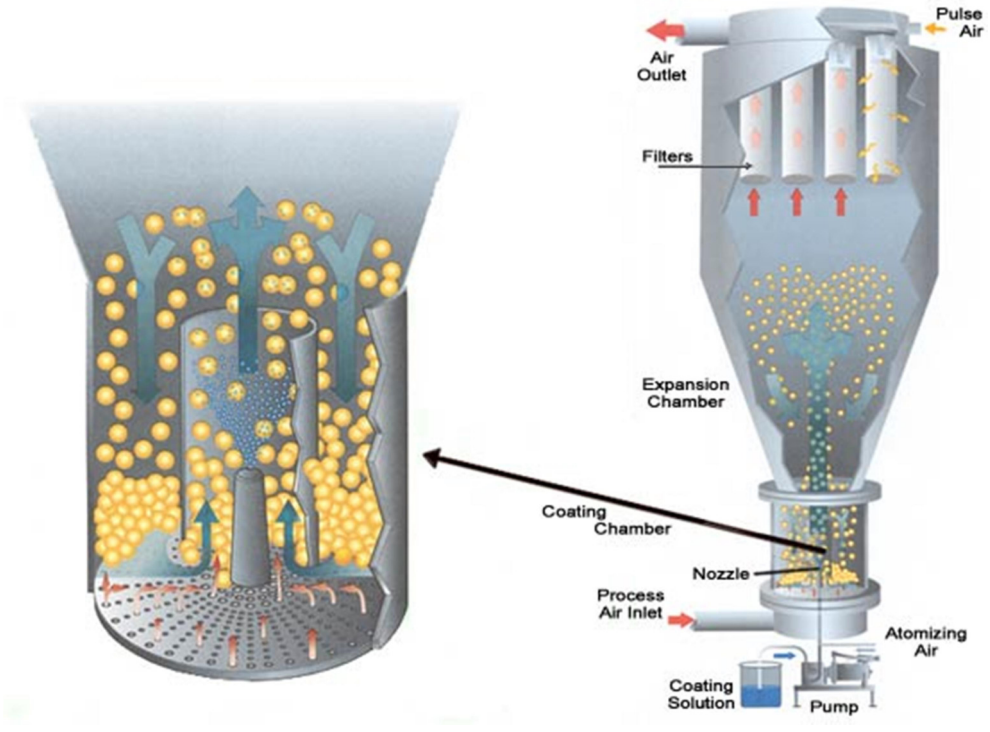

Figure 15 - Schematic diagram of a fluidized bed apparatus

2.3. Microencapsulation and vulcanization technology

Microencapsulation is not a totally new technology in the tire industry. Some methods for immobilization of sulfur in microcapsules are patented. Errasquin patented an encapsulation method for the controlled release of sulfur during the vulcanization process in order not to overcure the rubber sample[55]. Their system consists in the embedding of sulfur in a polymeric network (a resin) that retains the load at moderate temperature, while when the temperature increases, the embedding polymer is degraded, releasing the load. They use thermoset polymers – like silicone rubber, acrylic, epoxy or ethylene resins – as encapsulating polymer, but the encapsulation procedure and a more detailed description of the polymer structure is not given, thus raising doubts on what the authors effectively did and why. However, they disperse sulfur in water, then the resins are added, mixed, recovered and cured to form the protective shell. Another patent describes the encapsulation of sulfur in capsules made of melamine-formaldehyde resins and polyelectrolytes[56]. Eventually, some capsules are coated in a second step with other layers of resin. The capsule preparation is made using high performance agitation and dispersion apparatus (Ultra Turrax®). The second layer is deposited applying the same process on the formed microcapsules. Calcium alginate is also used as encapsulating material starting from the emulsion of aqueous sodium alginate with sulfur

dissolved in CS_2 and added to a calcium chloride solution by means of a capillary jet[57].

Most of the work is dedicated to sulfur[56,57], but there are only a few examples of encapsulation of other curing agents. Actually, there is only one paper about the encapsulation of accelerants. In this paper the encapsulation of two zinc derivatives in PMMA is presented[58]. The purpose of the work is the delayed delivery of accelerant during the vulcanization process in order to keep the rubber sample as processable as possible, in order not to vulcanize too fast for being shaped correctly. The capsules are prepared dissolving the accelerant in methylene chloride and emulsifying the solution with an aqueous PVA solution using an Ultra Turrax® dispersion apparatus. The obtained capsules have dimensions of 10-20 μm. However, the rubber matrix in which the samples are dispersed is liquid rubber, so the capsules are not undergoing a mechanical treatment. Guo et al. use plasma processing to coat sulfur and N-Cyclohexyl-2-benzothiazole sulfenamide (CBS) with different polymers[59]. Their work is oriented on the improvement of the rubber-curative interaction, and provides a very solid background study of the solubility parameters of the curatives in various polymers.

2.4. Our choice

Among all the techniques listed above, we chose to use the solvent evaporation from emulsion droplets. Coating techniques like spray drying or fluidized bed require expensive instruments and operate on

big scales in terms of mass output. We consider these techniques as the final step of our procedure, but we need to start from something more available on a laboratory scale. Solvent evaporation would allow us to operate with common laboratory equipment (i.e. mechanical stirrers or rotor/stator homogeneizers) without need of chemical reactions to happen, like in the case of interfacial and in-situ polymerization. Moreover, the output of the solvent evaporation method - even if performed on a laboratory scale – can, albeit with considerable practical difficulties, reach the hundreds of grams scale. As encapsulating material we chose to use a cellulose derivative – ethylcellulose – and the reason for this will be highlighted in the following section.

2.5. Cellulose ethers as encapsulants

Cellulose ether polymers have a wide diversity of applications ranging from organic soluble thermoplastic products to water-soluble food additives. Although many polymers are used in the pharmaceutical industry, the most widely used are the cellulose derivatives: methylcellulose, hydroxypropyl methylcellulose, hydroxypropyl cellulose, ethylcellulose, cellulose acetate phthalate and hydroxypropyl methylcellulose phthalate. All are derived from, and hence possess, the polymeric backbone of cellulose, which contains a basic repeating structure of R-anhydroglucose units; each unit having three replaceable hydroxyl groups (figure 16).

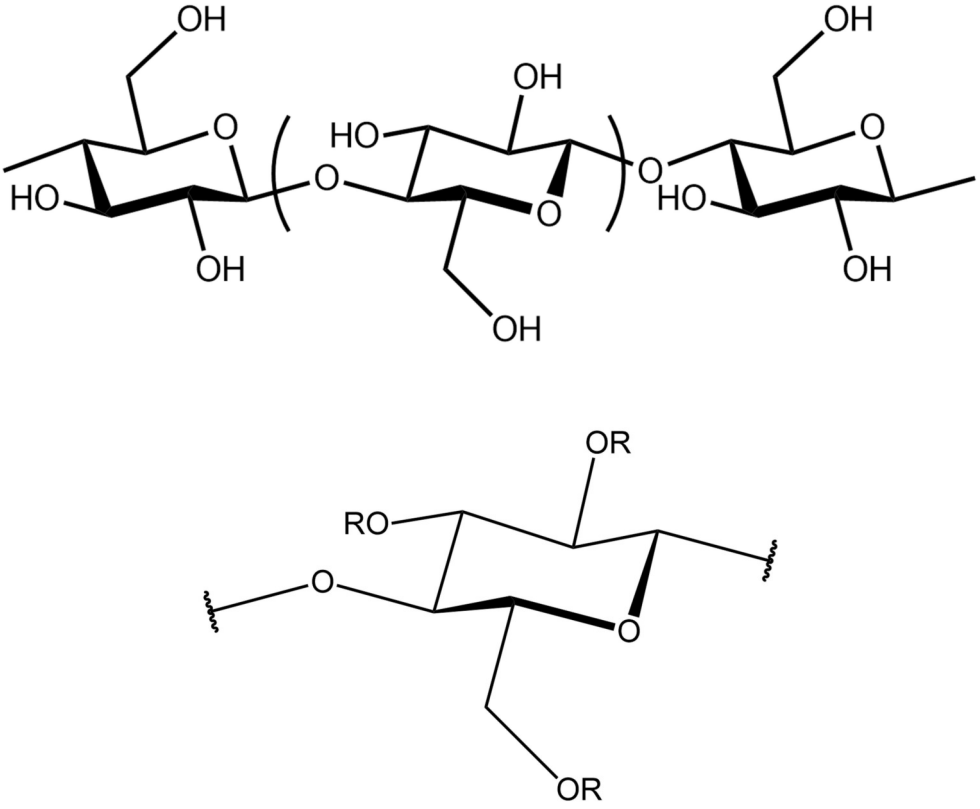

Polymer	Substituent groups	
Methylcellulose	—H	—CH_3
Hydroxypropyl methylcellulose	—H	—CH_3 —CH_2CHCH_3 (OH)
Hydroxypropylcellulose	—H	—CH_2CHCH_3 (OH)
Ethylcellulose	—H	—CH_2CH_3

Figure 16 - Molecular structure of cellulose backbone (top) and of some selected cellulose ethers (bottom)

The number of derivatized hydroxyl groups can be designated either by a weight percentage or by the number of points where the groups are attached - a concept known as degree of substitution (DS). If all the three

available positions on each anhydroglucose unit are substituted, the DS is designated as 3.

Ethylcellulose resins are white to light-tan granular powders. The differences in physical properties of the ethylcellulose products result largely from variation in the degree of etherification. The ethoxyl substitution values of commercial products range from a DS of 2.2 to 2.6 ethoxyl groups per anhydrous glucose units. This corresponds to an ethoxyl content of 44.5 to >49%.

Ethylcellulose is soluble in a wide variety of solvents, thus making it easier to use with solution processing methods. Among the useful solvents are the esters, aromatic hydrocarbons, alcohols, ketones, and chlorinated solvents. Solutions of ethylcellulose in aromatic hydrocarbons are highly viscous; consequently, solutions of low concentrations are practical when these solvents are used individually. On the other hand, solvents like ethanol and methanol yield solutions having lower viscosity; however, film properties are too poor for practical purposes.

Ethylcellulose is the most stable of the cellulose derivatives. It is resistant to alkalis – both dilute and concentrated – but is sensitive to acids. It takes up very little water from moist air or during immersion, and this evaporates readily leaving ethylcellulose unchanged. Light, visible or ultraviolet, has no discoloring action on ethylcellulose. Application of heat up to its softening point has little effect on ethylcellulose.

The softening point of ethylcellulose is between 150 and 160°C, depending on its substitution degree. This is consistent with the typical

vulcanization temperature range (150-170°C). Moreover, ethylcellulose is non-toxic, cheap and abundant, which makes it affordable from an industrial point of view[22].

In the tire industry, cellulose has been investigated as a filler[60,61]. Bare mixing of cellulose powder is not sorting any effect on the mechanical properties of the blend, while a more intimate mixing obtained treating a rubber-celluose xanthate mixture with an alkaline solution and riprecipitating the obtained solution with an acidic solution. The comparison of this blend with cellulose-free polymers (SBR, BR and NR) showed an enhancement of the curing time. Moreover, an increase of properties such the tensile strength and the modulus is observed, while the elongation and resilience decrease. However, those effects start to be relevant when cellulose the cellulose amount is greater than 5 phr, while the usual accelerator concentration spans between 1 and 3 phr. This was to show that actually cellulose derivatives, even if not common, are explored in tire technology.

3. Encapsulation of vulcanization accelerators

In this chapter will be showed the attempts and the optimized procedures developed for the accelerator encapsulation. A brief summary on the material that we decided to use is provided.

Accelerator (core material)

TBBS is a sulfenamide-based primary delayed action vulcanization accelerator for use in natural rubber and synthetic rubber such as SBR, BR, NBR and EPDM. TBBS provides high modulus and excellent physical properties, suitable for tire treads and mechanical goods. It is usually used in conjunction with secondary accelerators, such as diphenylguanidine. It is soluble in a wide range of organic solvents (ethanol, isopropanol, acetone, toluene, ethyl acetate, chlorinated solvents), while it is practically insoluble in water. Its melting point is between 104 and 110°C.

Ethylcellulose (encapsulating material)

We chose to use a very viscous (300 cP, 5% solution in toluene/ethanol 80:20) ethylcellulose (EC from now on) to be sure to have a homogeneous capsule surface. Its softening point is 157°C, while the ethoxyl percentage is 48%.

3.1. Reprecipitation technique

We identified the synthesis from emulsion as the best solution for our purposes, but we thought that it was worth a shot to try with an even simplest method, the reprecipitation method (figure 17). Basically, both the load and the wall material (which must be insoluble in water) are dissolved in a water-miscible organic solvent. Then, the solution is added to a water bath under sonication or high stirring. The solvent replacement induce the precipitation of both the wall and the core material, giving a matrix-type structure. This process is widely used for the synthesis of pigment nanocrystals[62] [refs] and has been used for the PMMA encapsulation of lanthanide chelates[63].

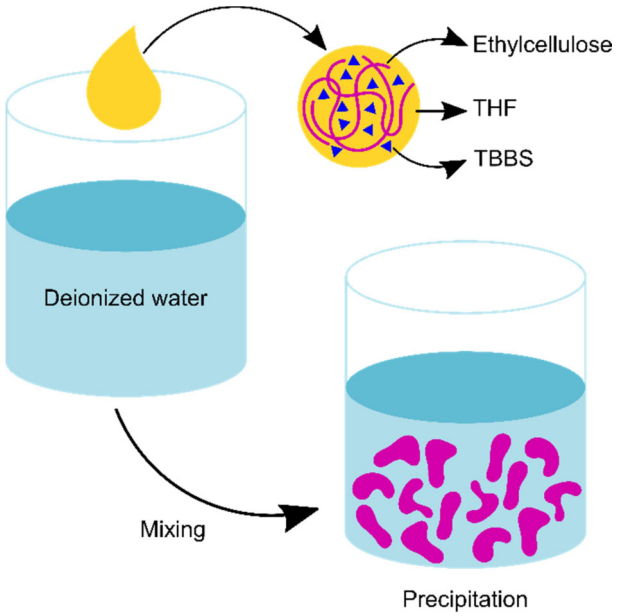

Figure 17 - Encapsulation of TBBS by reprecipitation from THF solution

We chose THF as good solvent for both TBBS and EC (TBBS/EC was set to 5:1), and in fact a clear solution is obtained, but the viscosity increases dramatically. This makes troublesome the addition of this phase to water, so we decided to add water to the organic phase. After water addition, the solution turns to a colloidal suspension, followed by the precipitation of a white solid. Unluckily, the precipitate aggregates dramatically while precipitating, forming some fibrous structures instead of a powder. Therefore, we moved on directly towards the emulsion technique.

3.2. Solvent evaporation from emulsion droplets

As pointed out before, TBBS is readily soluble in chlorinated solvents, toluene, alcohols and ethyl acetate. EC, on the other hand, gives readily clear solution only in chlorinated solvents. It is soluble also in ethyl acetate and toluene, but the solution obtained are hazy (ethyl acetate) or gel-like (toluene). By the way, this can be overcome by stirring the solution for longer time, or as we later discovered, by using a proper homogenizer to prepare solutions.[†] We decided to use dichloromethane

† Homogenizers are of course very well established in formulation technology. Same goes for probe sonication. However, due to the industrial constraints we already mentioned, we had to restrain to easily scalable techniques for most of the time. Only during the third year of the project we managed to acquire a rotor/stator homogenizer big enough to handle the typical 5 L vessels we routinely worked with.

(DCM from now on) for the organic phase, keeping in mind that this solution will fit the laboratory needs, but not the industrial ones. Later on we successfully managed to use AcOEt instead, yet the number of samples we have with this former solvent is limited. The most common surfactant used for EC encapsulation is polyvinyl alcohol (PVA), a non-ionic synthetic polymer.

We started to investigate TBBS/EC encapsulation with a modified literature procedure. The main change we made – apart from the core material – is a scaling-up of one hundred times in terms of amount of materials. The aqueous phase was prepared dissolving PVA in deionized water for 12 hours by means of mechanical stirring (400 RPM). Eventually, undissolved PVA (if any) is filtered off on a paper funnel.

TBBS is dissolved in DCM with magnetic stirring. Then, EC is slowly added to the solution. A rapid addition of EC will result in a massive agglomeration of the powder, and the dissolution time increases. Once fully dissolved, EC increase the solution viscosity dramatically. The organic phase is added slowly to the aqueous phase under high mechanical stirring (1000 RPM). A vigorous mechanical stirring is needed to disperse homogeneously the viscous organic phase, but this can result in the formation of foam, which can be disruptive for the formation of the emulsion droplets. Therefore, the addition is stopped when foam starts to develop, and it is restarted when the foam level stabilizes.

Component	Mass (g)	Volume (mL)
TBBS	30	-
EC	10	-
DCM	-	600
PVA	20	-
Water	-	2000

Figure 18 - Optimized recipe for TEC01 (TBBS/EC = 7:3)

Once mixed, the two phases are emulsified at 1500 RPM for 30 minutes, obtaining a white, milky solution. That solution is left stirring (500 RPM) until all the organic solvent evaporates (typically up to three days). This causes the precipitation of a white solid, which is collected, dried in vacuum oven at 60°C till constant weight and characterized. We produced several batches of particles pertaining to three families of TBBS/EC ratio to 7:3 (TEC01), 1:1 (TEC02) and 3:7 (TEC03).

We did also some tests using conventional magnetic stirring instead of mechanical stirrer to compare the two techniques. After a few trials, we managed to achieve a satisfactory reproducibility.

a

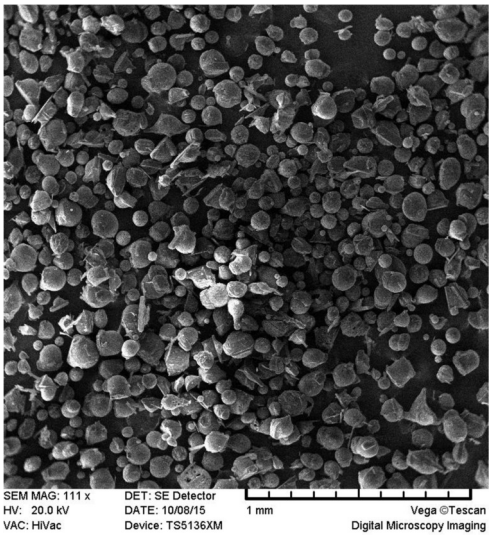

b

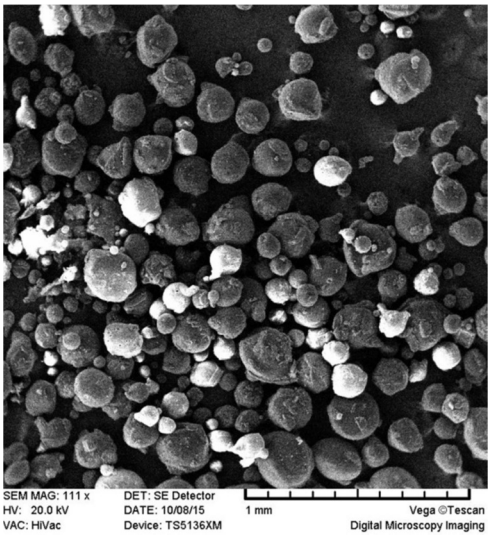

c

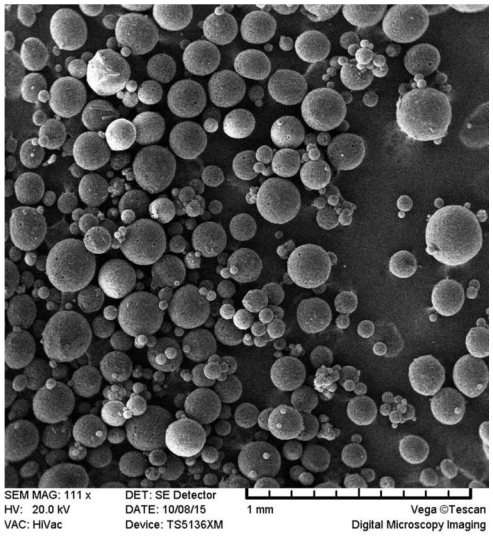

Figure 19- SEM micrographs of (a) TEC01; (b) TEC02; (c) TEC03

The SEM images (figure 19-20) shows that the powder is composed by spherical microparticles. The samples obtained *via* magnetic stirring have irregular shape, while a more homogenous shape is obtained with the

mechanical stirring. The particle surface is not uniform, showing some holes which may be related to the solvent evaporation[64,65]. Shifting the TBBS/EC ratio towards EC results in an increase homogeneity of the particle surface, as expected. The particles dimension span from 20 to 200 μm; we think that such big dimension and wide polydispersity are intrinsically related to the technique and the operative scale. It has been demonstrated that operating on lower volumes it is possible to obtain better results in terms of dimension and dispersity, yet the production of a single batch would require the repetition of the procedure a few tens of times, which is unpractical.

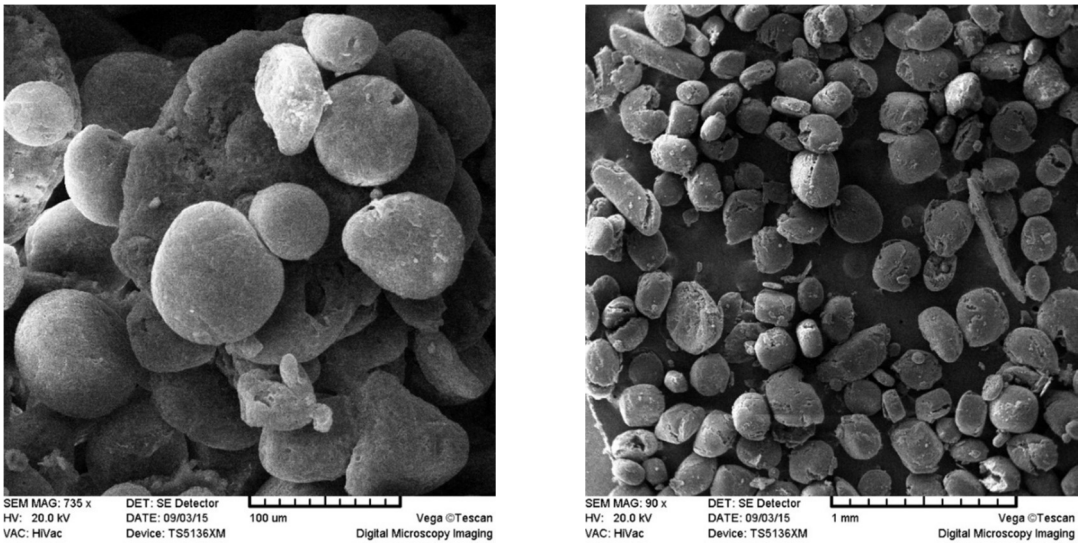

Figure 20 - SEM micrographs of TEC04 (left) and TEC05 (right)

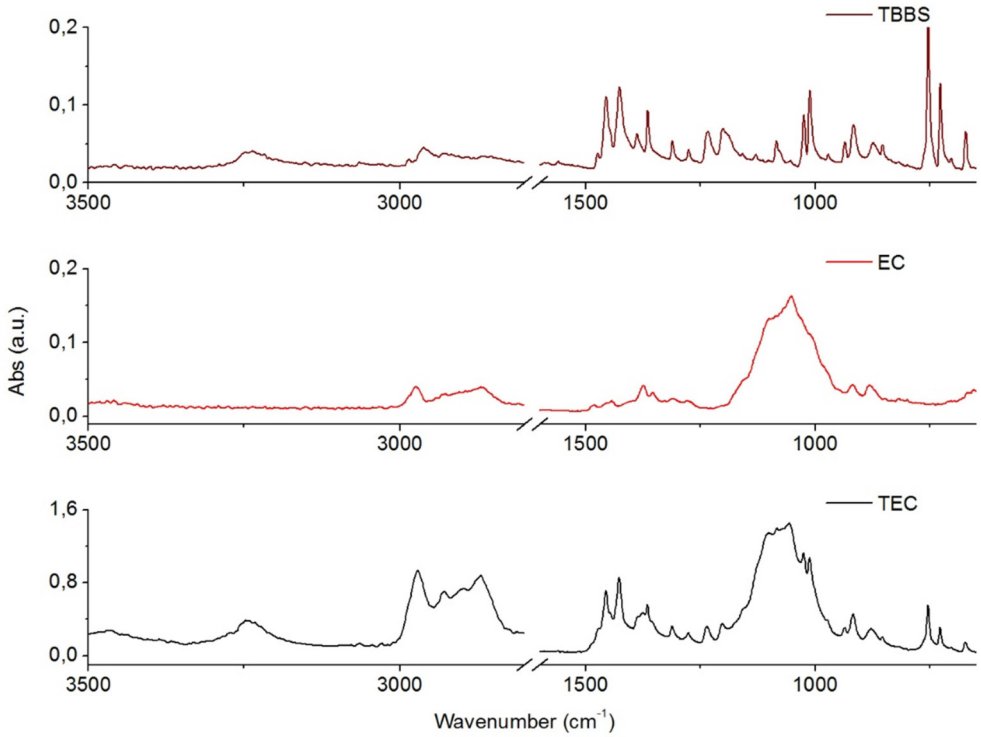

Figure 21 - IR spectra of TBBS, EC and TEC01

Figure 21 shows the IR spectra of TBBS, EC and TEC01, from which is possible to see the presence of both the components within the capsules. However, it is hard to obtain quantitative data from IR spectra, particularly when operating in the ATR configuration, as we did. In order to determine the amount of TBBS in the sample we used Uv/Vis spectroscopy (figure 22). First, we determined the molar extinction coefficient (ε_{279nm} = 12724 $Lmol^{-1}cm^{-1}$ in DCM) of TBBS, then we dissolved a small portion (few milligrams) of the encapsulated sample and, from the selected peak, we calculate TBBS concentration. The estimate was supported by solution NMR spectroscopy, by comparison of the integrals attributed to TBBS signals vs EC signals (figure 23).

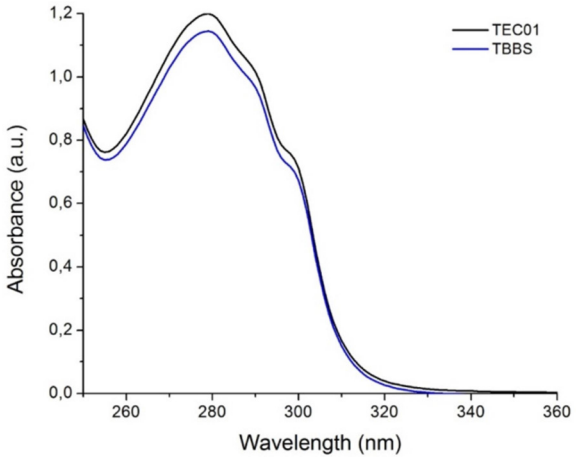

Figure 22 - Uv-VIs spectra of TEC01 (black line) and reference TBBS (blue line). It is possible to recognize that the only contribute to the spectrum comes from TBBS absorption.

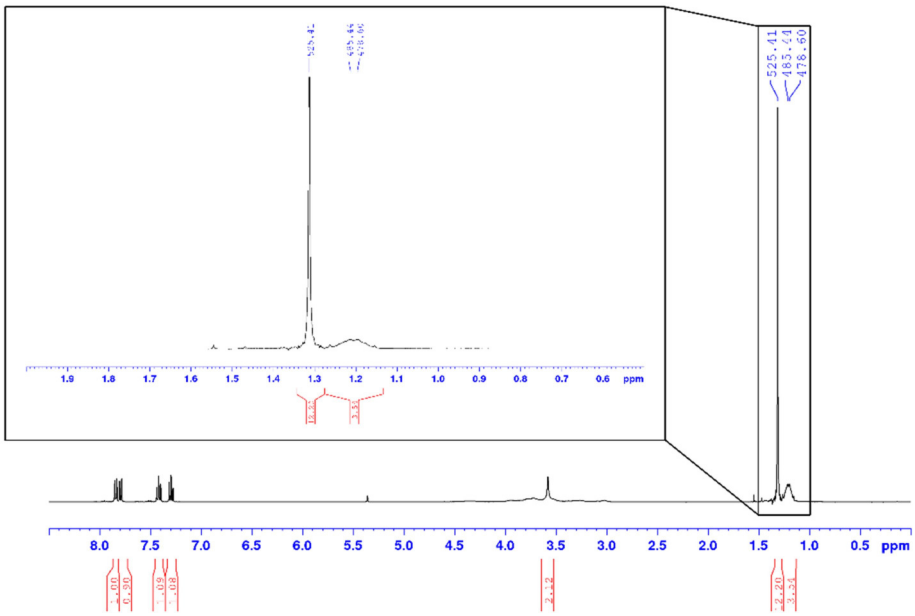

Figure 23 - NMR spectrum of TEC01 in CD_2Cl_2. The inset shows the integration of the signal attributed to the methyls of the t-butyl group of TBBS (sharp peak) and the signals of the terminal methyl of the ethoxyl substituents of EC.

The latter technique is clearly not as sensitive as Uv/Vis measurement. Moreover, the peak relative to the terminal –CH3 of the t-butyl moiety of TBBS is partially superimposed to some signals of ethylcellulose, messing up the integration. It is worthy to note that $CDCl_3$ is slightly acidic, and it reacts with TBBS, so we had to use CD_2Cl_2 as NMR solvent. Due to its simplicity and accuracy, we decided to keep Uv/Vis as the standard analysis to determine TBBS concentration. In terms of mass yield, we can produce in one run up to 40 g of product.

An intrinsic problem exists, since EC is partially soluble in all the most common organic solvents, there is no way to dissolve the non-encapsulated TBBS which remains in the sample. Therefore, we can determine how much TBBS is in our sample, but we cannot estimate the real percentage of encapsulated TBBS. However, TBBS recrystallize in needle-like structures, and their absence in the SEM images induces us to think that we can assume that all the TBBS found is encapsulated.

We tried to vary the ratio between organic solvent and water (TEC07, oil/water 1:10), but we did not see significant differences in terms of dimension. We tried to change the stirring blade, in particular we used a high shear blade, but we obtained a very poor result in term of encapsulation. In particular, lots of needles and platelets can be found mixed with the particles (TEC08). Figure 24 shows the SEM micrographs of the previous samples. We think that those platelets are non-encapsulated TBBS crystals. Macroscopically, the precipitate looks shinier, and TBBS is the only component that can form a crystalline structure. We decided to keep the method used for the production of

TEC01 as the standard operative method; the rest of the characterization described are conducted on what we consider is our optimized sample.

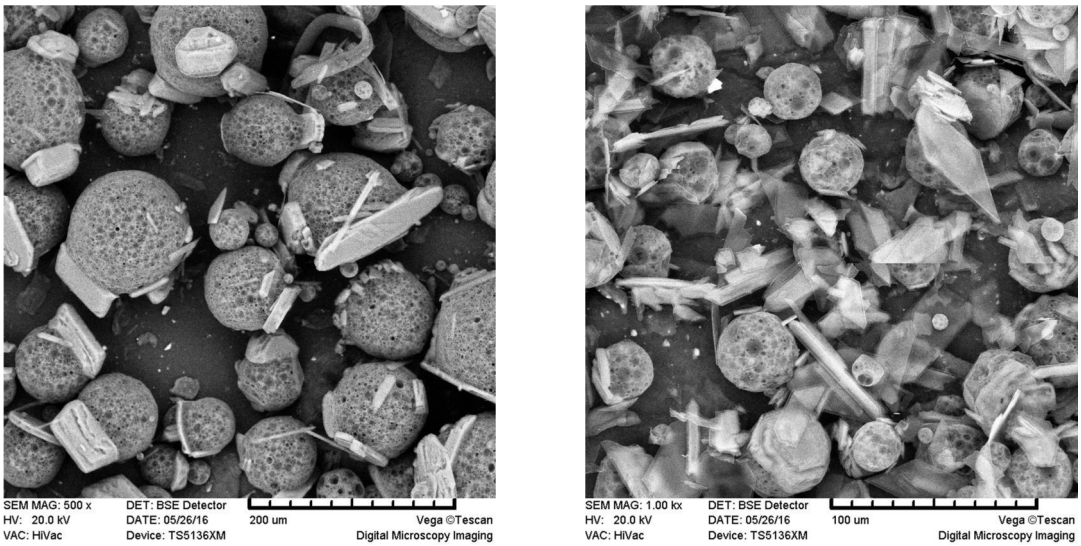

Figure 24 SEM micrographs of TEC07 (left) and TEC08 (right)

In order to have an idea of both the thermal stability of the capsules and of their inner structure (matrix versus polycore or core-shell), we carried out a DSC analysis.

This analysis turned out to be highly informative. Figure 25 shows the DSC curve of pristine TBBS (blue trace), encapsulated TBBS (TEC01, black trace) and a mechanical mixture of TBBS and ethyl cellulose we used as a reference (red trace). In all three cases the DSC trace shows a clear melting process happening in the 105-115 °C range. The TBBS trace is narrow and well defined as expected for a crystalline material. In contrast, the capsule trace is sizably broader and features a slight suppression of the melting point.

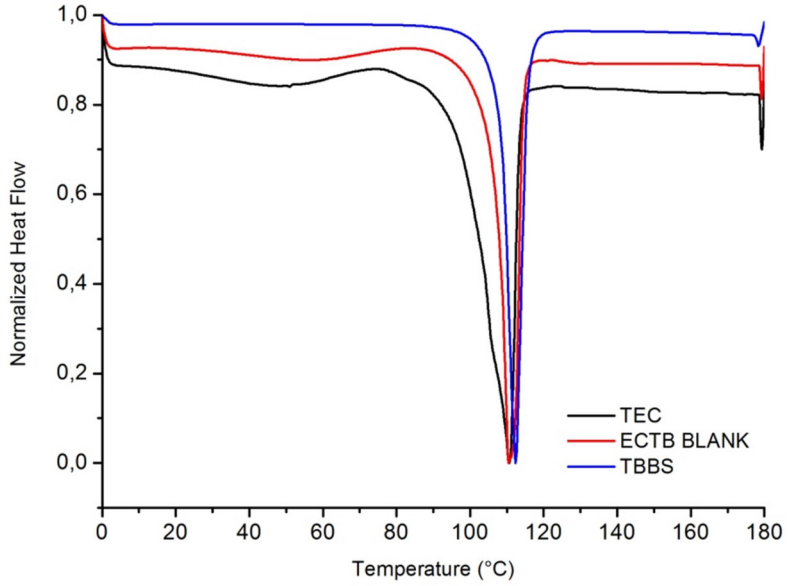

Figure 25 - DSC curve (first run) of TEC01 (black line), mechanical mixture of TBBS and EC (red line) and pristine TBBS (blue line).

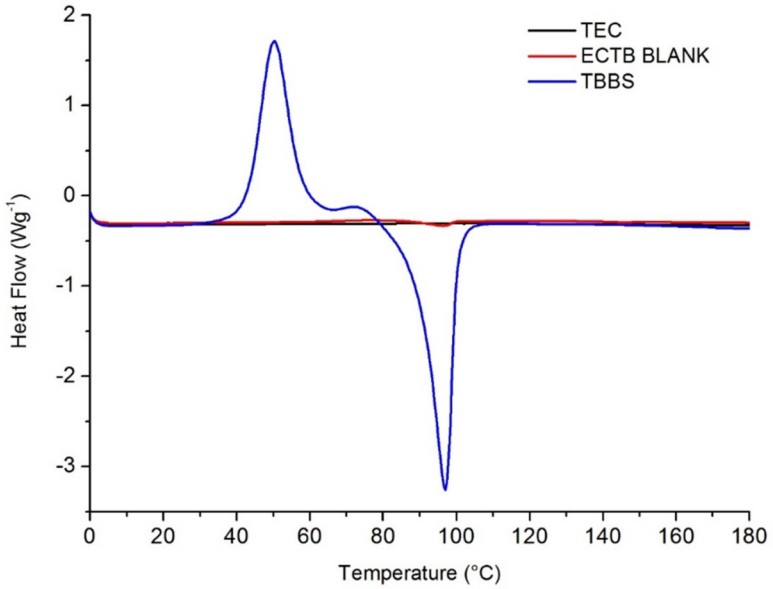

Figure 26 - DSC curve (second run) of TEC01 (black line), mechanical mixture of TBBS and EC (red line) and pristine TBBS (blue line).

Both characteristics are in agreement with the formation of very small crystals having a broad dimension's distribution. On the basis of this evidence, we can conclude that the capsules are not of a matrix type, as in this case no melting point would be observed.

Their spherical shape as well as the still in any case well defined melting (in particular when compared with the mechanical mixture) would rather suggest a core shell structure, yet a polycore one cannot be excluded on the sole ground of thermal characterization. It should be noted however that for the purpose of the present applications, a polycore and a core shell structure would have similar performances, thus a further discrimination is of little practical importance.

Figure 26 gives another very important clue on the behavior of the capsules. In all of the traces, the very same sample of Figure 25 is cooled down to room temperature, and then the thermogram is acquired again. Only in the case of pure TBBS (blue curve) the thermogram shows the exothermic peak at 50°C associated with the recrystallization of the materials (eventually melting again in this case at less than 100°C due to the poor quality of the crystals). In both the capsules and the mechanical mixture, the second run shows essentially no signal. This can be interpreted as the formation of a TBBS/EC solid solution. In fact above 120°C TBBS is a liquid, also acting as a solvent for the EC. In the second run the TBBS is still present but cannot crystallize as it is homogeneously dispersed in the EC polymer. Consequently, no melting point is observed. It is worthwhile nothing that EC itself is completely stable un

to 160°C, yet in the presence of molten TBBS, acting as a good solvent for EC, capsules are not expected to survive. This observation turned out to be very relevant when our solid formulation was tested in vulcanization experiments, as will be described in chapter 3.

To overcome this problem, we devised a crosslinking post-functionalization approach, which will be covered in the following chapter.

3.3. Encapsulation of TBBS in ZnO

One of the material that have an active role in the vulcanization process is zinc oxide, which is generated *in situ* in the rubber blend starting from zinc esters. It has been showed the possibility to prepare zinc-oxide based capsules containing a phase-change material[66]. We thought that, if successful, this could be an idea to bring two vulcanization components together in the same place in the mixing phase.

Zinc oxide can easily form from zinc salts (e.g. zinc chloride or zinc nitride) and their reaction in alkaline environment, according to the following scheme:

1. $Zn^{2+} + 2OH^- \rightarrow Zn(OH)_2$
2. $Zn(OH)_2 \rightarrow Zn[OH]_4^{2-}$
3. $Zn[OH]_4^{2-} \rightarrow ZnO + OH^- + H_2O$
4. $Zn(OH)_2 \rightarrow ZnO + H_2O$

There are two kind of mechanism; the first is a dissolution-reprecipitation, in which zinc hydroxide converts into zincate ion and then precipitates as zinc oxide, the second is an *in situ* crystallization of zinc oxide from the hydroxide by means of dehydration. Both of the mechanism work together for the formation of zinc oxide.

We used a reprecipitation approach, dissolving first TBBS in acetone, then reprecipitating it with an aqueous solution of zinc chloride. Zinc chloride concentration is calculated to produce, theoretically, zinc oxide stoichiometric with TBBS. During the whole process, the solution is kept under high magnetic stirring. We want to reprecipitate TBBS for two reasons: forming smaller crystals and using the formed crystals as nucleation center for zinc oxide. After the addition of the zinc chloride solution, TBBS precipitates from the solution, obtaining a shiny dispersion. Subsequently, a KOH aqueous solution is added to the dispersion, causing a massive precipitation. Also, we noticed the formation of a gel-like structure, because magnetic stirring became suddenly unable to mix homogeneously the dispersion. However, increasing the stirring speed causes the network collapse, and a powder precipitates at the bottom of the flask. The powder can be easily recovered on a paper funnel and dried in the oven.

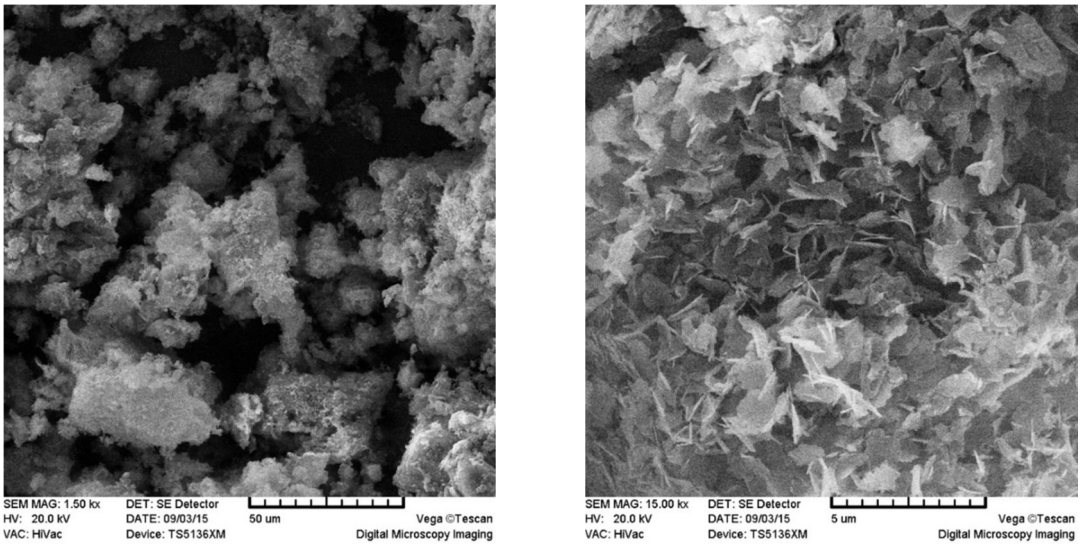

Figure 27 - SEM micrographs of ZnO/TBBS composites

SEM images of the powder shows that it is composed by big aggregates covered by scales (figure 27). Since zinc oxide is insoluble in all the common organic solvents, we washed the powder to remove non-encapsulated TBBS. Evaporating the acetone used for washing the powder, we found TBBS in every acetone sample used for the washing procedure. We concluded that, even if the encapsulation was successful, the shell formed is not dense enough to allow TBBS to be contained, and it will leak for sure above its melting point. Even if our results cannot exclude that encapsulation in ZnO might be possible, our proof of concept experiment was not encouraging enough to keep pursuing the approach alongside with our main encapsulation strategy.

3.4. Encapsulation of TBBS in polymethylmethacrylate

Being aware of the limits shown by EC as encapsulating material (see previous paragraphs), we considered possible alternative encapsulating materials. PMMA and bis-phenol A based polycarbonate were in this contest somewhat obvious choices both in terms of availability of samples and of solubility in molten TBBS. Both polymers in fact are available at molecular weight high enough to ensure a better resistance toward such kind of cargo. Is should also be noted that the use of such polymers in real tire application would be problematic, mostly due to the costs of such raw materials. Nonetheless we decided to explore alternative polymers, also to make sure that our encapsulation strategy was efficient for polymers other than EC.

Polymethylmethacrylate is a synthetic polymer, which find application in a plethora of technologies, from automotive, optics and buildings to biomedical applications, molecular separation and solar concentrators. It has a glass transition between 100 and 130°C, it is very resistant to aging and UV exposure, it has good thermal stability, very good optical properties and good compatibility with human tissue. In the field of microencapsulation, PMMA has been used to encapsulate phase-change materials or photochromic dyes[67].

To prepare PMMA encapsulated TBBS, we started from the developed protocol for EC simply substituting EC with PMMA. We prepared the organic phase dissolving PMMA and TBBS in DCM and, once dissolved, it is added dropwise to a PVA solution under mechanical stirring (1000 RPM). The emulsion forms readily, and once obtained, it is left stirring until all DCM evaporates.

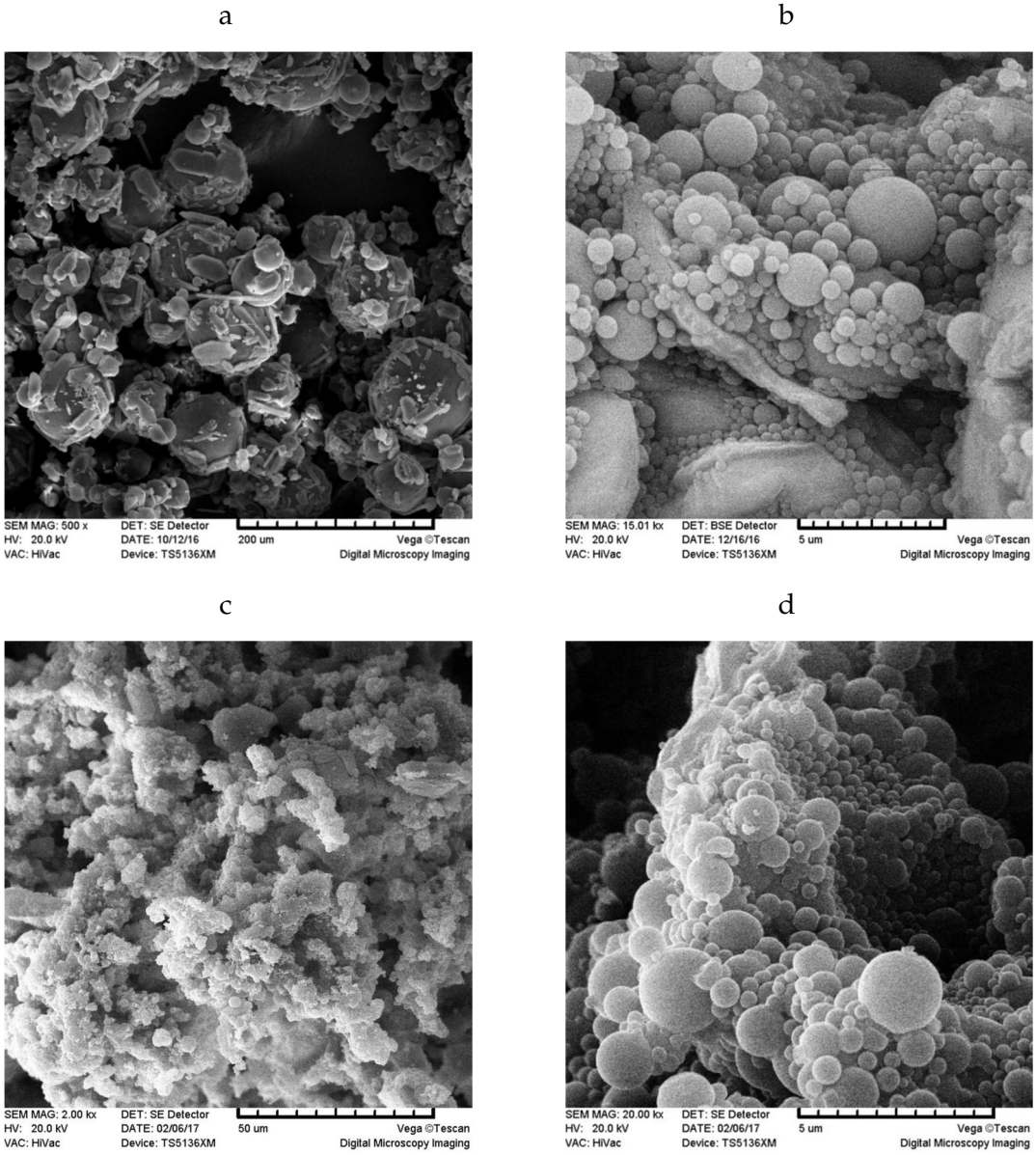

Figure 28 - SEM micrographs of: (a) PMTS01; (b) PMTS02; (c,d) PMTS03

A white, fine powder is obtained and it is collected on a paper funnel. The SEM images (figure 28a) shows the presence of some spherical particles along with some rod-like material. Moreover, the particle size is non-homogeneous.

While for EC encapsulation PVA is the mostly used surfactant, for the preparation of PMMA microcapsules along with PVA some other surfactant are used, like Triton X-100 and sodium dodecyl sulfate (SDS). We tried to modify our procedure using SDS (2,5% w/w) as surfactant instead of PVA. The emulsion is obtained through mechanical stirring at 2000 RPM. Instead of let the organic solvent evaporate from the emulsion, we evaporated it under reduced pressure. This procedure affords a very fine powder that cannot be filtered on a paper funnel, but must be harvested by centrifugation (4500 RPM for 30 minutes).

From the SEM images (figure 28b) we can see that the powder is composed by small spherical microsphere and some random aggregate.

We tested also a different solvent instead of DCM. The organic phase is prepared dissolving TBBS in ethyl acetate (AcOEt), then, when TBBS is completely dissolved, PMMA is added. PMMA dissolution in AcOEt takes more time if compared with DCM. The solution is left stirring for one night, then it is filtered through wool glass to remove eventually non dissolved material. The organic phase is then added dropwise to an aqueous SDS solution (1.6% w/w) and the two phases are mixed with a mechanical stirrer. Once emulsified, AcOEt is evaporated carefully at 40°C under reduced pressure. During the process lot of foam forms, so the evaporation phase must be done very carefully. When the majority of the organic solvent is evaporated, a white precipitate starts to deposit at the bottom of the flask.

The white solid is collected on paper funnel, dried in the oven and characterized. The powder is very fine and after the drying stage

agglomerates forming big white chunks. However, those chunks can be easily break with mortar and pestle.

The SEM images of this sample (figure 28c-d) shows that the powder is formed by small spherical particles, whose dimension spans from 2 μm to 500 nm. The particle surface looks smooth and without holes that may arise from evaporation. The TBBS loading determination can be done with Uv/Vis spectroscopy, as did with EC capsules.

3.5. Encapsulation of TBBS in polycarbonate

Polycarbonates (PCs) are a class of thermoplastic materials. One common precursor of polycarbonate is bisphenol A. PC is a durable material, with a high impact resistance, although with a low scratch resistance. It is widely used as coating for eyewear lenses and glasses. Its characteristics are quite similar to PMMA, but it holds better high temperatures; PC has a glass transition temperature of about 147°C and it flows at 155°C.

Polycarbonate has been used to encapsulate catalysts, phase-change material, drugs and dyes. The most common surfactant used is PVA. We tried to encapsulate TBBS in PC using the same protocol developed for EC encapsulation. The solvent choice is limited to DCM due to PC solubility. The two phases are emulsified using mechanical stirring. Once DCM is evaporated a whit suspension is obtained, but no precipitation is observed, probably due to the particle dimension. The suspension was centrifuged (30 minutes at 4500 RPM) obtaining a thick, white precipitate that is collected on a paper funnel and dried. Like for PMMA, after

drying the precipitate agglomerates, but it can be easily powdered with mortar and pestle.

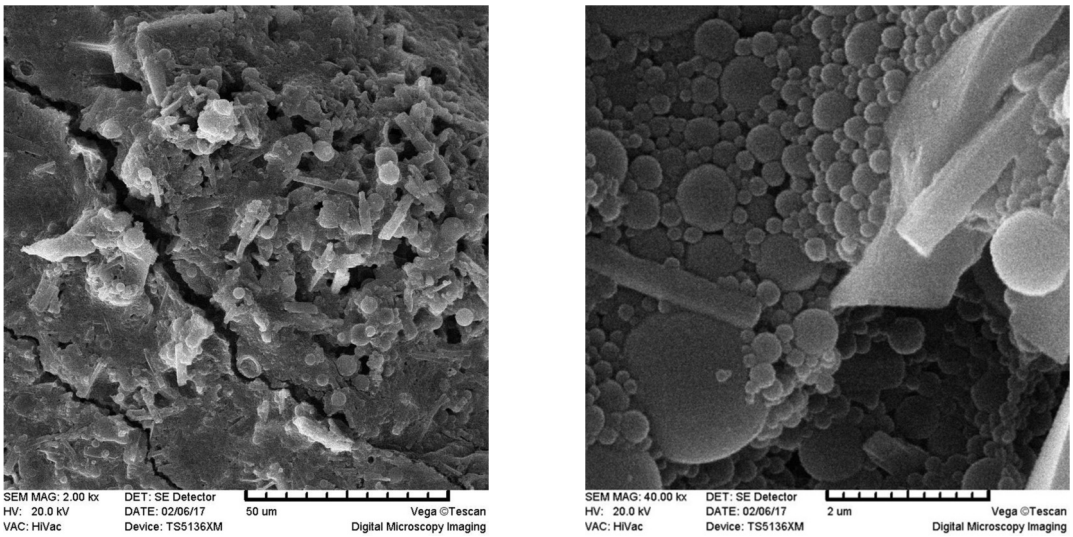

Figure 29 - SEM micrographs of PCTS01

SEM images (figure 29) show that the powder is composed of small spherical particles, very similar to the PMMA one. The particle dimension spans from 2 m to hundreds of nanometers. However, we can see that together with the microspheres there are some rod-like structures, which we cannot clearly identify.

Unlike EC and PMMA, the TBBS loading cannot be determined by means of Uv/Vis spectroscopy, because PC absorption spectrum overlaps with TBBS one. The only way to determine TBBS concentration, even if it is a rougher method, is NMR spectroscopy.

Both the capsules made using PMMA or PC as encapsulating agent were not tested in the vulcanization process. Those process were optimized in the last phase of the project.

3.6. Synthetic process for TBBS encapsulation in EC

General procedure:

The organic phase is prepared dissolving TBBS in DCM, then EC is added and the mixture is stirred – using magnetic stirring – until complete EC dissolution. In a second beaker, PVA is dissolved in water. The solution is mechanically stirred until all the PVA is completely dissolved.

The organic phase is slowly added to the aqueous phase. The stirring speed is set to 1000 RPM during the addition process. The addition is suspended when foam develops, and it is restarted when the foam level lowers. When the organic phase is completely added, the two phases are emulsified by mechanical stirring at 2000 RPM for 30 minutes, then the solution is left stirring at 500 RPM until total DCM evaporation. The obtained precipitate is isolated on a paper funnel and dried in the oven at 60°C. If necessary, the supernatant is centrifuged (4500 RPM for 30 minutes) to harvest the suspended material. The centrifuged material is taken up with the smallest amount of water, collected on a paper funnel and dried in the oven at 60°C.

TEC01

Organic Phase	
TBBS	15 g
EC	5 g
DCM	300 mL

Aqueous phase	
PVA	10 g
Deionized water	1 L

TBBS fraction = 68%

Encapsulation efficiency = 90.6%

TEC02

Organic Phase	
TBBS	10 g
EC	10 g
DCM	300 mL

Aqueous phase	
PVA	10 g
Deionized water	1 L

TBBS fraction = 45%

Encapsulation efficiency = 90%

TEC03

Organic Phase	
TBBS	12 g
EC	28 g
DCM	800 mL

Aqueous phase	
PVA	20 g
Deionized water	2 L

TBBS fraction = 29.7%

Encapsulation efficiency = 99%

TEC04

This sample is obtained following the same general procedure, but using magnetic stirring for all the mixing steps.

Organic Phase	
TBBS	10 g
EC	3 g
DCM	100 mL

Aqueous phase	
PVA	3 g
Deionized water	300 mL

TBBS fraction = 65%

Encapsulation efficiency = 86%

TEC05

This sample is obtained following the same general procedure, but using magnetic stirring for all the mixing steps.

Organic Phase	
TBBS	500 mg
EC	500 mg
DCM	15 mL

Aqueous phase	
PVA	500 mg
Deionized water	50 mL

TBBS fraction = 48.3%

Encapsulation efficiency = 96.6%

Synthetic process for TBBS encapsulation in polymethylmethacrylate

PMTS01

The sample is obtained following the same general procedure for EC, but using magnetic stirring for all the mixing steps.

Organic Phase	
TBBS	10 g
PMMA	25 g
DCM	250 mL

Aqueous phase	
SDS	10 g
Deionized water	1 L

PMTS02

Organic Phase	
TBBS	4 g
PMMA	4 g
AcOEt	150 mL

Aqueous phase	
SDS	4 g

Deionized water	250 L

The organic phase has been prepared following the same general procedure. Prior to be emulsified, the organic phase has been filtered through glass wool to filter off undissolved PMMA.

PMTS03

Organic Phase	
TBBS	4 g
PMMA	4 g
AcOEt	150 mL

Aqueous phase	
SDS	4 g
Deionized water	250 L

After emulsifying with mechanical stirring, the emulsion has been ultrasonicated for 3 minutes.

Synthetic process for TBBS encapsulation in polycarbonate

The sample is obtained following the same general procedure for EC

Organic Phase	
TBBS	8 g
PC	8 g
DCM	150 mL

Aqueous phase	
SDS	4 g
Deionized water	250 L

4. Crosslinking of EC capsules

As we have discussed in the previous chapter, the use of EC as the shell materials in the microcapsules was dictated by two reasons: it is a cheap material already employed in the tire industry and EC softening point is within the same range as the vulcanization temperature. Unfortunately, as it is shown by the thermal characterization and will also be clear form he vulcanization tests discussed later on in the thesis, the solubility of EC in molten TBBS brings about the collapse of the capsule at a temperature that is well below the target one.

It might be surprising at this point that we decide to use the simple TBBS/EC capsules in vulcanizations tests anyway, instead of using directly the crosslinked ones, discussed in detail in the present paragraph. As it will be soon clear, the task of crosslinking our capsules was not an easy one. It took us the best part of two years to figure out a viable solution, during which time we started to test all available materials doing our best to tune the vulcanization conditions in order to see a confinement effect even with capsules not fulfilling the original requirements. This issue will be discussed in more deails in the following chapter.

The idea of crosslinking EC is based on the fact that the particular materials we had been using has an ethoxyl grade of 49%, meaning that the remaining hydroxyl groups can be further functionalized (figure 30). The main issue we had to resolve on doing this was merely practical: all

crosslinking agents that can be used in solution are soluble in the same solvents where EC is soluble as well. We thus had no way of using solution processing methods to crosslink capsules after their assembly, without completely ruining their supramolecular arrangement. Crosslinking in water, the only solvent where EC is insoluble, was also problematic due to the lack of suitable chemicals. The only other approaches for ex-post crosslinking were a vapor phase process, which we tested under several different configuration, the inclusion of a crosslinking agent during the microencapsulation process and the pre-functionalization of the cellulose with a cross-linker.

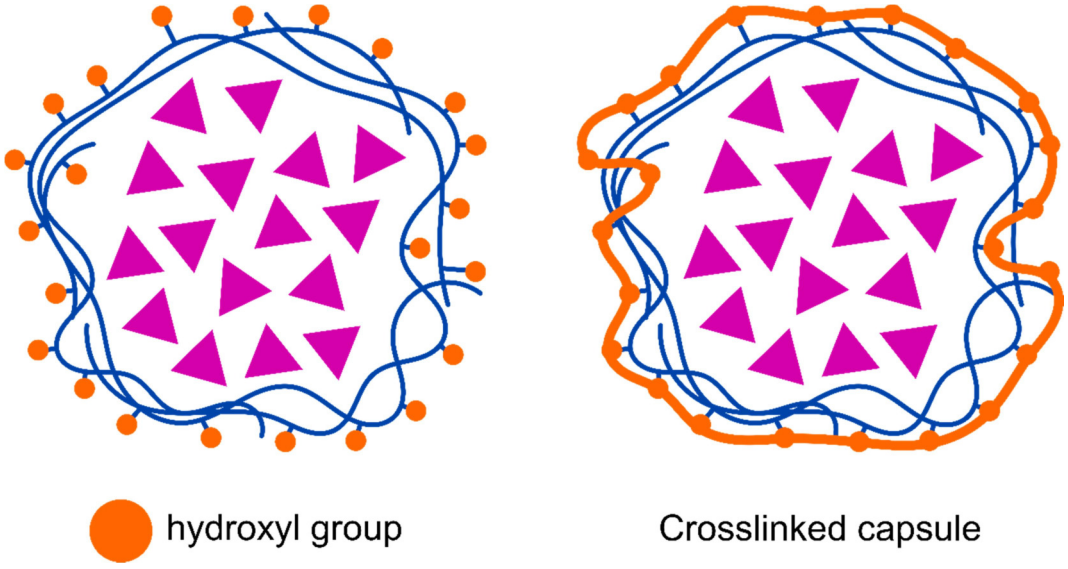

Figure 30 - Scheme of the crosslinking of ethylcellulose non-ethoxylated hydroxyl groups

4.1. Epoxy crosslinking

Epoxy-based glue are an extremely diffuse material[68]. Their working mechanism is based on the crosslinking reaction between a pre-polymer containing epoxy moieties, and a second component called hardener, which include polyfunctional amines, acids, anhydrides, phenols, alcohols and thiols. Like for vulcanized rubber, once crosslinked those polymers change dramatically their properties, gaining high mechanical modulus, chemical and temperature resistance. Epoxy are used in a wide range of application, including metal coatings, electronics, electrical insulators, adhesives and reinforcement. The most common and reactive hardeners are amino- and anhydride-based, but, as said before, epoxy can react with alcohols, so it would be possible to crosslink EC by reacting the hydroxyl groups of EC with bifunctional epoxides. We chose to use two different epoxides (figure 31), bisphenol A diglycidyl ether (DER 332) and trimethylolpropane triglycidyl ether (TMPG). Both of them are well known and easily available components of commercial epoxy formulations.

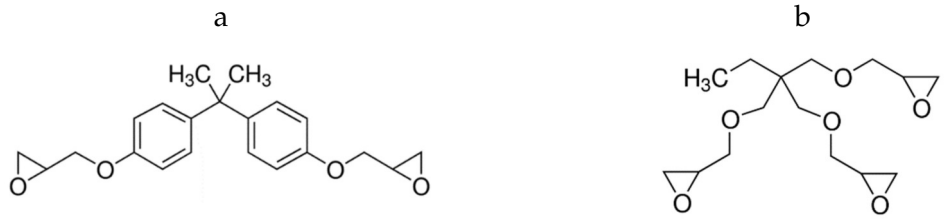

Figure 31 - Structure of (a) bisphenol A diglycidyl ether (DER) and (b) trimethylolpropane triglycidyl ether (TMPG)

We started adding DER to our optimized process dissolving it into the organic phase (DER-TEC-01). The amount of DER added is stoichiometric with respect to the free hydroxyl groups of EC.

The number of free hydroxyl groups can be estimated looking at the cellulose structure; approximating the substitution degree to 50%, the cellulosic chain can be viewed as the repetition of a monomer consisting of two D-glucose unit, with one unit fully ethoxylated. The calculation of the amount of crosslinking agent are based on this assumption.

What we expect here is to enclose the epoxy inside the EC shell, in order to perform the crosslinking reaction during the drying phase.

No remarkable changes were observed during the synthetic process. After the drying phase, the portion of powder which was in contact with the paper funnel actually adhered with it. We interpreted this as consequence of the epoxy presence, confirming its reactivity. However, the SEM images shows a very messy composition of the powder. The majority of the powder is composed by scale-like structures mixed with deformed spheroidal particles. We tried to prepare a new batch lowering DER concentration, using a DER/EC ratio of 1:10. In the SEM images, we see that instead of having many small scales, we have big aggregates with irregular shape (figure 32).

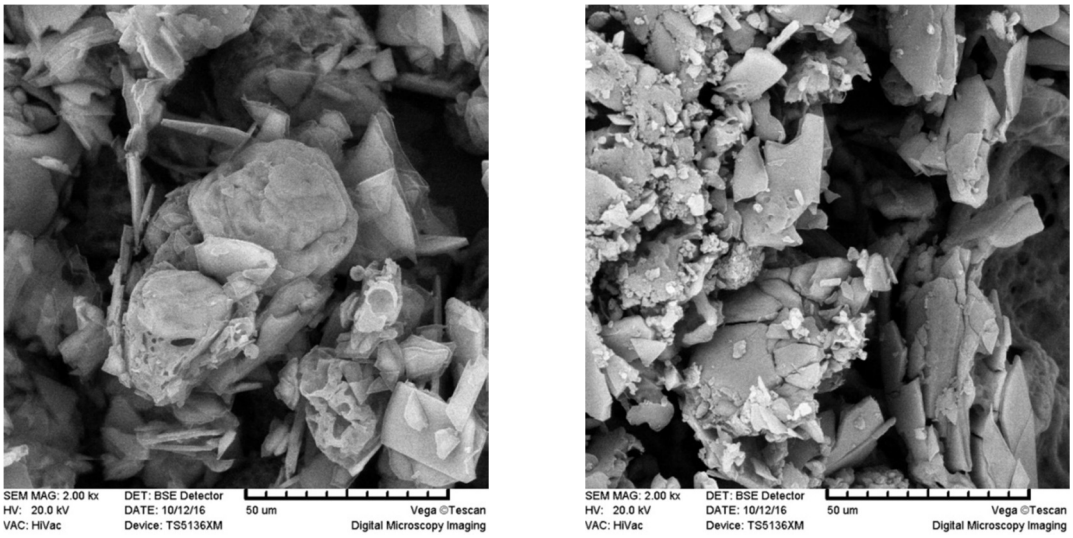

Figure 32 - SEM micrograph of DER-TEC-01 (left) and DER-TEC-02 (right)

The obvious limit of this method is that instead of having one single molecular material constituting the cargo and one single polymeric materials constituting the shell (or matrix), we now have two molecular materials. One of them is also reactive, which is against the standard guidelines of formulation chemistry. Likewise, DER is co-localizing with TBBS in crystalline aggregates, eventually evolving in the irregular plaques evidenced by the SEM images. Also, it cannot be ruled out that PVA is reacting with DER during encapsulation, thus completely changing the nature of the emulsion.

We tested several other stoichiometric ratios, as well as TMPG instead of DER as the epoxide yet to no avail. A literature search was not supportive on this side: the MESE method was not reported as being compatible with a crosslinking approach[69].

The breakthrough that showed us a way out of such stalemate came serendipitously. As it is mentioned in the previous chapter, when assembling the capsules according to the standard protocol, the solutions of TBBS and EC is added slowly to the vigorously stirring solution of PVA in water. The process on a large scale is so slow that it takes hours.

When testing strategies to incorporate TMPG into the capsules, we prepared a solution of EC, 10 % by weight TMPG with respect to EC and TBBS and we decided to carry out the dropwise addition slowly overnight. Unexpectedly, the viscosity of the organic solution increased considerable during the addition to the point that only a small portion of the same had been added to the water solution in 8 h. Puzzled, we checked the composition of the organic solution by IR and we found out that the epoxyde had already partially reacted with the EC, bringing about partial crosslinking. This effect was the cause of the steep increase in the viscosity.

We thus prepared a fresh organic phase using a TMPG concentration of 10% w/w with respect to EC concentration and we aged it for 48 h, observing the same increase in the viscosity. We thus added the TBBS and proceeded according to the standard protocol with the only difference that stirring was performed with an Ultra Turrax® dispersing tool, also due to the extremely high viscosity of the organic phase (figure 33).

The addition must be stopped multiple times because if the formation of sticky aggregates that cannot be immediately dispersed.

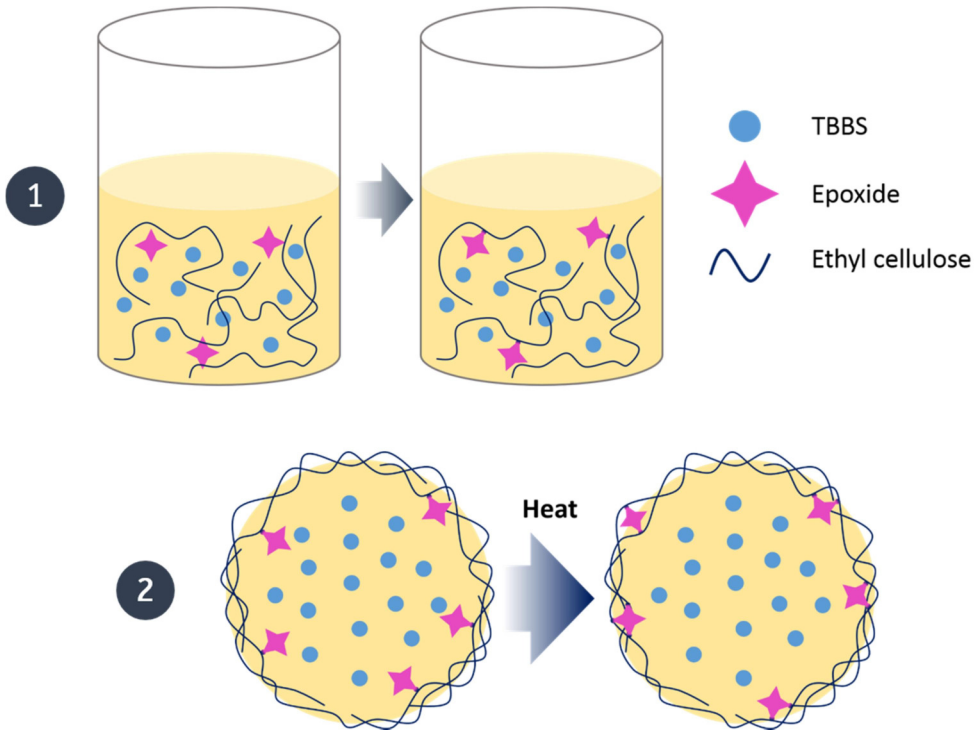

Figure 33 - Scheme of the epoxy-crosslinking of EC: (1) prefunctionalization of EC in solution; (2) post-encapsulation thermal crosslinking

In this case, the speed was increased until no sign of aggregates was visible, and the addition was started again. No foam develops during the whole addition process. When all the organic phase has been mixed, homogenization is prolonged for further ten minutes, then the milky emulsion is left stirring magnetically until solvent evaporation. When DCM (but the process is also fully compatible with AcOEt) is evaporated, a fine powder precipitates at the bottom of the flask, but the supernatant retains a milky look, hint of the presence of dispersed capsules. The supernatant is separated from the white precipitate; the precipitate is taken up with the smallest amount of water and filtered on a paper funnel. When redispersed in water, the precipitate behaves like a non-

newtonian fluid (like corn starch aqueous dispersion), and it takes a long time for water to separate out from the dispersion.

The supernatant is centrifuged (4500 RPM for 30 minutes), harvesting one third of the final mass. Even after the centrifugation process, the supernatant maintains a white color, meaning that still some material is well dispersed. We tested this process two times, increasing the scale up to almost ten times the amounts of reagents used in TMPG-TEC-01. We also substituted DCM with AcOEt, in order to test the efficiency of the method with an industrial-friendly solvent. It is worth to notice that the preparation of TMPG-TEC-03 afforded almost 300 g of product.

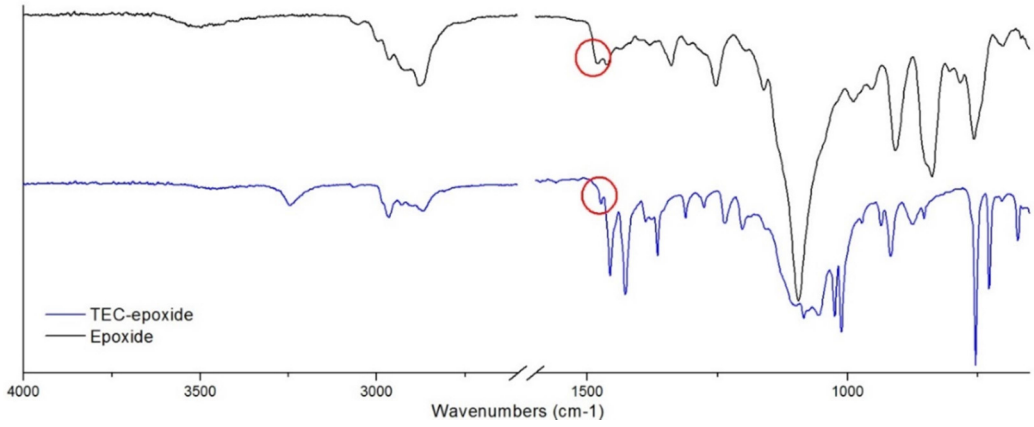

Figure 34 - IR spectra of TMPG (black line) and TMPG-TEC (blue line). The circled band is the chosen one to follow the crosslinking process

The IR spectrum of the capsules (figure 34) shows the presence of the three components. In particular, we identified a band located at 1474 cm^{-1} that is relative to the epoxide structure, and that can be easily identified

in the TBBS-EC-blend. The two fractions isolated – the precipitated and the centrifuged one – show different EC/TBBS ratio; in particular, the centrifuged solid is richer in EC. We can suppose that, since EC positions at the droplet interface, the smaller the droplets are and the more concentrate will be EC. The presence of the 1474 cm^{-1} stretching means that not all the epoxide residues have reacted while in solution, thus leaving room for a further cross linking to be carried out after the isolation of the capsules. The breakthrough of this method consists on the fact that the crosslinking agent acquired the characteristics of the polymeric materials, thus being localized within the same compartment of the capsules. Even if the quality and homogeneity of the functionalized epoxy containing capsules (Figure 35 shows the SEM micrographs) is not as good as that of the parent preparations carried out without epoxyde, the difference between these samples and those shown in Figure 32 is quite strong; even if aggregated, the particles retain a spherical shape. It is also worthwhile nothing that this is the first example of cross linkable microcapsules produced with the MESE method.

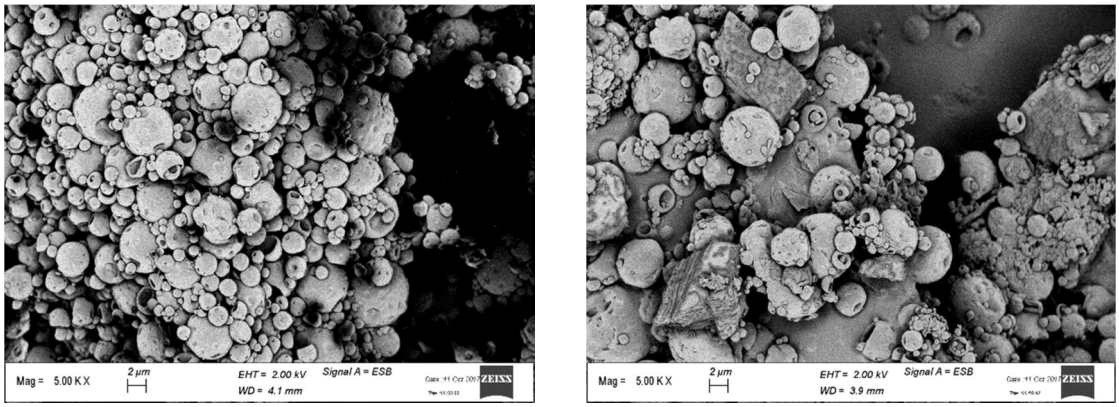

Figure 35 - SEM micrographs of the centrifuged sample (left) and of the precipitate (right).

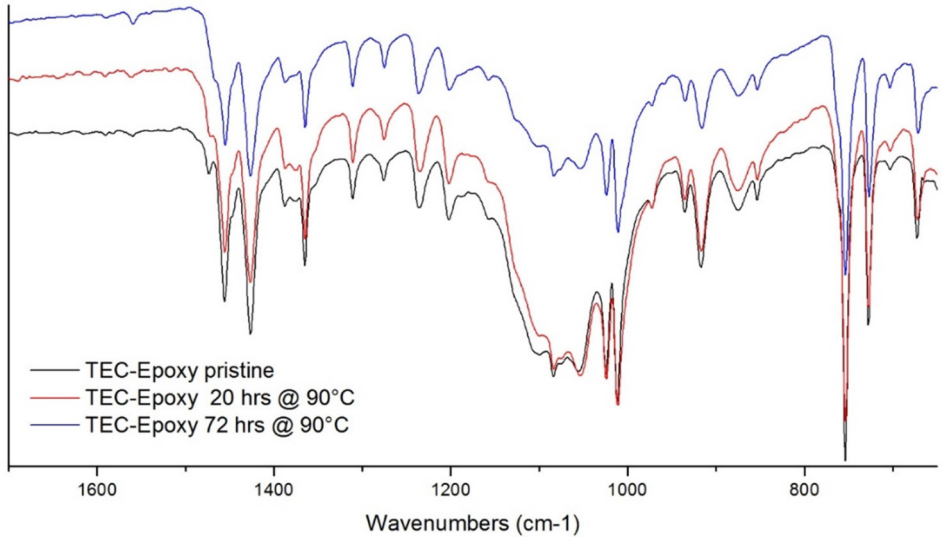

Figure 36 - Time evolution of TMPG-TEC at 90°C; t = 0 (black line); 20 hours (red line); 72 hours (blue line).

The SEM images (figure 35) shows also that the two fractions look slightly different. In the precipitate sample the capsules are less homogeneous and some aggregates are present, while in the centrifuged sample the particles appear more defined. It is noticeable that the particle

dimension are less than 5 μm in both the samples, confirming that it is possible to reduce the particles size even on a large scale. It is worth to notice that we produced 300 g of particles, and with our equipment, a precise control over morphology, aggregation and size dispersion is unlikely to be achievable.

The crosslinking process consists of a thermal treatment after that the particles have been dried. We tested the process both at 90°C and 120°C to see how TBBS melting can influence the outcome of the crosslinking process and the behavior of the crosslinked capsules in the blend. The process can be followed with the IR spectroscopy (figure 36) because the epoxy band at 1474 cm-1 decrease in intensity meanwhile the crosslink reaction goes on. After 72 hours at 90°C the band disappears, and we concluded that the crosslink process is finished.

Before the crosslinking process, the material looks like a powder; after the crosslinking process, a terrific coarsening happened, converting the powder in a dense block, hard to break even with mortar and pestle. One major issue is clearly to find a proper way to perform the thermal treatment keeping the particles enough separated not to aggregate during the process. We tried to do the thermal process distributing the powder on aluminum foils; this prevented the formation of a big hard chunk, but still the powder underwent a certain amount of coarsening, as witnessed by the SEM images (figure 37). With this procedure, the thermal treatment at 120°C is extremely inefficient; the capsules collapse and form an amorphous agglomerate that, eventually, crosslinks in a thick, dense film on aluminum foil.

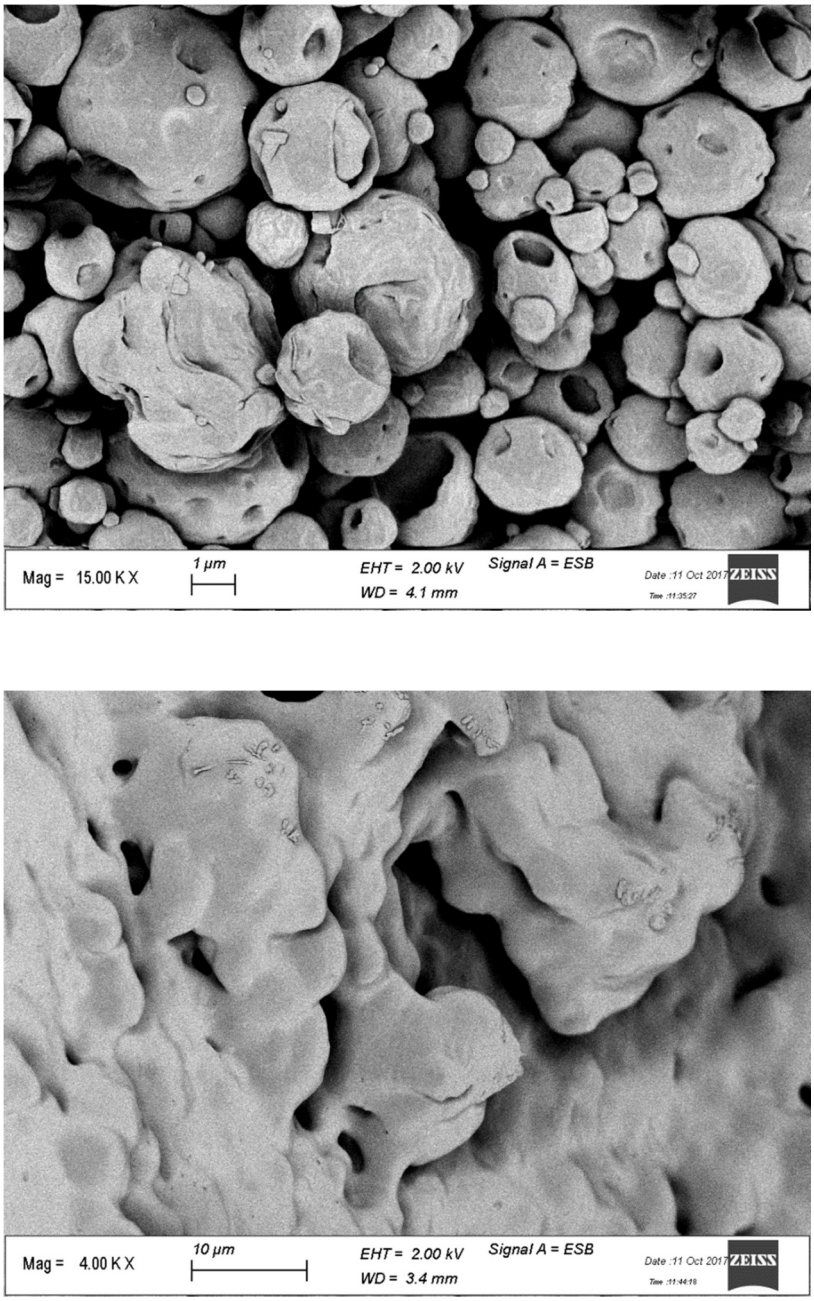

Figure 37 - SEM micrographs of TMPG-TEC before (top) and after the thermal treatment (90°C)

We were struggling to find an oven – or a similar piece of equipment – that could simultaneously heat and keep the powder in motion. Then, we realized that a simpler solution could be used: we suspended the capsules in water using mechanical stirring, and then we heated up the

dispersion to 90°C. A Vertex® temperature controller keeps the temperature constant. The suspension is stirred for 5 hours, and during this time, some extra water is added to compensate the water loss due to evaporation.

After 5 hours, the epoxy band disappears completely. The powder is then collected on a paper funnel and dried at room temperature. Potentially, this process can be done on the raw powder right after the organic solvent evaporation phase, making the whole synthetic process a one-pot procedure. Macroscopically, a small degree of coarsening happened, but this process is the one that gave the best result in terms of agglomeration. Moreover, the powder can be refined with mortar and pestle.

We tried two different heating set-up, using an oil bath as a heating medium or using directly the heating plate. Of course, an oil bath is better in terms of heat distribution, but from a practical point of view it is very hard to find a suitable oil bath for very large beakers. This process allows us also to wash any PVA residue on the particle surface.

The SEM images (figure 38) of the capsules crosslinked with this method show that the conglomeration degree of the capsules after the thermal treatment is way lower if compared to the oven treatment. Keeping the particles stirred in a homogeneous medium is an efficient way to prevent a strong particle aggregation. However, the morphology of the particles of the small batch is very different if compared with the particles of the big batch. This problem may arise from the heat source that was used: the small batch was heated using an oil bath, while due to the big dimension of the second batch, we used directly the heating plate.

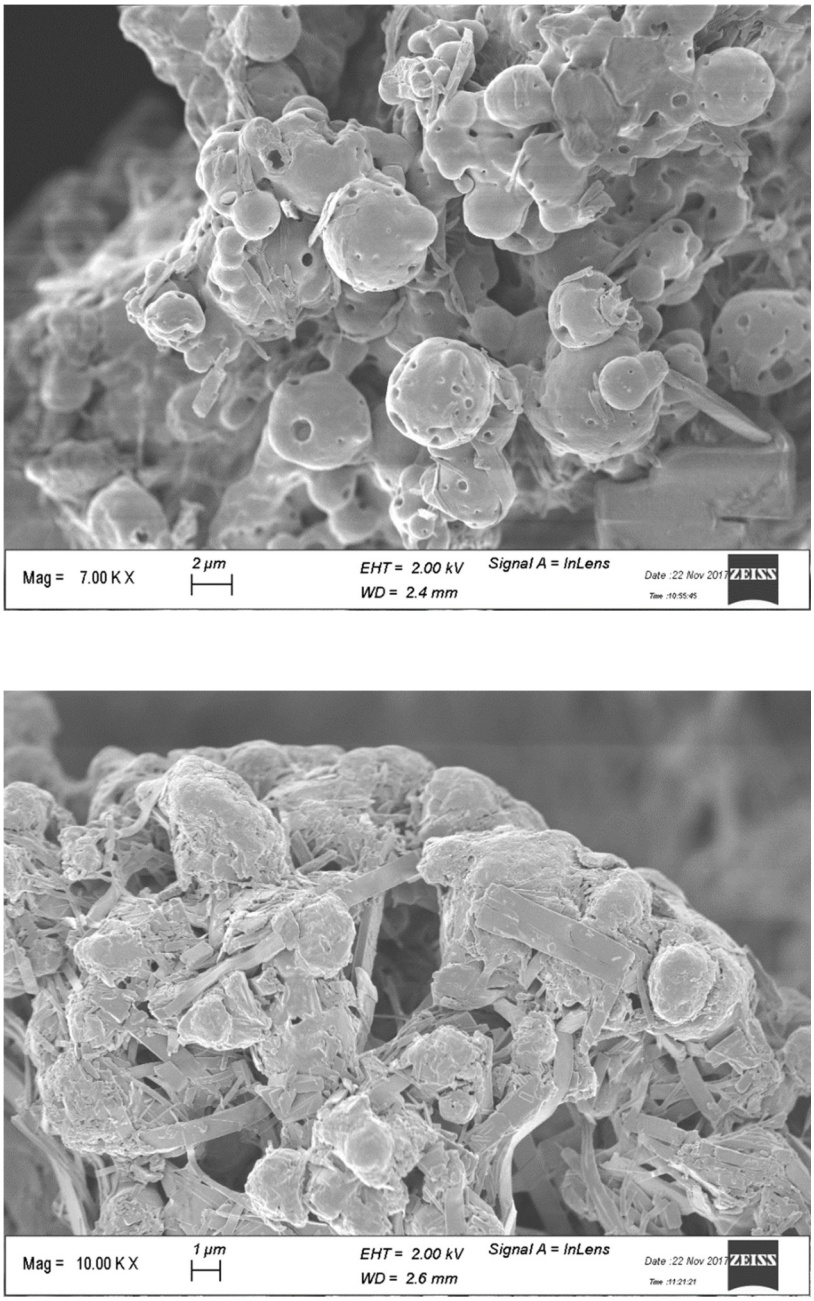

Figure 38 - SEM micrographs of TMPG-TEC crosslinked in water suspension with (top) and without the aid of an oil bath (bottom)

In this way, the bottom of the flask is directly in contact with the heat source. The temperature controller keeps the suspension at a constant temperature, but in practice, the plate can reach temperatures much

higher than the set temperature. The part of the suspension directly in contact with the plate may be exposed to higher temperatures with respect of the rest of the suspension, even if the mixture is stirred.
Some rod-like and strip-like structures can be seen in the latter sample; those structure may be composed by leaked TBBS. This gives an idea of how delicate is the system that we are dealing with.

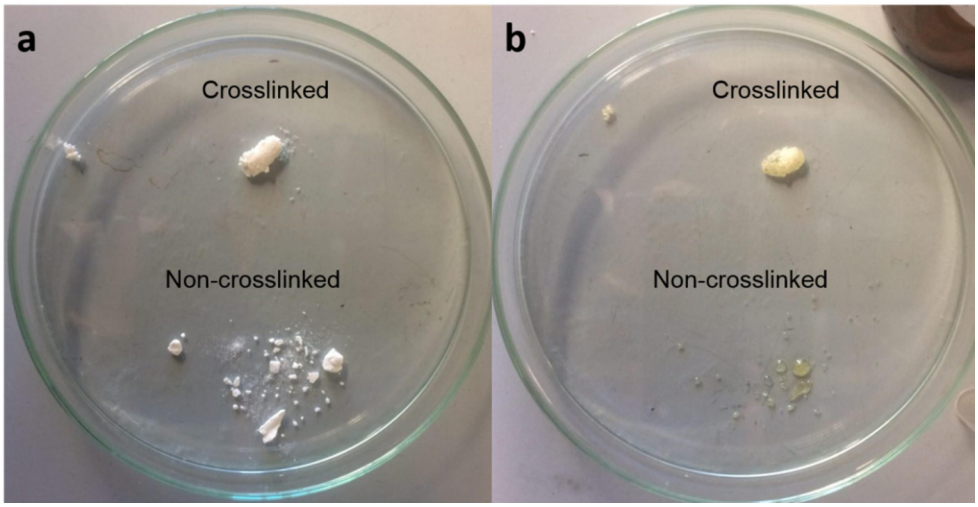

Figure 39 - Samples of crosslinked and non-crosslinked capsules before (a) and after (b) a thermal treatment of 24 hours at 120°C

Once crosslinked, the thermal stability of the capsules changes dramatically. In figure 39 is shown a sample of non-crosslinked powder and a crosslinked one before and after a thermal treatment at 120°C for two hours. While the non-crosslinked sample collapse after TBBS melting, the crosslinked sample maintain its shape and does not collapse. The melting process of the capsules, which can be followed with a simple

melting point apparatus, gives a significative indication about the capsules thermal stability[‡].

Figure 40 shows the melting grade evolution of the crosslinked capsules sample compared with non-crosslinked capsules and pristine TBBS. The graph clearly show that, when the capsule is crosslinked, no collapse is observed until 140°, while the non crosslinked capsules immediately collapse when TBBS melts.

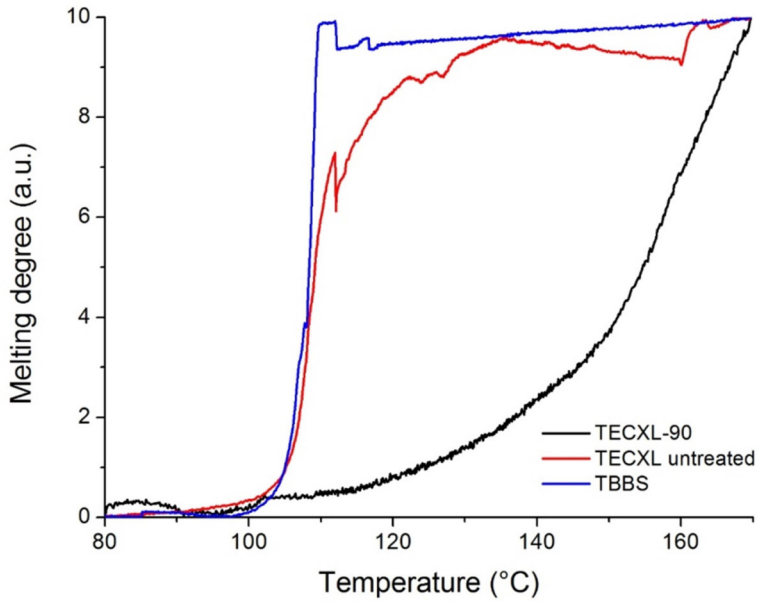

Figure 40 - Melting grade of epoxy-crosslinked capsules at 90°C (TECXL-90, black line), non-crosslinked capsules (TECXL untreated, red line) and pristine TBBS (blue line).

[‡] The instrument operative manual is not specifying at all how the melting grade is determined. However, it is most likely related to light transmission through the sample. As showed in figure 39, when the non crosslinked capsules collapse, the sample looks like a very viscous liquid. Therefore, we associated the evolution of the melting grade of the sample to the structural stability of the capsules.

To conclude, it is worth to underline that this is the first example of an original method of epoxy pre-functionalization of EC and its subsequent crosslink process. Moreover, is a very simple method, since the components are just mixed together, without involving any kind of catalysis or purification protocol, and potentially allows a one-pot procedure.

4.2. Silane crosslinking

One possible way to crosslink hydroxyl moieties is the reaction with alchoxysilanes. Alcoxysilanes are widely used in the sol-gel process (summarized in figure 41), one of the most important wet-chemistry method for material synthesis[70,71]. Briefly, it involves the hydrolysis and condensation of – in the most general case – metal alcoxides, obtaining a colloidal solution that, in a second step, evolve towards a gel-like bicontinuous structure.

Alcoxides are replaced by the formation in the first instances of hydroxyl moieties, then, the hydroxyls form oxo bridges between the metal centers. Acid or basic catalysis is needed to start the hydrolysis-condensation reactions. In addition, pH act as a driving force towards the formation of linear chains (acid catalysis) or branched structures (basic catalysis)[72]. We want, therefore, to form a silica shell by the reaction of the free hydroxyl groups with organosilicon precursors.

In tire technology, silica is widely used as filler. One issue that people dealt with is the aggregation of silica nanoparticles and how to maximize

the rubber-filler interaction. A solution that actually is used is the addition of some bifunctional polysulfide-bridged silanes.

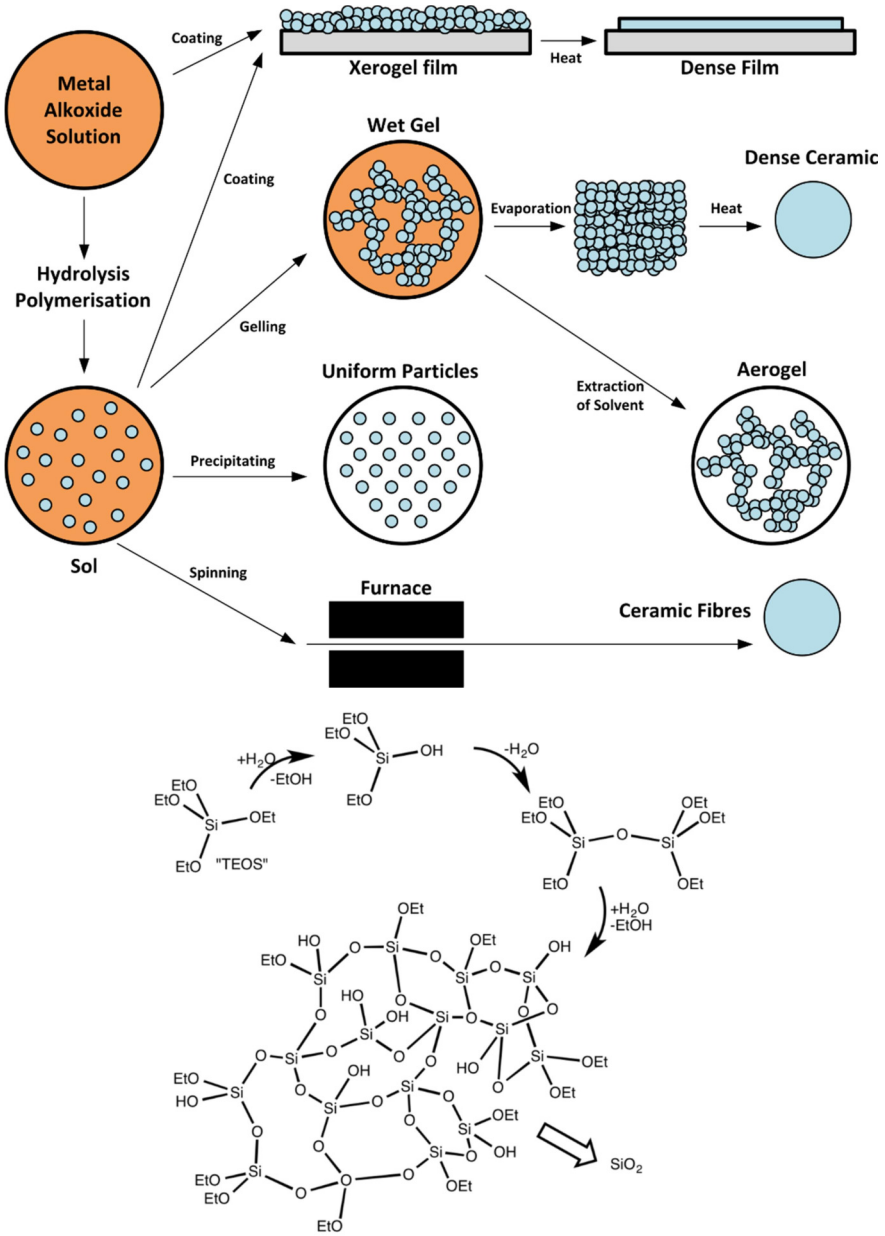

Figure 41 - Schematic representation of the sol-gel process (top) and simplified structure of the hydrolysis-condensation reaction of TEOS (bottom)

Those molecules are able to form covalent bond with the nanoparticle surface and their organic bridge allows them to have a better interaction with rubber. Both of the solution will be interesting for our purpose, since making the capsules more rubber-friendly would be of great interest.

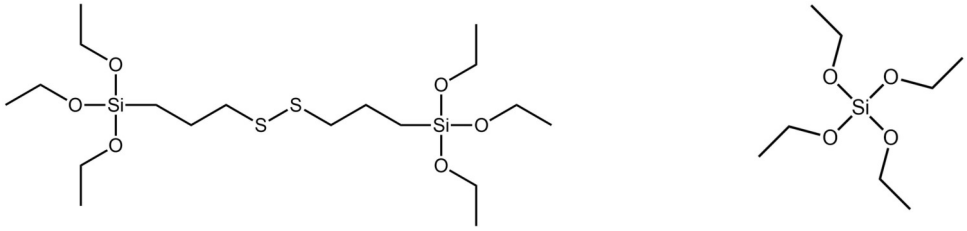

Figure 42 - Molecular structure of bis(3-triethoxysilylpropyl)disulfide (TESPD, left) and tetraethyl ortosilicate (TEOS, right)

We started modifying our standard synthetic procedure by adding a disulfide-bridged silane (TESPD, figure 42 left) into the organic phase in order to incorporate it directly inside the capsules. For the first test, we introduced an amount of TESPD stoichiometric to the number of estimated free hydroxyl. After the drying phase, we obtained an extremely sticky material; most likely, we obtained a gelation of the whole silane that embedded the rest of the material. Despite the macroscopic rubbery appearance, the SEM micrographs reveal that the sample is composed by sintered spheroidal structures, most likely capsules embedded in a polysiloxane matrix (figure 43).

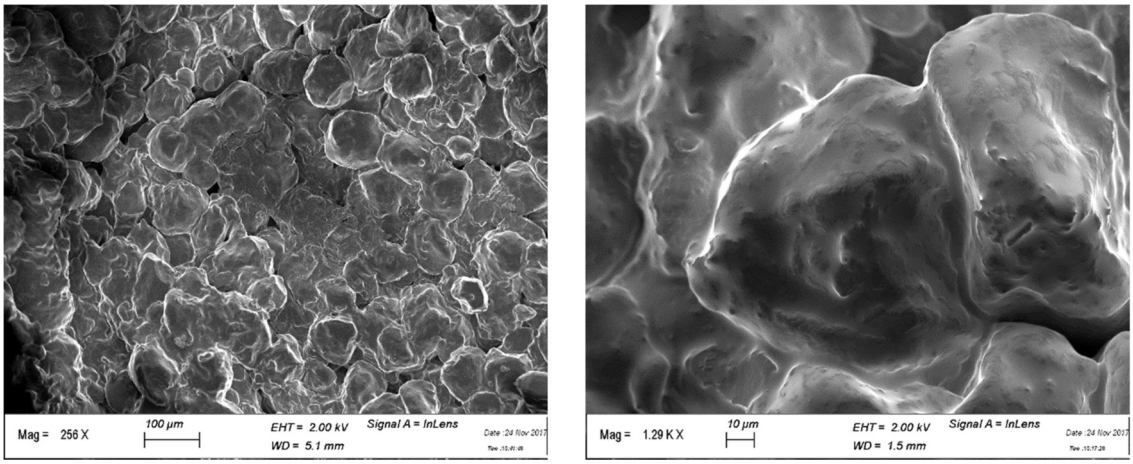

Figure 43 - SEM micrograph of TESPD-TEC

We then tried to do a post-functionalization of the capsules (1 g of TEC01) dispersing them with TESPD (1 mL – TESPD-TEC-1 – and 0.3 mL – TESPD-TEC-2) in a hydroalcoholic medium (ethanol/water = 1 : 4). From the IR spectra, however, is hard to tell if the surface crosslinking took place (figure 44).

We tried also to use an extremely common silica precursor, TEOS (figure 42 right). Since we cannot use water, we tried to suspend the capsules in heptane, which is not supposed to dissolve EC. To be sure to protect the core from leaking, we used capsules with an EC/TBBS ratio of 1/1 (TEC02). The capsules can be easily suspended in heptane, then TEOS is added to the suspension. After being stirred for 24 hours, the capsules are collected on a paper funnel and dried.

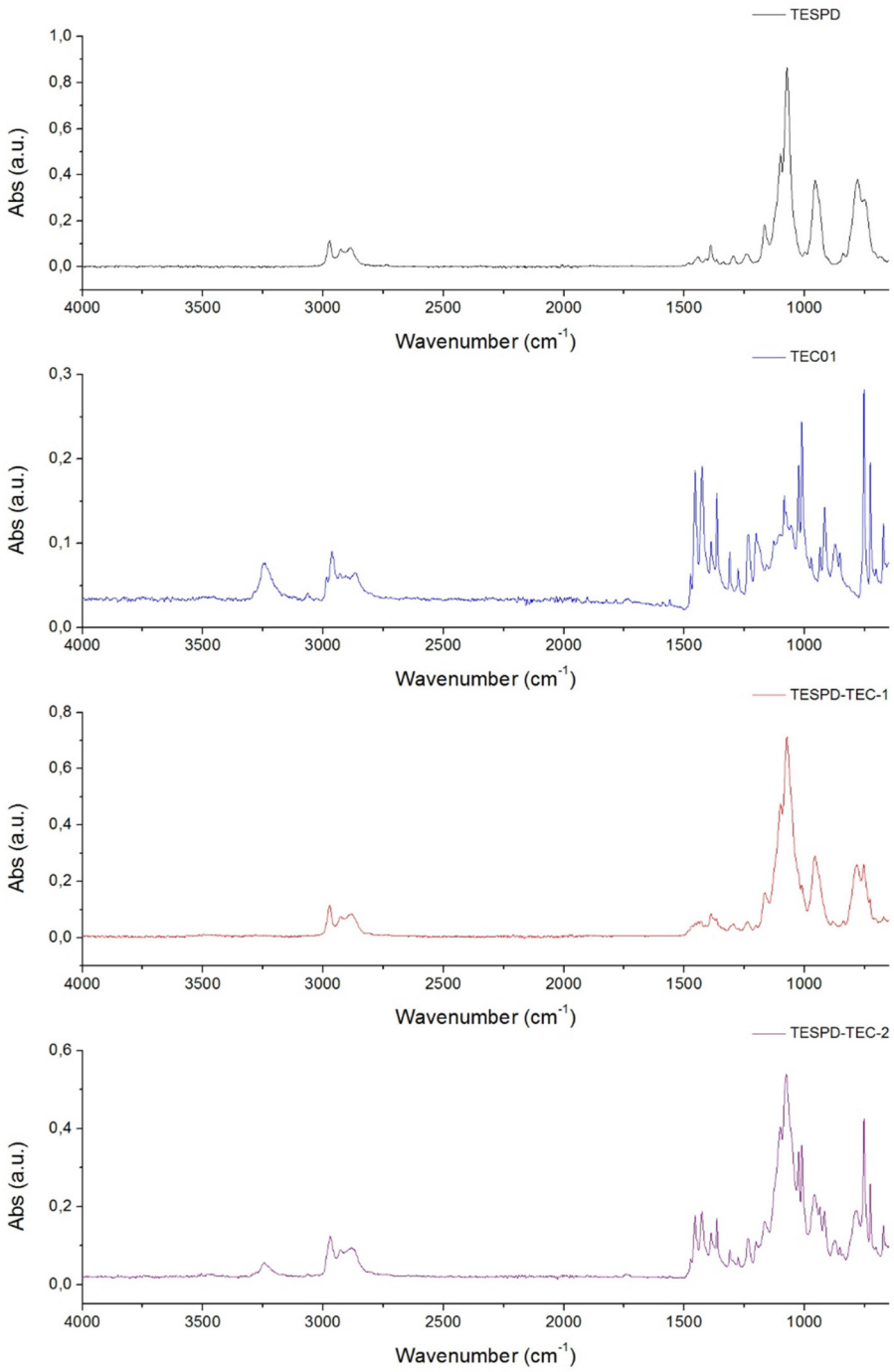

Figure 44 - IR spectra of: TESPD (black line), TEC01 (blue line), TESPD-TEC-01 (red line) and TESPD-TEC-2 (purple line)

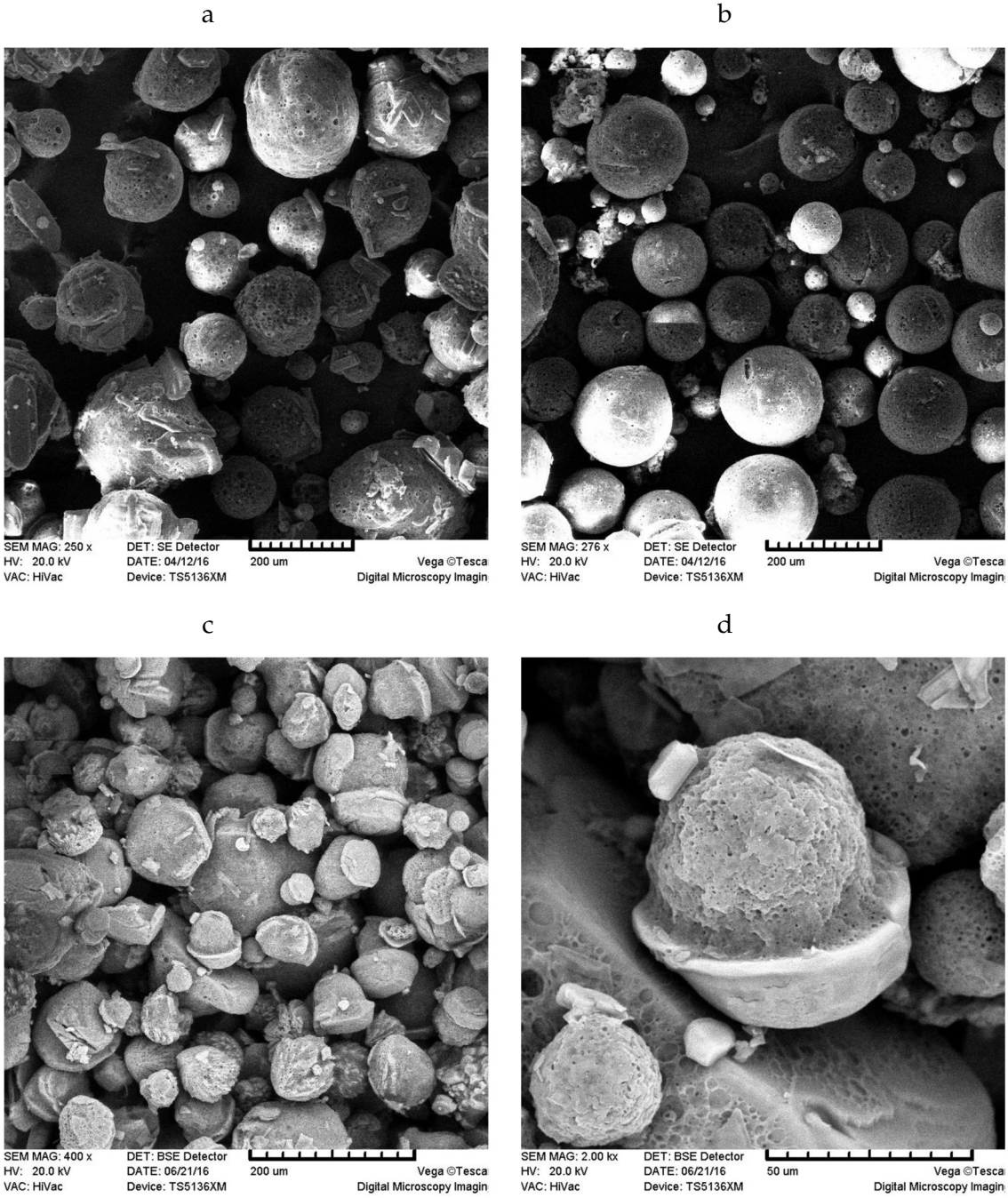

Figure 45 - SEM micrographs of: (a) pristine TEC02; (b) TEC02 reacted with TEOS in heptane; (c) TEC02 reacted with TEOS in heptane and ammonia

The SEM images shows that the surface of the capsules looks slightly smoother, but it is the only difference that can be perceived between the two samples. We tried to add a small amount of ammonia to heptane to catalyze TEOS condensation (even if aqueous ammonia is not soluble in heptane). What we noticed from the SEM images is that some capsules have a second dense layer on their surface; however, this layer only covers a portion of the capsule (figure 45). We concluded that this method is totally inefficient for a post-functionalization of the capsules.

We tried to use volatile silane precursor to functionalize our capsules with a vapor-phase method. Cellulose fibers can be functionalized with chlorosilanes simply exposing them to their vapors in a sealed flask. Vapors of the silane precursor fill the flask and react with the hydroxyl group. This method has been used to realize hydrophobic tissues and fibers[73]. At first we tried to build a small system like the one showed in figure 46.

- The powder is put inside a flask equipped with a stirring bar;
- The chlorosilane is put in another flask, immersed in an oil bath on a heating plate;
- The flasks are connected using rubber pipes. Argon is used as carrier;
- A drechsel bottle filled with a NaOH solution is connected at the end of the chain to purge the flow from unreacted silane and from byprodutcs (mainly HCl).

To contain the powder and to keep it in motion, we designed a plastic box with proper connection that could be placed over a vibrating plate to mime the effect of a fluidized bed. However, the box had some serious

leaks due to the absence of a proper sealing, so we replaced that element with a round bottomed flask. Actually, the vibrating plate provides an efficient mixing of the powder even if it is placed in the flask (figure 46).

Figure 46 - Working scheme for vapor-phase silanization of TEC02: (1) silane supply; (2) reaction chamber; (3) purging flask

We observed a color change of the powder from white to yellow while the reaction proceeded. We checked the IR spectrum of the powder and we found that the spectrum is different from the original spectrum. We realized that this degradation of the powder is due to the development of HCl as byproduct, which can react with TBBS. We then stopped any further experiment in this direction.

4.3. Synthethic attempt for epoxy-crosslinked TEC

DER-TEC-01

Organic Phase	
TBBS	30 g
EC	10 g
DER 332	10 g
DCM	600 mL

Aqueous phase	
PVA	20 g
Deionized water	2 L

The encapsulation was performed following the general encapsulation procedure.

DER-TEC-02

Organic Phase	
TBBS	30 g
EC	10 g
DER 332	1 g
DCM	600 mL

Aqueous phase	
PVA	20 g
Deionized water	2 L

The encapsulation was performed following the general encapsulation procedure.

TMPG-TEC-01

Organic Phase	
TBBS	20 g
EC	20 g
TMPG	2 g
DCM	400 mL

Aqueous phase	
PVA	10 g
Deionized water	1 L

The organic phase is aged for 48 hours. The solution viscosity enhances. The organic phase is dropped slowly into the aqueous phase. The mixture is emulsified using a Ultra Turrax dispersing apparatus. The mixing speed is increased from 10000 to 16000 RPM during the addition of the organic phase to maximize the dispersion. Once the organic phase is completely added, the mixing speed is set to 20000 for 10 minutes, then

the emulsion is stirred mechanically until total evaporation of the organic solvent. When the solvent is evaporated, the suspension is allow to decant at the bottom of the flask. The supernatant is discarded and the white solid is collected on a paper funnel and dried in the oven at 50°C.

TMPG-TEC-02

Organic Phase	
TBBS	90 g
EC	90 g
TMPG	9 g
AcOEt	1.4 L

Aqueous phase	
PVA	18 g
Deionized water	1.8 L

The sample is prepared the procedure used for the previous sample. Due to the stirring volume range of the dispersing apparatus, the two phases were mixed in two different batches of 1.5 L each (in total).

TMPG-TEC-03

Organic Phase	
TBBS	160 g

EC	160 g
TMPG	16 g
AcOEt	2.5 L

Aqueous phase	
PVA	36 g
Deionized water	3.6 L

The sample is prepared the procedure used for the previous sample. Due to the stirring volume range of the dispersing apparatus, the two phases were mixed in two different batches of 1.5 L each (in total).

5. Test of capsules in polymer blends

In the previous chapters, we have shown how to produce and characterize EC based capsules loaded with TBBS. We also discussed how those capsules can be produced using PMMA or PC as shell materials. We gave evidences that the melting of the TBBS core causes the capsule collapse and that this can be avoided by increasing the capsule rigidity by means of crosslinking. After different tests with silane precursor and epoxides, we found that tetramethylolpropane triglicidyl ether is the crosslinking agent that allow us to produce thermally stable capsules. In this chapter will be presented the effects of the capsules (both non-crosslinked and crosslinked) on the vulcanization kinetics of polymer blends. Obviously, the results are not presented in chronological order, some of the vulcanization experiments were performed long before the full characterization of capsules (crosslinked and not) was available.

5.1. Blend preparation

The material chosen for the rubber blend are butadiene rubber (BR) and a copolymer styrene-butadiene rubber (SBR) in a ratio BR/SBR 3/7.
Diphenylguanidine is added as a secondary accelerator; zinc octanoate is the zinc oxide precursor. We chose not to add any filler to have an ideal blend in which all the attention can be focused on the accelerator's effect. Figure 47 summarized the ingredients listed previously.

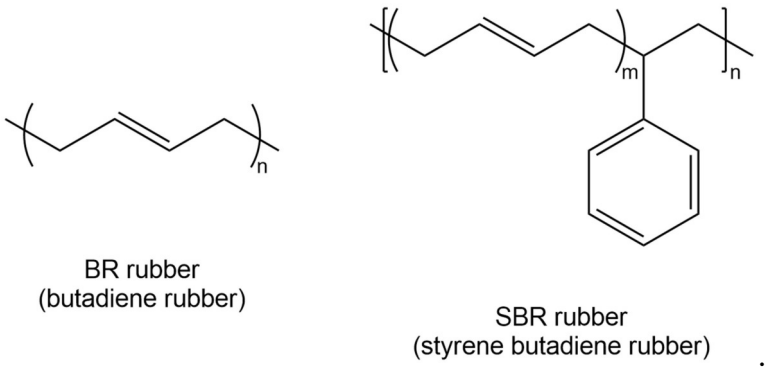

Curative name	Role
TBBS	Primary accelerator
DPG	Secondary accelerator
Sulfur	Curing agent
Zinc octanoate (zinc octoate)	Vulcanization activator

Figure 47 - Molecular structure of the polymers used in the rubber blends (top) and table of the components of the cure package (bottom)

The components of the blend are mixed together in a Haake type mixer, equipped with an hourglass-shaped chamber equipped with two blades rotating in the opposite direction. This process is called mastication. After the mastication process, the composite is processed through a two-roll miller for further homogenization of the blend. When the capsules are used, it can be noticed that the rubber sample shows some white spots, which can be attributed to the capsules aggregation (figure 48).

We followed two strategies for the incorporation of the vulcanization accelerants. The first one, and the simplest, is the mixing of all the curing agents with both the polymer that compose the blend. The second

strategy is called masterbatching, and is a preformulation of one or more components in one single polymer. The obtained composite is called masterbatch, and will be mixed in a second stage with the other polymers and curing agents.

Figure 48 - Unvulcanized blend sample. The visibles whide dots results from capsules segregation.

Masterbatching is a technique employed mainly to deal with the curative diffusion. To prevent a curative depletion from the phase in which the solubility is lower, the curatives are mixed directly in that phase. Then, the curative-rich phase is mixed with the other polymer. The polymer in which the selected curative is less soluble become the curative reservoir. This strategy is not preventing the curative from diffusing into the other phase, in fact the mechanical properties increase just slightly.

5.2. Reference test with BR and SBR

The first test that we made was the vulcanization of samples of the polymers that compose the blend (BR and SBR). The vulcanization temperature was set at 170°C, according to existing recipes at Pirelli Tire. Vulcanization kinetics are different for the two rubbers; in particular, BR vulcanizes faster, reaches a higher value of maximum torque compared to SBR and shows a reversion behavior. SBR vulcanize slower, but once vulcanized, its torque value reaches a plateau.

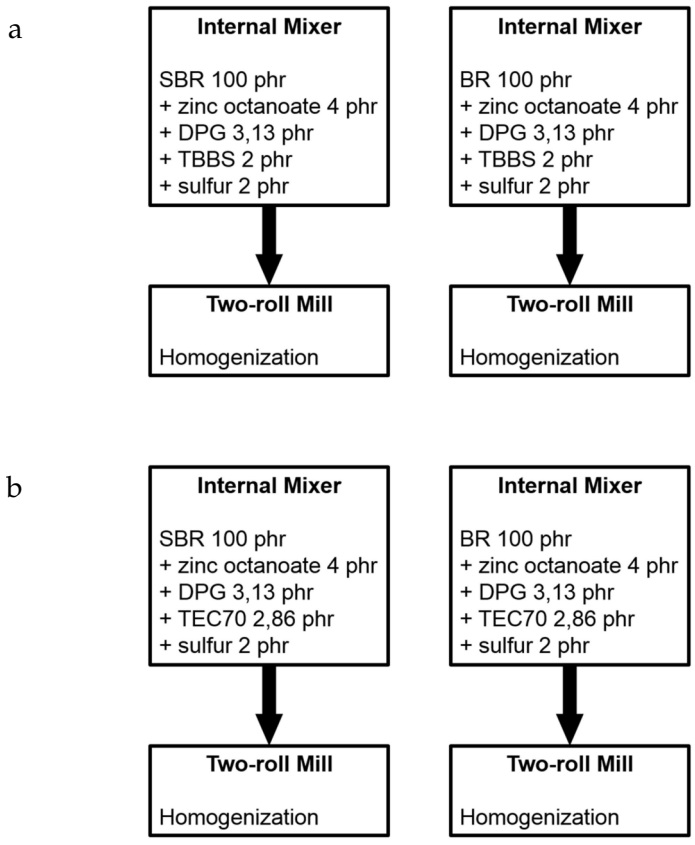

Figure 49 - Mixing methods for the preparation of: (a) SBR-TS and BR-TS; (b) SBR-TEC and BR-TEC

The vulcanization curves of encapsulated TBBS (BR-TS and SBR-TS), when compared to the non-encapsulated one (BR-TEC and SBR-TEC), shows very little differences both in terms of torque maximum and in terms of vulcanization kinetics. The encapsulated sample in BR seems to delay slightly the onset of the vulcanization process, but also the maximum torque value is inferior to the one reached with the non-encapsulated one. On the other hand, there are no differences in the vulcanization kinetics for the two SBR samples using encapsulated TBBS instead of non-encapsulated, even if the final torque level is slightly higher. It should be noted however that the differences shown in figure 50 should be considered within the experimental error of the machine. On this respect, and by direct admission of the industrial technicians, reproducibility in vulcanization experiments is a serious issue. Only samples pertaining to the same experimental campaign can be compared directly. The status of the machine, along with environmental variables like temperature and moisture level, affect both the mixing and curing steps of the process. As such in the following experiments, direct comparisons should be done only amongst curves shown within the same picture. The absolute torque values are also relative to the specific measurement campaign and should not be considered as absolute performances indicators.

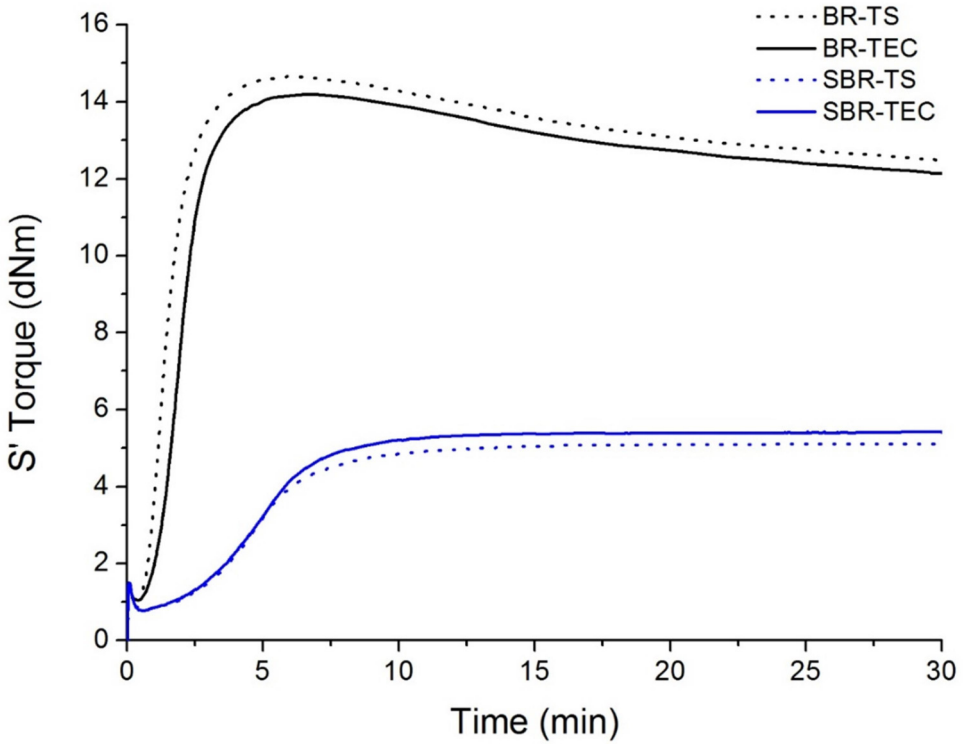

Figure 50 - Vucanization curve of BR (black lines) and SBR (blue lines) at 170°C containing pristine TBBS (dotted lines) and TEC01 (solid lines)[§]

Essentially the message we got from the experiments shown in Figure 50 is that the simple formulation of TBBS and TEC does not improve the vulcanization process at single component level. It should be however noted that TEC does not interfere with vulcanization. This is a very important finding as it validates the use of this component in blend. In principle in fact the use of TEC could interact in an unwanted way with the vulcanization curatives leading to an overall decrease of performances.

[§] The notation S′ refers to the real part (the one which gives information about the elastic properties) of the complex shear modulus, which can be written as S* = S′ + *i*S′′ (where S′′ is the shear loss and is related to the sample viscous component).

5.3. Rubber blends

In order to test the possible influence of the formulation strategy on the repartition of TBBS between the two different polymeric phases, we decided to test vulcanization in blends even though the behavior of the single elastomers was unaffected. We tested a blend having a BR/SBR ratio of 3/7. According to the general way of operation we described in the previous paragraph, a reference blend with non-encapsulated TBBS was also tested. The vulcanization temperature was again set at 170 °C.

The polymers and the curing agents are mixed in one stage (no masterbatching). The vulcanization curves of the blend with encapsulated TBBS and non-encapsulated TBBS show almost no difference, nor in terms of induction time, neither in terms of maximum torque values (figure 51). This result was somewhat expected based on the evidences discussed in Figure 50, yet again the presence of TEC (a third polymeric compound within the blend) did not interfere with vulcanization.

From the standpoint of the working hypothesis – the capsules help in controlling the release of TBBS – we expected a delay effect in the vulcanization kinetics. At this stage we did not yet had proof of the poor thermal stability of the capsules, although this seemed to be at least an educated guessing.

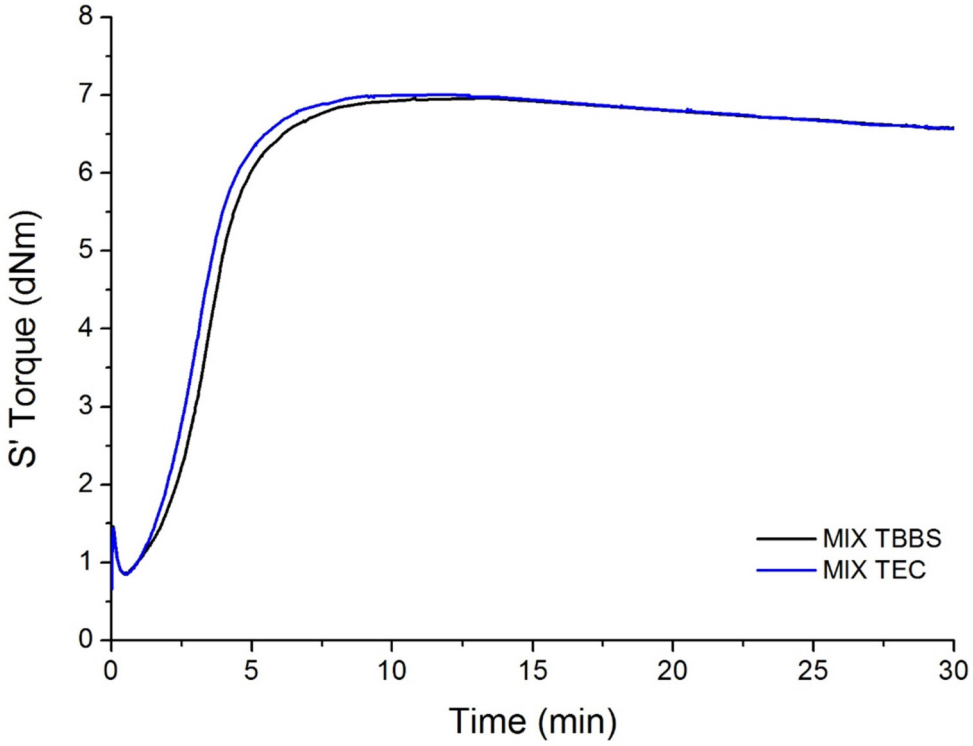

Figure 51 - Vulcanization curve of the rubber blend (SBR/BR 7:3) containing pristine TBBS (black line) or TEC01 (blue line). The vulcanization temperature is set to 170°C.

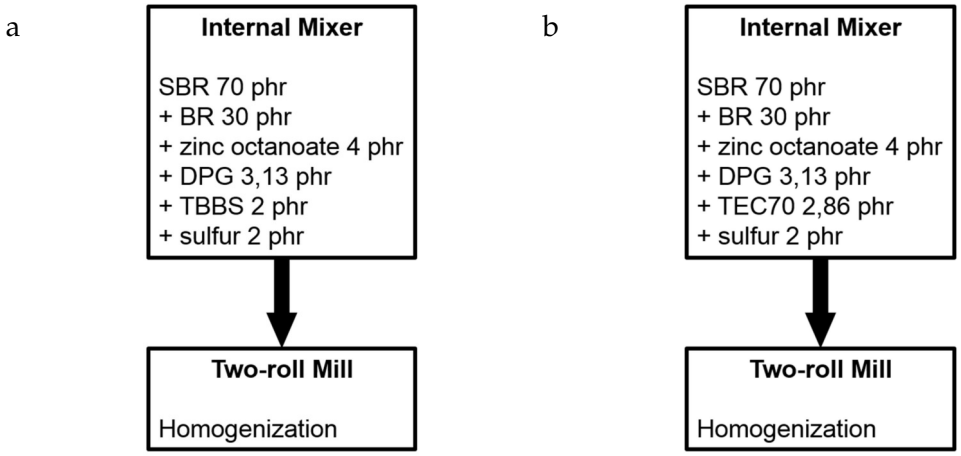

Figure 52 - Mixing methods for samples MIX TS (a) and MIX TEC (b)

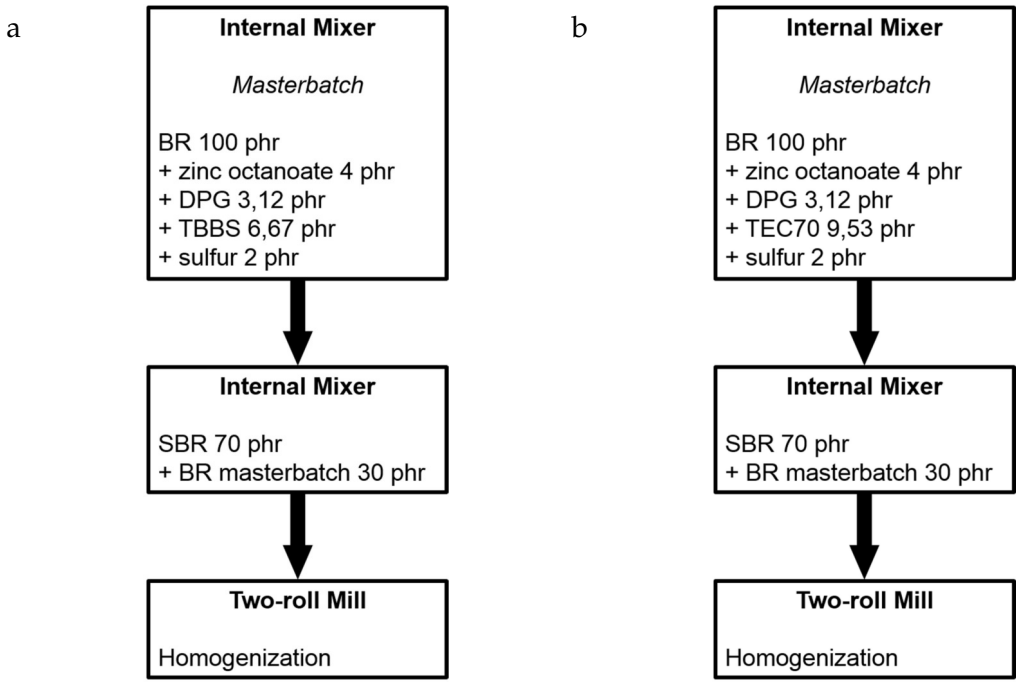

Figure 53 - Mixing methods for samples MB-BR-TS (a) and MB-BR-TEC (b)

In order to evaluate a possible processing agent effect exerted by TEC even if the capsules did collapse earlier than expected, we tried anyway to then to pre-formulate the encapsulated TBBS in BR according to the masterbatch strategy. The underlying idea was that, given the immiscibility of TEC in BR and the favorable polar-polar interaction of TBBS and TEC with respect to TBBS and BR, droplets of TBBS dissolved in TEC could also act as accelerant reservoirs during vulcanization.[**] As usual, we had to compare the results with an identical sample where TBBS alone was also masterbatched in either BR or SBR for comparison.

[**] This whole section describes experiments performed in parallel with the work on crosslinking of the capsules. Very likely, should the work on crosslinking had been easier we would had not tried so hard to see an effect even with simple capsules. Yet, the results at least validated the use of TEC as an innocent excipient in tyres, an evidence we needed anyway.

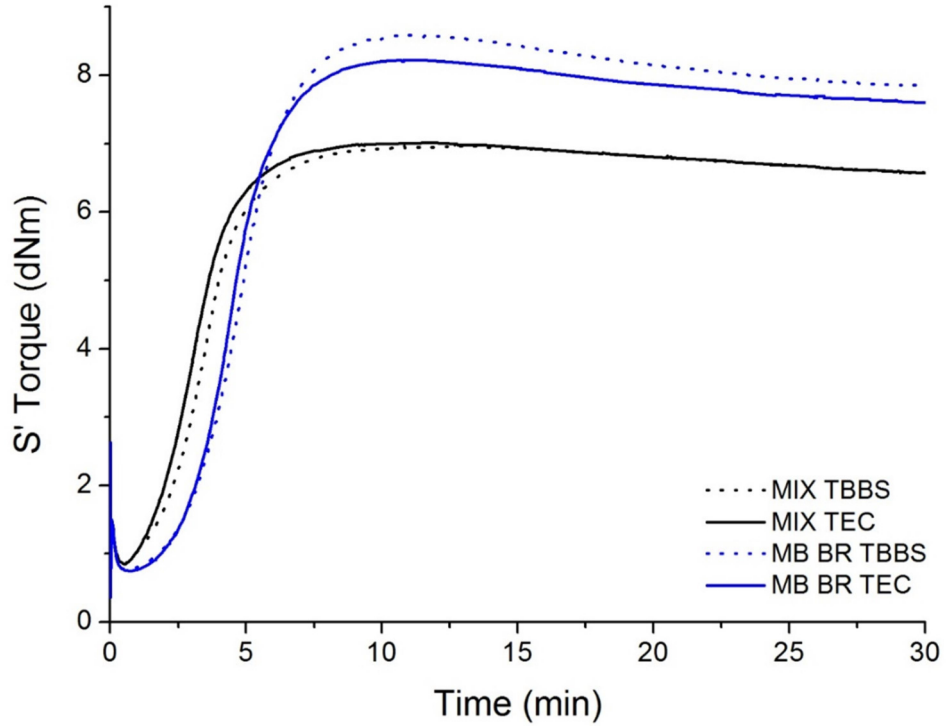

Figure 54 - Vulcanization curves of SBR/BR blends produced with a one-step mixing process (black lines) or with a pre-formulation of the accelerator in a BR masterbatch (blue lines). Samples contain either pristine TBBS (dotted lines) or TEC01 (solid lines)

The first relevant finding shown in Figure 54 is that indeed the masterbatching process brings about an increase of the scorch time – thus a delay in the vulcanization kinetics – associated with a general improvement of the final Torque value. A closer inspection of the final portion of the curing profiles shown that the vulcanization reversion is more evident for the masterbatched samples that it is for the standard ones. As the reversion is a phenomenon closely associated with the BR phase, a likely guess is that in masterbatched samples the latter is more efficiently vulcanized than it is in the standard mixture. The overall

improvement of the torque is coherent with this interpretation as well. It should be noted however that, as it is shown in Figure 50, the scorch time of BR is *shorter* than that of SBR. This is somewhat not coherent with the idea that the accelerant concentration in BR is higher in samples where TBBS is directly masterbatched in said polymer.

As for the effect of the encapsulation, the two curves corresponding to direct mixing are – as we discussed above - essentially superimposable. Conversely, in the case of the msterbatched samples, the encapsulation leads to a slight decrease in the peak torque value along with a little decrease on the scorch time. Even if the differences are barely noticeable, this result will be useful when discussing what we observed with crosslinked samples.

We performed further studies – both on polymer mix and on masterbatch – varying the temperature from 150 to 170°C (figure 55-56), and in no one of these cases, some appreciable changes can be observed.

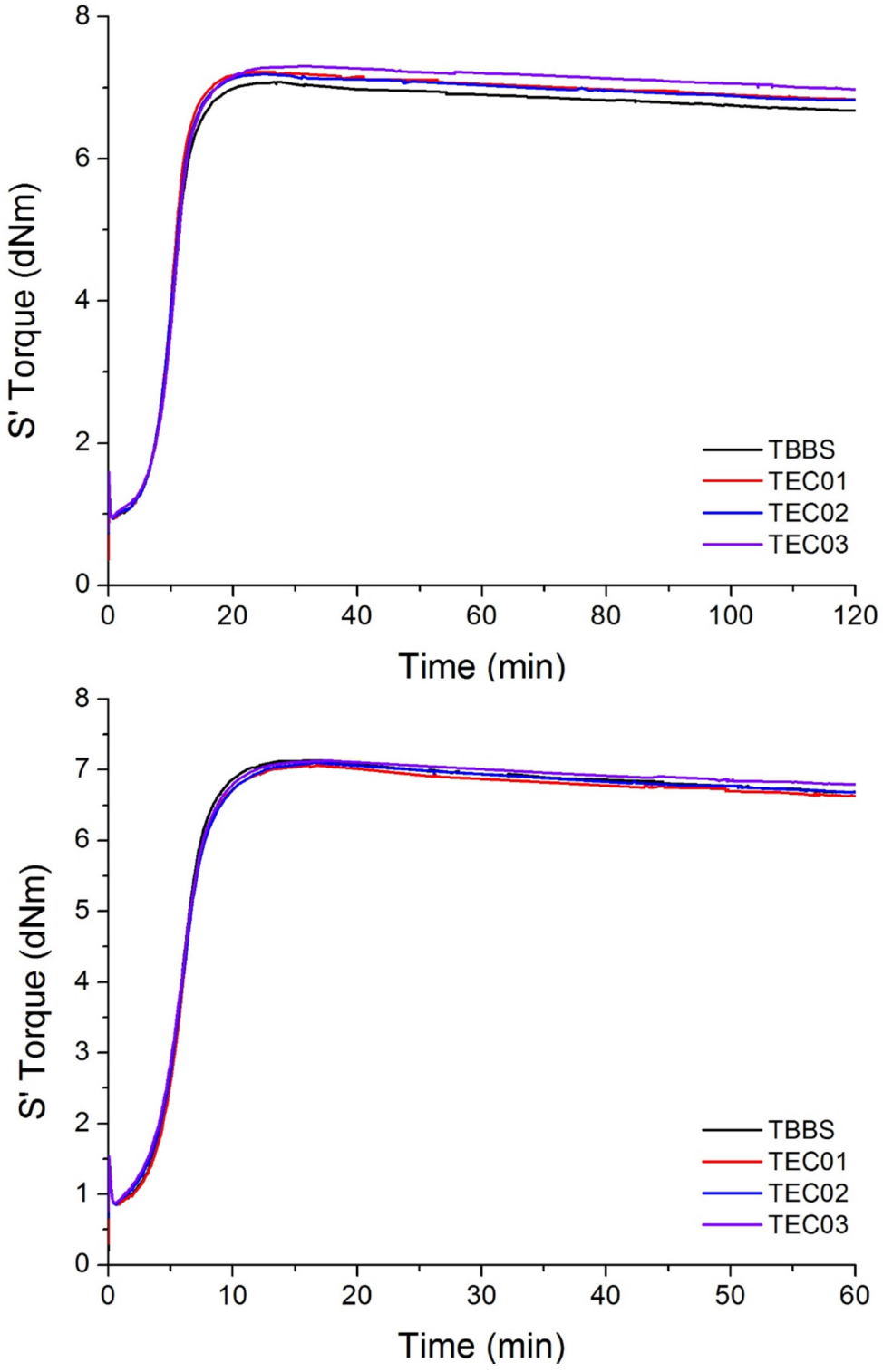

Figure 55 - Vulcanization curve of the rubber blends using capsules with different EC/TBBS ratio; The curves are recorded at 151°C (top) and at 160°C (bottom)

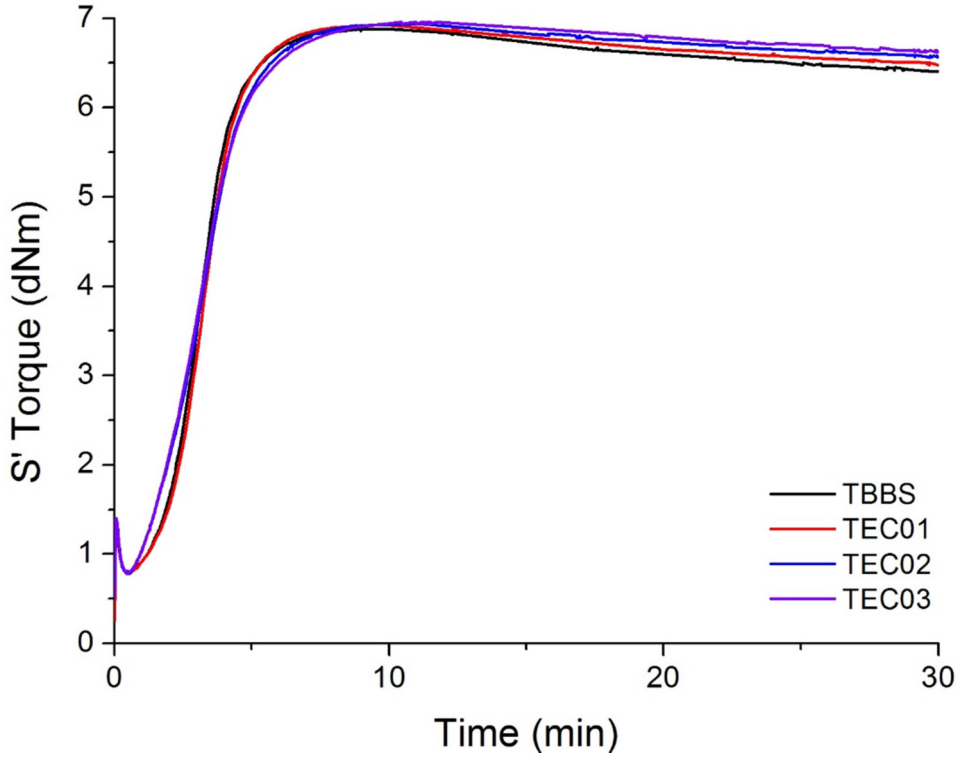

Figure 56 - - Vulcanization curve of the rubber blends using capsules with different EC/TBBS ratio; The curves are recorded at 170°C.

We tried to prepare some blends using encapsulated TBBS with different EC/TBBS ratio. Capsules with an EC/TBBS ratio shifted towards EC should have thicker shell, so we expect to see a trend in the release behavior. Unfortunately, the vulcanization curves show only slight differences. The EC/TBBS ratio is not influencing dramatically the performance in blend of the encapsulated TBBS. Actually, the capsules with a higher EC content show a little delay, but the overall effect is negligible.

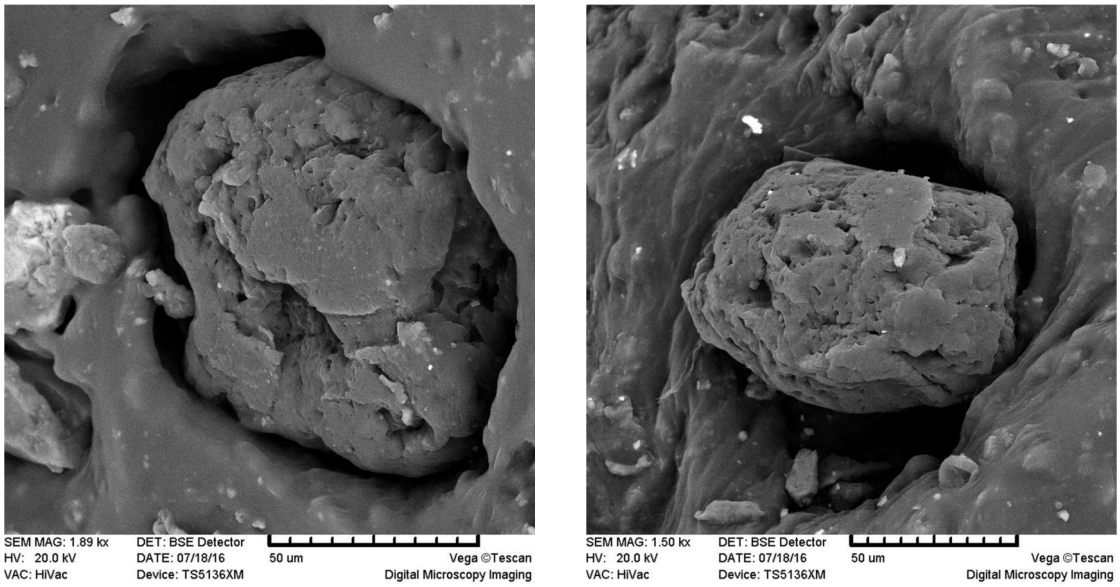

Figure 57 - SEM image of a sliced crude sample of rubber blend containing TEC01 capsules

We identified three main issues that can be responsible for the inefficiency of the capsules in the blends:

1. The capsule shell is not acting as a diffusional barrier;
2. The capsules are not surviving the mixing phase – the shear stress that the sample experience during the mixing phase is breaking the capsules;
3. The thermal collapse of the capsule nullifies the presence of the capsule itself.

We made some SEM images of polymer blends right after the compounding process to look for the capsules; the samples were prepare cutting the rubber blend in small pieces, and then cutting from them small slices. From the images that we obtained, it seems that the capsules can be found mixed with the polymers (figure 57). However, it is hard to

define exactly what we found as the capsules, so further efforts are still in progress to obtain some TEM images of the processed samples.
The characterization of the efficiency of the EC barrier against the load diffusion has been performed using a soluble derivative of quinacridone, a popular pigment. The detailed discussion of the experiment can be found in appendix A.

5.4. Vulcanization of secondary accelerator-free blends

So far, we compared the vulcanization of blends using a standard procedure in which the accelerant was replaced with the encapsulated one, and we see that no significant difference can be spotted in the two set of measures. However, in standard vulcanization recipes TBBS is paired with a secondary accelerator, DPG, which decrease noticeably the induction time. We thought that removing DPG from our samples, and thus slowing significantly down the process, we could get the chance to see some effect caused by the encapsulation process.
Of course, since DPG is a component that is normally used in all the preparation, it is impossible to think about an industrial recipe without DPG, so the DPG-free tests will only have the purpose of looking closer to the encapsulation effect.
The polymers used in this study are still BR and SBR in a 3/7 (BR/SBR) ratio. Only TBBS, pristine or encapsulated, is pre-formulated in a BR masterbatch. The other curing additives (apart from DPG that is

completely absent in this set of samples) are added in the second step of the mixing process together with SBR.

The kinetic curves without DPG look very different from the sample in which DPG is present. Indeed, the induction time is longer and the torque value of the vulcanized blend reaches the plateau only when vulcanized at 170°C. However, there are some important observation that we can do, while looking at the vulcanization curves of the various samples (figure 58).

In the vulcanization curve recorded at 151°C, the behavior of control and encapsulated samples of the sample display different regimes. In the black trace (the control sample), there is essentially no scorch time as the torque almost immediately, albeit very slowly, starts to increase. After 30 minutes the process nearly reaches a plateau, eventually fully entering into phase II after 45 minutes. This behavior could be interpreted as a first vulcanization of the fast responding component (BR), followed by full vulcanization also interesting the slower phase (SBR). The blue trace (the capsules), shows a clear scorch time extending till minute 10, followed by a linear regime. Around minute 45 the process enters phase II with a slightly faster kinetics as the control experiment. Just like in the case of Figure 50 (section 5.2), the peak torque value is smaller for the encapsulated sample than it is for the control.

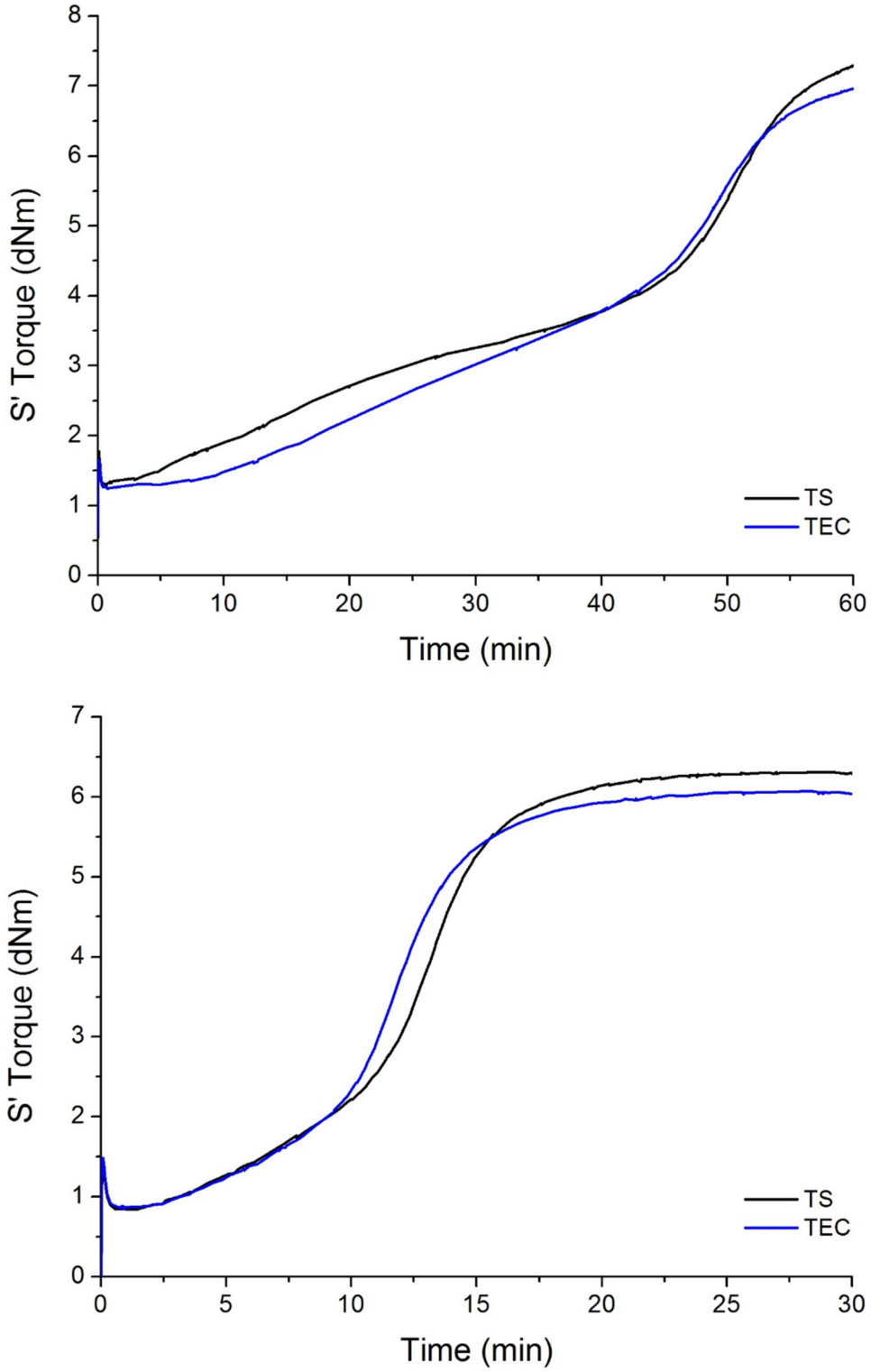

Figure 58 - Vulcanization curvs of SBR/BR blends without DPG at 151°C (top) and at 170°C (bottom). Samples contain pristine TBBS (black line) or TEC01 (blue line)

Our interpretation of the data is that the effect of the TEC is – in the first 30 minutes - the averaging of the different kinetics characterizing the two components of the blends we used. When, the same experiment is carried out at 170°C, the aforementioned affect essentially disappears. As for the slight reduction of the "averaged" scorch time, this is consistent for the two experiments: whenever TEC is present, the vulcanization is in the overall faster and slightly less effective. The importance of this observation will be fully appreciated when comparing these results with those obtained with crosslinked capsules.

5.5. Crosslinked capsules in polymer blends

From what was discussed in the previous chapter, non-hardened capsules are not likely to resist at temperatures above the melting point of TBBS, as such the slight differences observed in samples vulcanized at 150 or 170°C cannot be ascribed to an encapsulation effect but rather to the presence of TEC as a third phase where TBBS can accumulate, to eventually be released in the rubbers.

From now on, all described vulcanization tests have been carried out on crosslinked samples obtained via a procedure that was still largely under optimization. As such, even though general trends are consistent, a batch to batch variation in the quantitative behavior of the various samples tested was not unexpected. It should be also stressed that crosslinked samples became available for vulcanization only within the last 4 months of the project.

The capsules used in these studies are the epoxy-crosslinked one described in chapter 4; all the capsules used have the EC/TBBS ratio fixed to 1:1, and the epoxy content is 10% w/w with respect to EC. The samples will follow this coding:

- TECXL-1-120 – the capsules are crosslinked in the oven at 120°C for 10 hours; the batch dimension is around 20 g;
- TECXL-2-120 – same crosslinking strategy used for the previous sample, but the mass scale is one order of magnitude higher (180 g). Moreover, ethyl acetate was used instead of methylene chloride for the organic phase during the capsules preparation;
- TECXL-90 – the capsules are crosslinked in the oven at 90°C for 10 hours.

Figure 59 shows the vulcanization curves recorded at 151°C for the samples TECXL-1-120. This was the very first crosslinked sample we made. As we have described in the previous chapter, the crosslinking procedure is non-trivial as the capsules tend to consolidate upon thermal treatment. In this particular batch, the crosslinked sample was so coalesced that a mechanical milling became necessary prior to vulcanization tests. Likewise, such strong coalescence was the result of a too high crosslinking temperature. In this case in fact we operated at 120°C, that is significantly above the melting point of the TBBS.

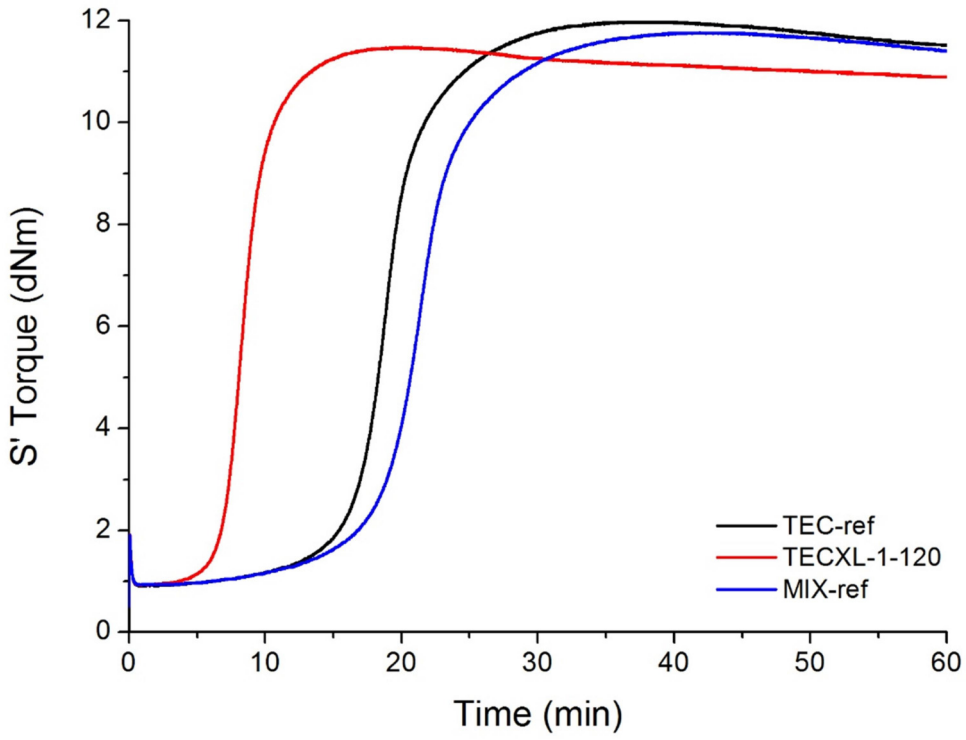

Figure 59 - Vulcanization curve of BR/SBR blend at 151°C containing TECXL-1-120 (red line), non-crosslinked capsules (TEC ref, black line) and the reference mixture of the ingredients (blue line)

The three curves of Figure 59 refer to a mechanical mixture of TEC, TBBS and epoxy (blue curve), capsules containing the epoxy but not crosslinked prior to vulcanization (black curve) and finally the crosslinked capsules.

The behavior of the crosslinked capsules is strongly different from that of both the reference sample and the one containing non-hardened capsules. In in fact the difference between the black and blue curve is minimal – we observe the now familiar slight reduction in the scorch time for the capsules with respect to the mechanical mixture – the red trace shows a drastically faster vulcanization connected with a noticeable decrease in the peak torque value.

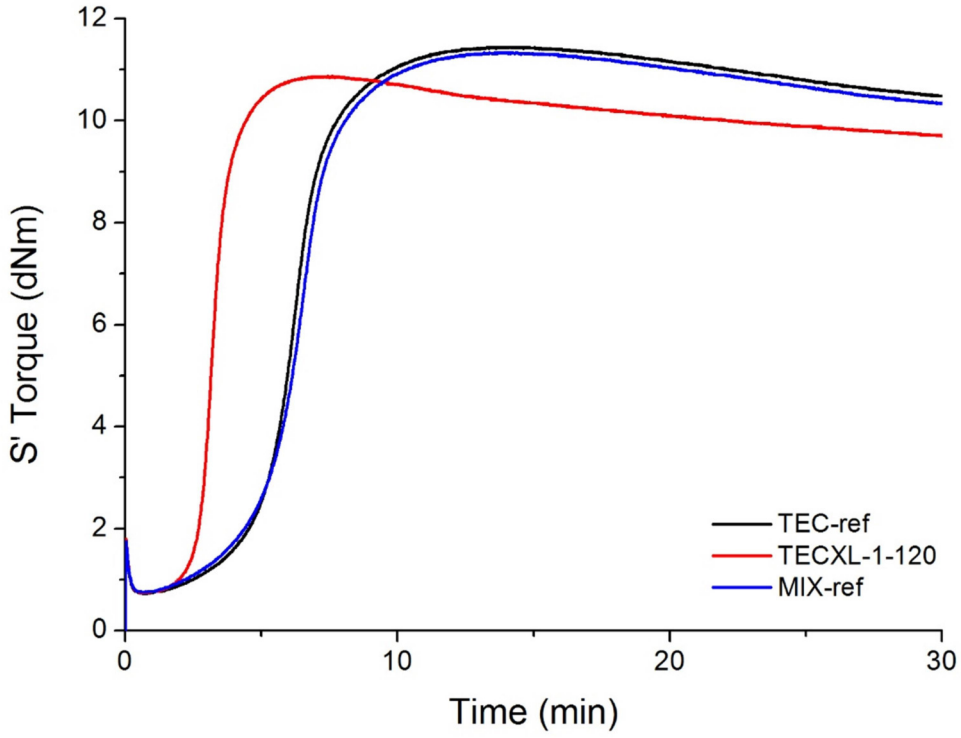

Figure 60 - Vulcanization curves of BR/SBR at 170°C containing TECXL-1-120 (red line), non-crosslinked capsules (TEC-ref, black line) and the reference mixture of the ingredients (blue line)

While there is very little doubt that in this case the presence of the capsules makes a drastically difference in the vulcanization behavior, the observed affect is opposite to the one we expected. In fact, as we already discussed elsewhere, the delayed release of the vulcanization curatives was expected to bring about an overall slowing down of the vulcanization itself. The vulcanization curve recorded at 170°C (Figure 60) shows a similar behavior: the sample containing the crosslinked capsules vulcanizes faster with respect to the sample containing the non-crosslinked one. In this set of tests, the differences between mechanical mixture and non-crosslinked capsules is barely noticeable (again in

agreement with the trend established in all previous experiments where crosslinking was not involved).

The experiments described in Figure 61 shows the vulcanization curves recorded at 151°C for the samples containing capsules crosslinked at 90°C (TECXL-90). As in this case the hardening was carried out at a temperature below the melting point of the cargo, the coalescence effect that so strongly affected sample TECXL-1-120 was less severe. We nonetheless had to recur to milling of the hardened sample prior to vulcanization tests.

In this case, the two curves refer to crosslinked capsules (blue trace) and a mechanical mixture of TBBS, TEC and epoxy also crosslinked at 90°C for the same amount of time as the capsules (black trace). This experiment was carried out to discriminate the formulation approach, leading for the reasons discussed in Chapter 2 to either polycore or core-shell capsules, from the pure crosslinking effect. In fact, also in the case of the black trace, TBBS is delivered as a solid solution in crosslinked TEC. The main difference between the two samples is in the dimension of the grains, in the order of tens of microns for the capsules, much larger for the reference sample. Much to our initial surprise, the acceleration effect we observed for the crosslinked capsules versus the non-crosslinked ones (Figure 59) is even stronger in the case of the crosslinked mechanical mixture of the components.

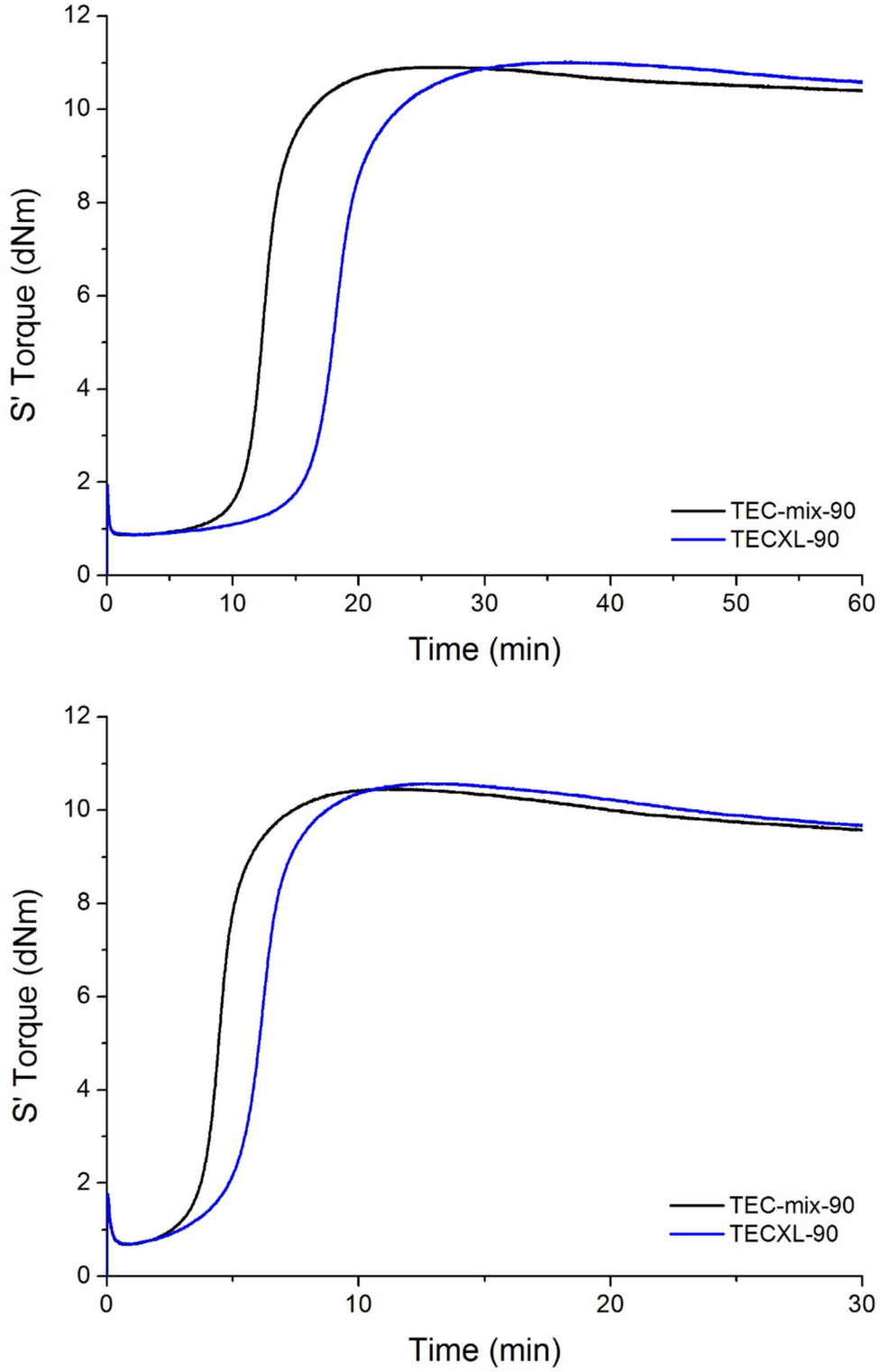

Figure 61 - Vulcanization curves of BR/SBR blends at 151°C (top) and 170°C (bottom) containing TECXL-90 (blue line) and the thermally treated mixture of components (TEC-mix, black line)

In fact in both the 150°C and 170°C experiments shown in figure 61, the black trace is associated with a faster process with respect to the blue one.

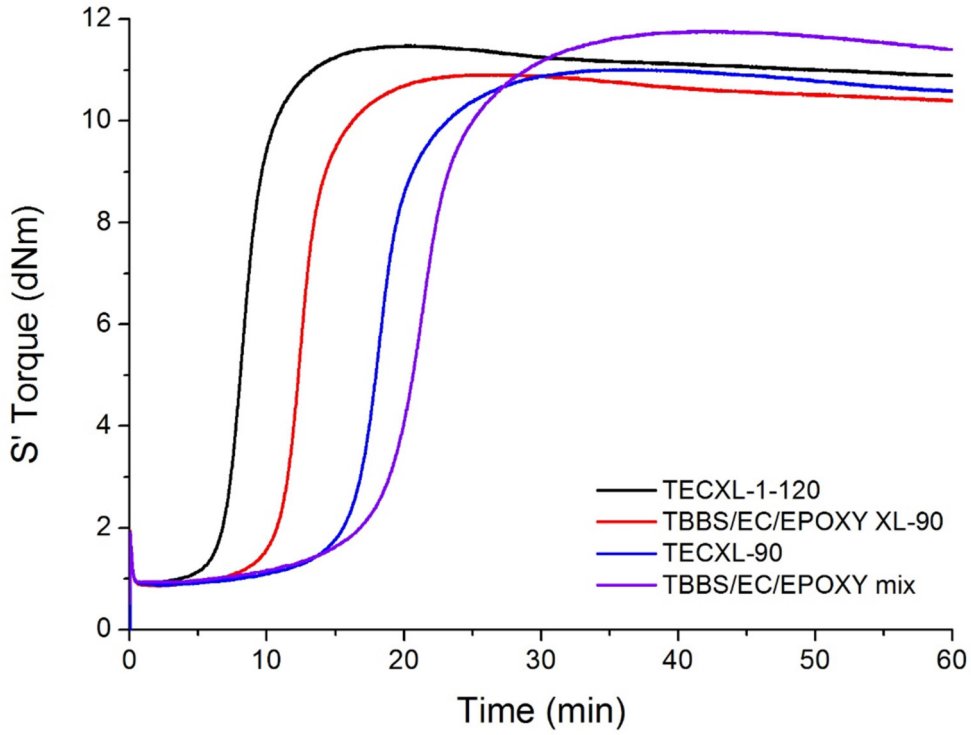

Figure 62 - Vulcanization curves of TBBS/TEC/epoxy non crosslinked mechanical mixture (violet), mechanical mixture crosslinked at 90°C (red curve), capsules TECXL-90 (blue curve) and capsule TECXL-1-120 (black curve). Conditions: 150°C on BR/SBR rubber blend.

Indeed, it would have been better to include in the same data sate also a true reference sample not containing the epoxide. This was the original intention but not in all vulcanization tests we had the opportunity to introduce as many samples as we wanted.

Slightly abusing the reliability of the data, we anyway present in figure 62 collection of data coming from two different measurements

campaigns: TECXL-90 and TECXL-1-120. Figure 62 shows that in all of the cases where crosslinked TEC is present, formulated or not, the overall effect is an acceleration of the vulcanization kinetics. No further elaboration can be done dealing with the maximum torque as the samples have not been acquired within the same measurement campaign. As in both TECXL-90 and TECXL-1-120 measurements campaigns we worked masterbatching the vulcanization curatives in BR, we wondered whether the acceleration effect could be related to the faster kinetics of BR over SBR in vulcanization. In short, supposing that the capsules or crosslinked matrix do not migrate in the second rubber introduced after masterbatching, the acceleration could be due to the fact that kinetics is dominated by the response of the rubber where the accelerant is masterbatched in (BR in our case).

To evaluate this further point, we made a third measurement campaign on crosslinked capsules, this time master batching both in BR and SBR. The particular batch of capsules we used in this case was the first one obtaining on replacing CH_2Cl_2 with AcOEt in the MESE formulation approach. Crosslinking was still carried out via direct thermal treatment at 90°C of the capsules in an oven.

Again, we observed partial coalescence of the capsules and the final crosslinked sample had to be milled. Dimension of the particles was again in the tens of microns regime (see previous chapter).

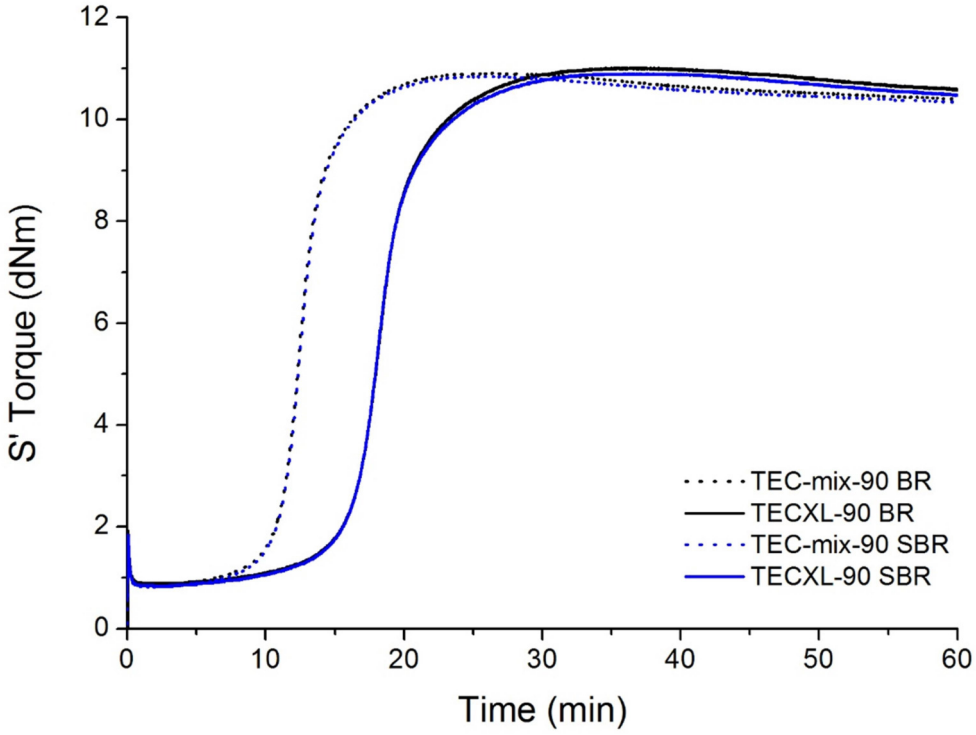

Figure 63 - Vulcanization curves of TBBS/TEC/epoxy crosslinked mechanical mixture masterbatched in BR (black dotted curve) and in SBR (blue dotted curve) and of crosslinked capsules masterbatched in BR (black solid curve) and SBR (blue solid curve).

Much to our surprise, masterbatching made no difference whatsoever for both capsules and crosslinked mechanical mixture. Indeed, Figure 63 shows that the curves pertaining to the two masterbatches of capsules and reference crosslinked mixture are essentially superimposable. The otherwise now familiar trend of capsules leading to a faster vulcanization kinetics is clearly observed.

We made a final measurement campaign, in this case only masterbatching in BR, using capsules produced with AcOEt and crosslinked at 120°C. This was done as in the very first measurement campaign capsules crosslinked at this temperature gave the largest

variation with respect to the standard. We were thus interested in verifying the generality of the effect when using capsules obtained via a more standardized assembly process.

Figure 64 shows at the three different vulcanization temperatures of 120, 150 and 170 °C the behavior of crosslinked capsules (blue trace) and non-crosslinked mechanical mixture of TBBS/TEC and epoxy (black trace).

In all of these three samples, we can see that the presence of the crosslinked capsules enhances dramatically the vulcanization process; in particular, the acceleration at 120°C is terrific, because the sample containing the capsules starts to vulcanize one hour earlier if compared to the samples containing pristine TBBS. On the other hand, the maximum torque value recorded in the samples containing the crosslinked capsules is always inferior to the torque level obtained using pristine TBBS. However, the vulcanization curve reaches a plateau, while usually the curves enter in reversion mode after that the maximum torque value has been reached.

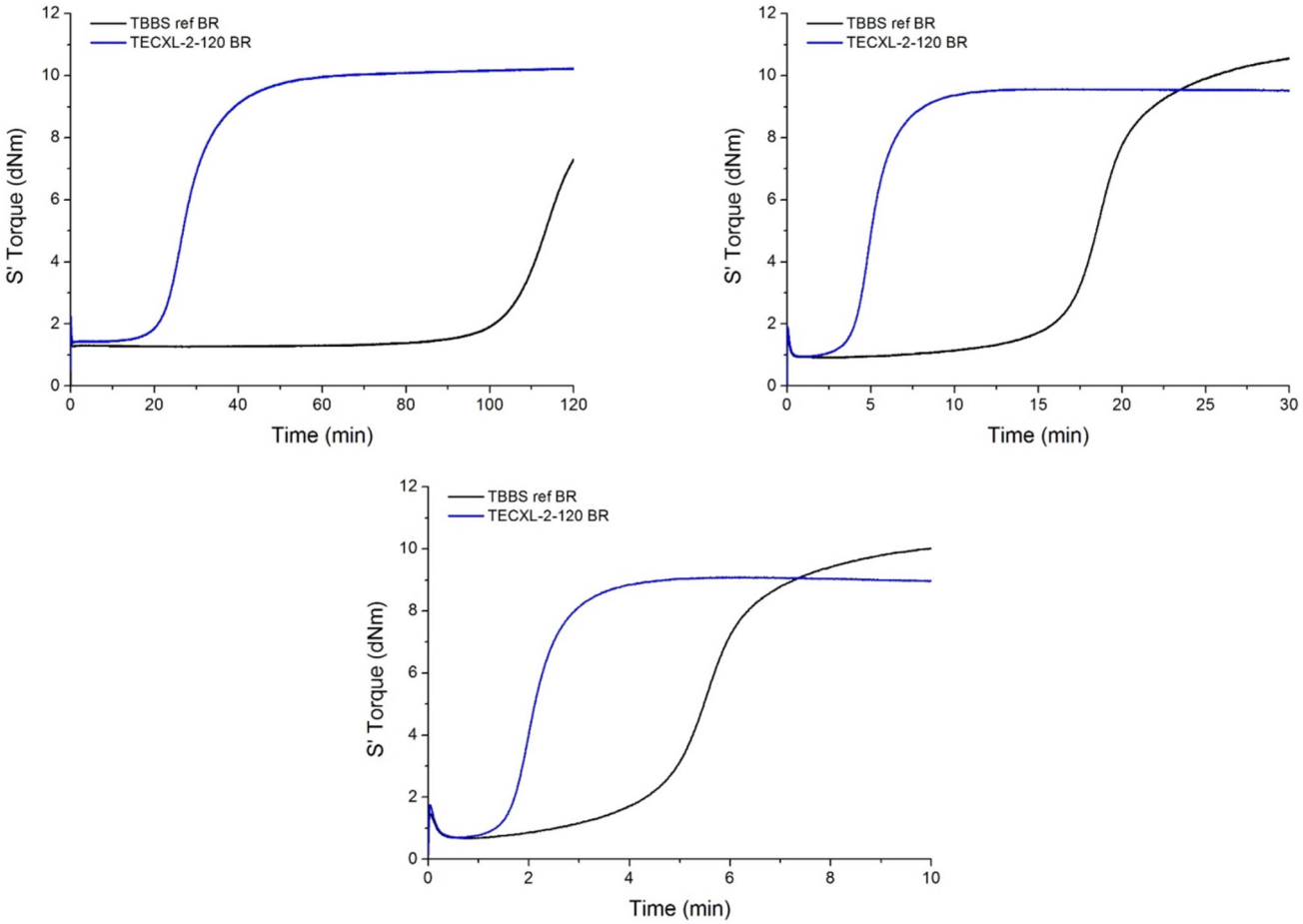

Figure 64 - Vulcanization curves of SBR/BR blends at 120°C (top), 151°C (middle) and 170°C (bottom) containing TECXL-2-120 (blue line) or pristine TBBS (black line)

To sum up all we observed in the various measurement campaign:

1. Crosslinking of the ethyl cellulose always lead to an acceleration of vulcanization kinetics
2. The acceleration effect is more pronounced for capsules crosslinked at 120°C than it is for those hardened at 90°C

3. The behavior of a mechanical mixture of TBBS/TEC and epoxy crosslinked at 90°C is intermediate between that of capsules crosslinked at 120°C and at 90°C
4. The stronger is the acceleration effect, the lower is the maximum torque achievable (and thus the overall extent and homogeneity of the vulcanization)
5. Masterbatching, effective in the case of non-crosslinked capsules and mixtures, has no effect whatsoever in the case of crosslinked TEC samples both in the case of capsules and simple mixture.

In order to formulate a model that could explain all such, somewhat counterintuitive observation, it is important to take into account three relevant facts:

a) All vulcanization campaign made on crosslinked capsules also used the secondary accelerant DPG.

As DPG is a polar molecule, in the presence of a TEC domain during the mixing phase, DPG will concentrate there due to polar affinity. This will be not the case for non-crosslinked capsules as, above 110 °C we do not expect to see any surviving capsule due to melting of the TBBS core.

b) The crosslinking alters the structure of the capsules due to coalescence.

For all the reasons discussed in the previous chapter, any attempt to crosslink capsules that are in close contact with each other leads to a more or less extended aggregation and coalescence. This is particularly true for capsules crosslinked at 120°C, where the molten core increases deformations and thus contact areas.

c) The domains of the two different rubbers in a blend have dimensions in the order of the micron.

If we put together all such evidences, a tentative interpretation of the data can be given.

The capsules are big to begin with and becomes bigger after crosslinking. The reason why masterbatching has no effect is that capsules are bigger than the different rubber domains. Also, capsules are crosslinked and thus immiscible with the rubbers. They will thus localize at the interphase between different rubber domains, hence no difference is correctly expected with respect to different masterbatching strategies. The capsules are in any case homogeneously distributed in the blend.

Also, the capsules are the only source of TBBS in the blend. We can assume that the capsule distribution is homogeneous in the blend, but the TBBS concentration will have a spike in correspondence of the capsules, while between the capsules the concentration is zero. If DPG localize around the capsules, the primary accelerant – trapped in a dense shell – is surrounded by the secondary accelerant. When the temperature is high enough to let the TBBS flow outside the capsule, TBBS will be in

the most reactive environment ever possible. This also mean that rubber starts to vulcanize around the capsules, building a very efficient diffusive barrier. This barrier will prevent TBBS to diffuse further in the blend, preventing a homogeneous vulcanization of the sample – which macroscopically reflects in the lower level of the torque maximum of the samples containing the crosslinked capsules.

The difference in the behavior of capsules crosslinked at different temperatures with respect to the crosslinked mechanical mixture of the components can be traced down to the different dimension of the crosslinked particles. Working at 120°C while crosslinking leads to extensive coalescence and thus to very big particles. The opposite is true when working at 90°C. The situation of the mechanical mixture is intermediate as the starting sample has no microstructure and particles are only produced by mechanical milling, after the crosslinking.

Thus, the difference between the expected effect of encapsulation (a delay in the vulcanization) and what we consistently observed (an acceleration) is due to the dimension of the particles we get after the crosslinking process.

As it is stated in the previous chapter, we now have a strategy to efficiently crosslink capsules while at the same time avoiding coalescence. A macrosample of 300 g has been synthesized, demonstrating that the method can be efficiently brought to a higher scale. The obtained particles have been crosslinked at 90°C in both the way illustrated in section 4.1 (oven treatment or water-mediated heating) and tested in rubber blends without any masterbatching (since we

showed that this process is not affecting the vulcanization kinetics). A non-crosslinked capsules sample has been used as reference, since its behavior is not different from the pristine TBBS one during the curing process.

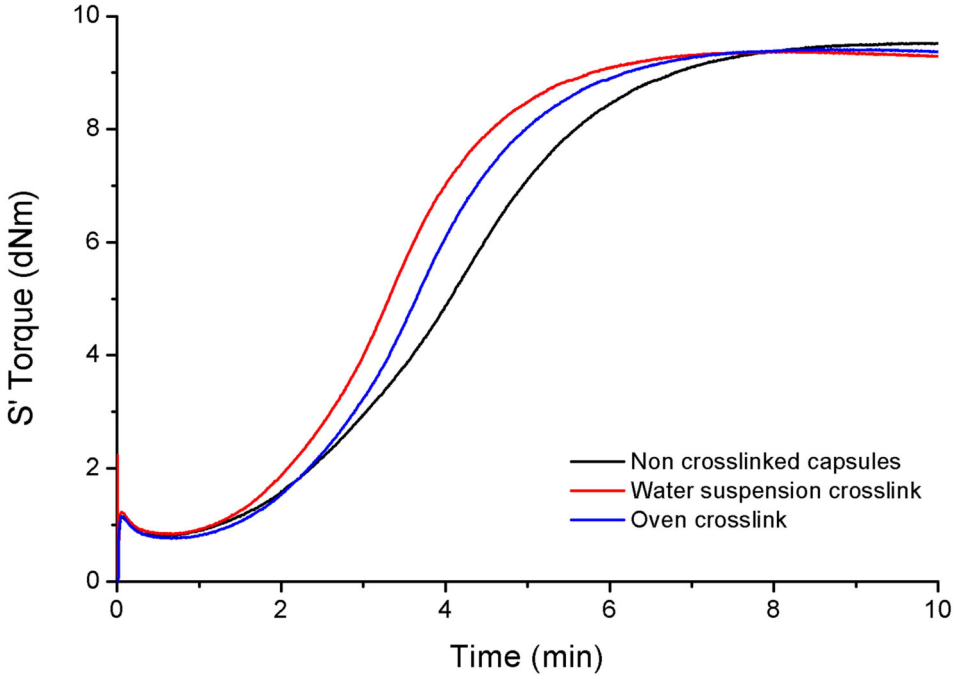

Figure 65 - Vulcanization curve of SBR/BR blend recorded at 170°C containing suspension-crosslinked capsules (red trace), oven-crosslinked capsules (blue trace) and non crosslinked capsules (black trace). Crosslinking temperature is 90°C.

As we can see from Figure 65, the trend in the acceleration of the vulcanization kinetic is preserved. Suspension-crosslinked capsules induce a faster curing than the oven-crosslinked ones. This can be attributed to the suppression of the coarsening effect arising from the crosslinking process, providing a better dispersion of the powder in the rubber blend and, hence, a higher number of accelerator sources available.

Recipes for rubber blends preparation

TECXL-1-120 series

Masterbatch (MB1)

Name	Quantity (phr)
BR	100,00
TECXL-1-120	13,33

Masterbatch (MB2)

Name	Quantity (phr)
BR	100,00
TEC ref*	13,33

Masterbatch (MB2)

Name	Quantity (phr)
BR	100,00
Ref mix*	13,33

Blend

Name	Quantity (phr)
MB1	34,00
SBR	70,00
Zinc octoate	4,00
Sulfur	2,00
DPG	1,00

Blend

Name	Quantity (phr)
MB2	34,00
SBR	70,00
Zinc octoate	4,00
Sulfur	2,00
DPG	1,00ù

*Non crosslinked capsules

Blend

Name	Quantity (phr)
MB2	34,00
SBR	70,00
Zinc octoate	4,00
Sulfur	2,00
DPG	1,00

*TBBS/EC/TMPG mechanically mixed and not cured.

TECXL-90 – BR masterbatch

Masterbatch (MB1)

Name	Quantity (phr)
BR	100,00
TECXL-90	13,33

Masterbatch (MB2)

Name	Quantity (phr)
BR	100,00
XL mix*	13,33

Blend

Name	Quantity (phr)
MB1	34,00
SBR	70,00
Zinc octoate	4,00
Sulfur	2,00
DPG	1,00

Blend

Name	Quantity (phr)
MB2	34,00
SBR	70,00
Zinc octoate	4,00
Sulfur	2,00
DPG	1,00

*TBBS/EC/TMPG mechanically mixed and cured at 90°C.

TECXL-90 – SBR masterbatch

Masterbatch (MB1)

Name	Quantity (phr)
SBR	100,00
TECXL-90	5,70

Masterbatch (MB2)

Name	Quantity (phr)
BR	100,00
XL mix*	5,70

Blend

Name	Quantity (phr)
MB1	30,00
SBR	74,00
Zinc octoate	4,00
Sulfur	2,00
DPG	1,00

Blend

Name	Quantity (phr)
MB2	30,00
SBR	74,00
Zinc octoate	4,00
Sulfur	2,00
DPG	1,00

*TBBS/EC/TMPG mechanically mixed and cured at 90°C.

TECXL-2-120 series

Masterbatch (MB1)	
Name	Quantity (phr)
BR	100,00
TBBS	6,67

Masterbatch (MB2)	
Name	Quantity (phr)
BR	100,00
TECXL-2-120	13,33

Blend	
Name	Quantity (phr)
MB1	32,00
SBR	70,00
Zinc octoate	4,00
Sulfur	2,00
DPG	1,00

Blend	
Name	Quantity (phr)
MB2	34,00
SBR	70,00
Zinc octoate	4,00
Sulfur	2,00
DPG	1,00

6. Functionalization of TBBS

We told previously that we would not try to synthesize a brand new accelerant that could be homogeneously dispersed in blend of different rubbers. We also told that we would not focus on the study of diffusivity of TBBS among different rubber, since we decided to use a different approach that could bypass the problem. However, it would be interesting being able to map the diffusion of TBBS in order to have at least a rough picture of its distribution into the rubber blend. For this purpose we decided to try to functionalize the molecule with some detectable moieties. For detectable moiety we mean functional groups that can be recognized with some experimental techniques (e.g. EDX, MS-TGA).

We designed two different derivatives, the first bearing a t-BOC moiety and the second bearing a bromine, as showed in figure 66-67. The t-BOC moiety is a common protective groups used for amines[74]; it can be removed with acid catalysis or with heat. The thermal cleavage gained importance in the last decades because of a clever usage in the field of pigments[75].

6.1. BOC-TBBS design and synthetic attempts

Pigments are, by definition, insoluble in almost all the most common organic solvents. However, pigments usually have conjugated structures, which makes them interesting for application in organic electronics.

Solution processibility is one of the key issue for achieving low-cost devices (e.g. OFETs). Pigments can be solubilized with alkyl chains, but the process is irreversible, and sometimes dyes are less stable than pigments. The latent-pigment technique allows the conversion of a pigment in a soluble form, which can revert to the pigment structure with a thermal treatment. This procedure has been illustrated for the first time by Zambounis et al. on a diketopyrrolopyrrole substrate, showing the working principle[75]; the same technique has been used to prepare quinacridone based field-effect transistors[76] or to efficiently disperse pigments acting as fluorophores in luminescent solar concentrators[77].

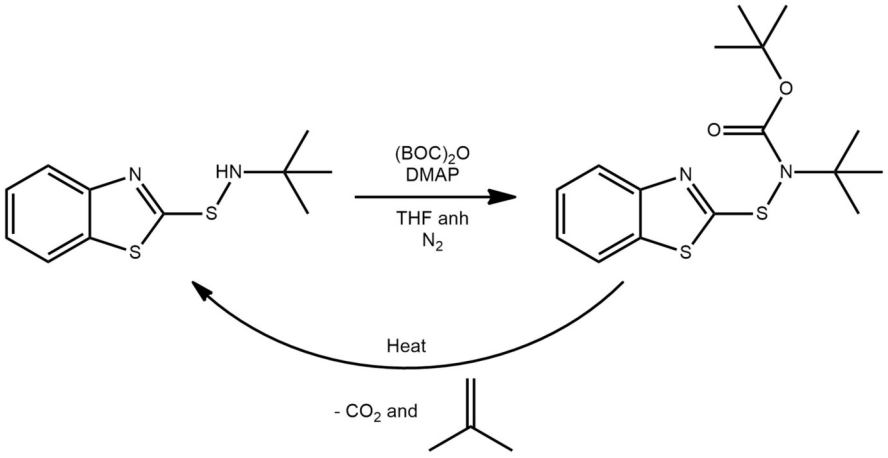

Figure 66 - Proposed synthetic pathway for BOC-TBBS and its thermal cleavage

The byproducts of the thermal treatment are always CO2 and isobutene, which can be viewed as footprints of BOC cleavage. Being a sulfenamide, TBBS has a –NH moiety that, theoretically, can be furthermore functionalized. Our idea is to functionalize TBBS with BOC in order to mix it into the rubber blend and then analyze with a TGA-MS the rubber

samples (figure 66). Tracking isobutene evolution will let us map the distribution of TBBS in the blend.

We used the standard synthetic method used for the BOC functionalization of quinacridone. TBBS is reacted with BOC anhydride in presence of dimethylaminopyridine (DMAP), which catalyze the reaction. The reaction is performed in dry THF under nitrogen atmosphere at room temperature. The color changes from a light yellow to a deep yellow. TLC plates shows that another specie is forming, however the reagent is still present. After four days of stirring, the solvent is evaporated under reduced pressure; the solid is triturated with ethanol, affording a yellowish solid, which is purified by silica chromatography (eluent DCM), obtaining three different fractions. However, the NMR analysis shows that none of them contains the desired product. We tried the reaction in the same condition another time, obtaining the same results.

Another way to insert the BOC protection is the formation of a nitranion-bearing intermediate, like for the perylene-diimide BOC functionalization. However, we considered that this strategy could be not worth the result, so we decided to change the type of tracking moiety.

6.2. Synthesis of Br-TBBS

The idea is to insert a bromine on the benzothiazole ring and use it as a contrast source for EDX imaging. We could have tracked TBBS using

sulfur, but we should not have put sulfur in the rubber blends, which is not clearly possible, so we opted for a bromine moiety.

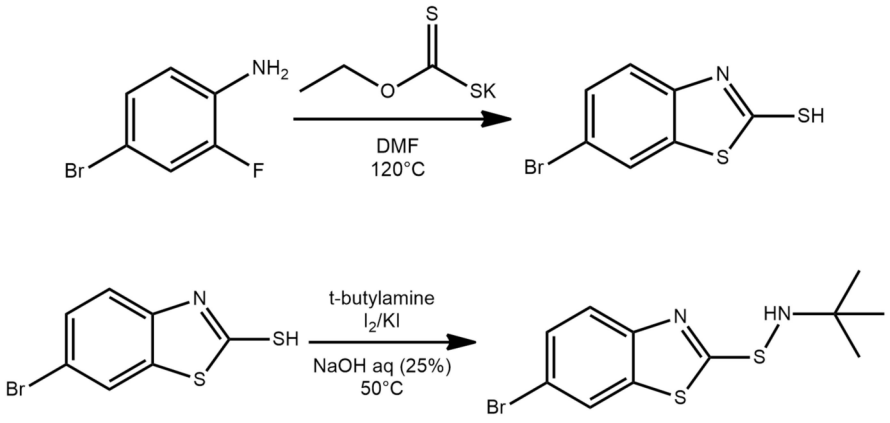

Figure 67 - Synthetic route for BrMBT (top) and BrTBBS (bottom)

We chose to synthesize Br-TBBS from the relative mercapto-benzothiazole and obtaining the desired product by reaction with t-butylamine (figure 67). Zhu et al. reported an easy and high-yield route to obtain the brominated mercaptobenzothiazole (BrMBT) by reaction of 4-bromo-2-fluoro aniline with potassium ethyl xanthate in DMF at 90°C, which we followed[78]. We used conventional heating plates instead of microwave heating for a mere matter of amount of reagent used (the biggest microwave vessel that the instrument support contains 20 mL of solution). Therefore, the reaction was stirred for 48 hours and at 120°C. After the acid workup, the precipitated product is collected on a Buchner funnel and dried in the oven. The yield is almost quantitative, and no further purification is needed.

The formation of the S-N bond is trickier. The only literature procedure comes from an old paper of D'amico, who by the way lists an enormous amount of mercapto-benzothiazole derivatives[79]. BrMBT is dissolved in a NaOH solution (25% w/w) then t-butylamine is added. The coupling between the thiol and the amine is mediated by iodine, which is added dropwise to the reaction. The iodine addition causes the formation of a white precipitate, which is collected on a Buchner funnel and purified by soxhlet continuous extraction. The pure product is obtained removing the solvent under reduced pressure. The yield of this step is pretty low (around 34%).

6.3. Test of BrTBBS in rubber blends

BrTBBS was encapsulated in EC following the same procedure that has been used for normal TBBS, but on a smaller scale (5 g of BrTBBS, figure 68). The encapsulated BrTBBS is then mixed in rubber pre-formulated in a BR masterbatch. The rubber blend is finally vulcanized at 151°C. A sample of both the uncured blend and of the vulcanized blend were analyzed with EDX mapping in order to look at the distribution of Br in the rubber blend (figure 69). In the crude sample, it is impossible to make some consideration about the distribution of BrTBBS in a single polymer phase.

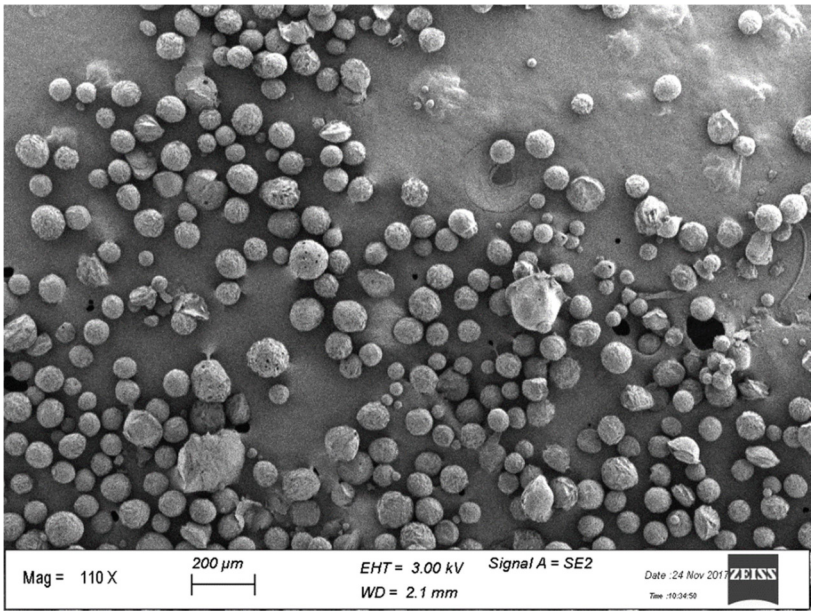

Figure 68 - SEM micrograph of encapsulated BrTBBS in EC

We can observe that:

- There are regions with high concentration of both zinc and bromine. This suggests that BrTBBS and zinc concentrates in the same regions. This would also mean that BrTBBS leaked outside the capsules.
- The bromine concentration is particularly elevated in two spots. Moreover, in those spots the zinc imaging is completely dark. Those spots can be recognized to be the BrTBBS-loaded capsules. This can tell us that, actually, capsules can still be found in the crude sample before that the vulcanization process starts and that they are loaded with the accelerant.

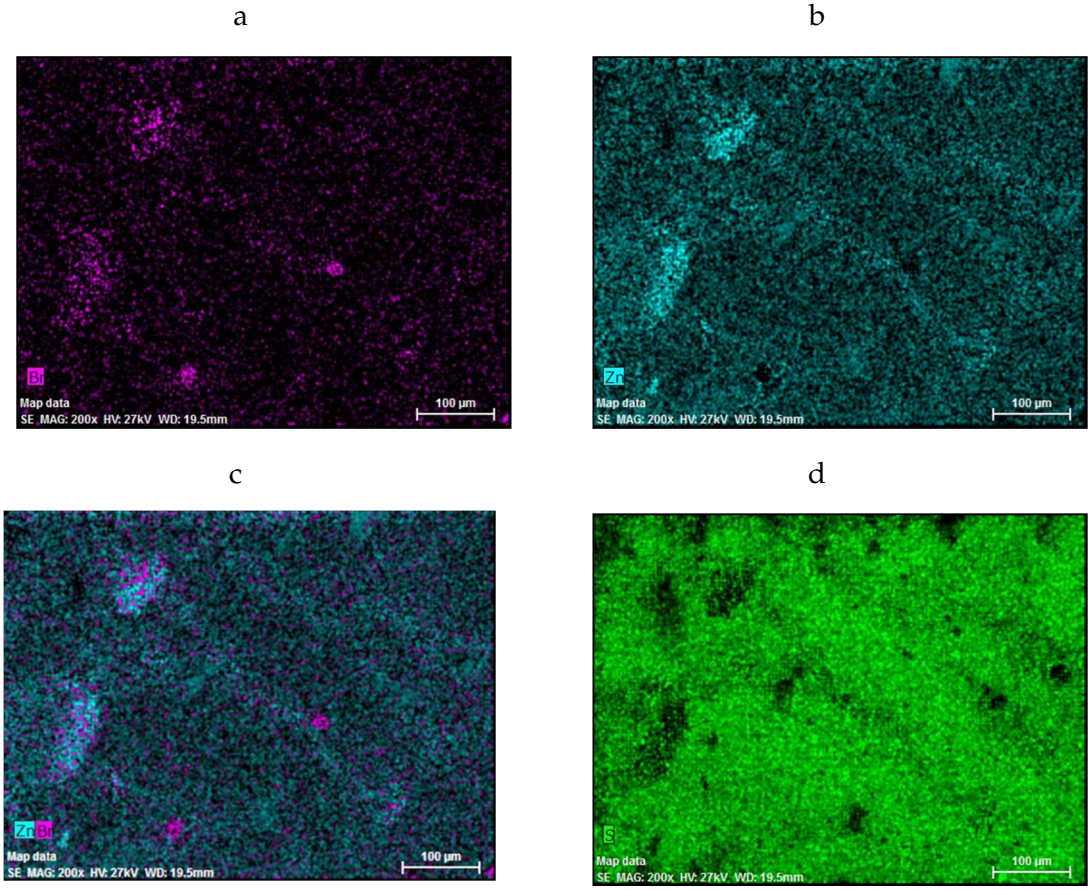

Figure 69 - Elementals map of the uncured SBR/BR blend containing encapsulated BrTBBS. Map refers to (a) bromine, (b) zinc, (c) overlap bromine-zinc and (d) sulfur

What we guess from this images is that the capsules can survive the mixing phase and be still loaded with the accelerant. The interaction between zinc and BrTBBS can be due to the zinc-sulfide complex formation. The dimension of the spot may originate from the breaking of the bigger capsules. It is possible to imagine that if a capsule breaks during the mixing phase, its load would disperse in the region nearby the capsule.

The vulcanized sample, unfortunately, is not possible to image, most likely because of its roughness.

7. Conclusion

We approached the issue of the curative diffusion in rubber blends proposing a pre-formulation approach. The microencapsulation of curatives is not a new idea, but it was explored only for sulfur encapsulation. A very few examples are reported in literature for the encapsulation of accelerators. We chose ethylcellulose as encapsulating material due to its softening point (150-160°C), which is compatible with the vulcanization temperatures. The chosen accelerant to be encapsulated is TBBS, a primary sulfenamide-based accelerant.

We approached the encapsulation process using the solvent evaporation from emulsion droplets technique since it is the simplest technique that could be performed in a laboratory environment that allows a tenth-grams scale output. We optimized the encapsulation process on different TBBS/EC ratio, obtaining spherical and homogeneous microcapsules. DSC analysis shows that the melting process of TBBS starts at lower temperatures and that the recrystallization process in hindered. Those observation are in accord with the behavior of a material in a confined environment. We showed also that it is possible to encapsulate TBBS in other materials as polymethylmethacrylate and polycarbonate, obtaining smaller microcapsules.

The effect on the curing process of obtained capsules have been tested in SBR/BR blends. The preliminary results showed that the vulcanization kinetics on the single components (SBR and BR) and on the blend is not

affected by the encapsulation, both in terms of induction time and maximum torque value. Changing EC/TBBS ratio is not even affecting the curing process.

We removed a secondary accelerant – diphenylguanidine (DPG) – from the blend recipe in order to slow the process. We observed that, without DPG, the encapsulation of TBBS actually causes a delayed release of the accelerator in the blend. We also checked that the capsules are intrinsically thermally instable due to TBBS melting at 110°C. We checked the efficiency of the capsules as diffusive barriers using a fluorescent pigment. Therefore, we concluded that our capsules need to be reinforced to enhance their stability by a surface crosslinking treatment.

We tried different crosslinking agents. We tried to deposit a silica layer using alcoxysilane precursor, but we observed that the reaction, when happened, was only partial. We tried to use chlorosilanes in vapor phase to crosslink the particles surface, but TBBS is not stable to the acidic byproducts that forms. Therefore, we decided to use polyfunctional epoxy to crosslink the particles. Ethylcellulose can be prefunctionalized with the epoxy simply by means of prolonged stirring; an increase of the viscosity of the solution accompanies the process. Once encapsulated, the crosslinking process can be terminated with a thermal treatment. The heating condition are crucial, because mixing of the powder is needed in order to prevent the agglomeration of the sample. To solve this problem, we perform the crosslinking process heating a water suspension of the material. In this way, it is possible to obtain a fine powder of crosslinked

particles. The degree of crosslinking can be estimated with the IR spectroscopy. We tested the crosslinking process at two different temperatures (90 and 120°C).

The crosslinked capsules show an unexpected behavior during the curing process. We observed that the capsules crosslinked at 120°C causes a dramatic acceleration of the vulcanization kinetic, even at low curing temperature. Despite the acceleration, the maximum torque level reached is inferior compared to the one reached with pristine TBBS. We hypothesized that the acceleration effect may be due to a dredge effect operated by ethylcellulose. Because of its polarity, ethylcellulose act as an aggregation center for DPG. In this way, the environment around the capsules is rich in DPG and the vulcanization process can start immediately. The reduced maximum torque value can be a consequence of a hindered diffusion of the accelerant through the vulcanized material.

Appendix A – Materials and instruments

All the reagents were purchased from Sigma Aldrich and used without any further purification. 1H and 13C NMR spectra were recorded by using a Bruker AMX-500 spectrometer operating at 500 and 125.70 MHz, respectively. Absorption spectroscopy was performed by using a Jasco V570 spectrophotometer. IR spectra were collected with a PerkinElmer FT-ATR spectrophotometer Spectrum 100. Melting points were recorded on a Buchi M-560. DSC thermograms were recorded using a Mettler-Toledo DSC 1 STAR^{e} System. The SEM micrographs were acquired using a Tescan VEGA TS 5136XM and a Zeiss GeminiSEM 500 (equipped with Bruker EDX and EBDS microanalysis).

For mechanical stirring, an IKA EUROSTAR 20 digital overhead stirrer was used. The impeller used was a collapsible blade impeller (R 1352 centrifugal stirrer, IKA) and a high-shear impeller (R 1300 dissolver stirrer, IKA). For homogenization, a T-25 basic IKA Ultra-Turrax was used. The dispersing tool is a S 25 N – 25 F rotor-stator.

For rubber blend preparation, a Thermo Haake Reomix lab station internal mixer (250 mL mixing chamber, 0.7 filling factor) was used. Rubber blend characterization was performed on a Moving Die Rheometer (RPA 2000, Alpha Technological) under the following

conditions: ±1° oscillation angle and 4.3 bar pressure (temperature and duration was varied according to the experiment).

Appendix B – Synthesis of TBBS derivatives

Synthesis of 6-bromobenzo[d]thiazole-2-thiol (BrMBT)

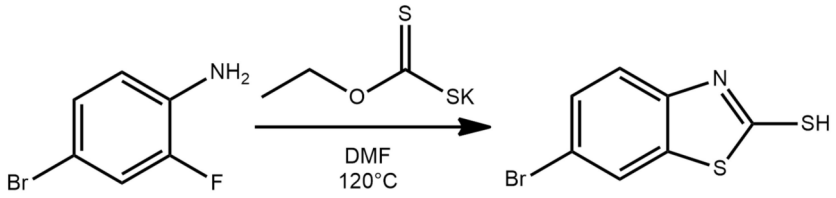

	MW ($gmol^{-1}$)	M (g)	n (mmol)	V (mL)
4-bromo-2-fluoroaniline	188.96	20	105.84	-
Potassium ethyl xanthate	160.29	37.3	232.70	-
DMF	-	-	-	200

4-bromo-2-fluoro aniline and potassium ethyl xanthate are added to a 500 mL round-bottomed flask and dissolved in 200 mL of DMF, obtaining a yellow solution. The solution is heated up to 120°C and kept at this temperature for 48 hours under magnetic stirring. During this time, the solution color changed to deep red. The solution is allowed to cool down at room temperature, then it is poured into 800 mL of ice-cold water, obtaining a yellow suspension.

To this suspension, 200 mL of an ice-cold 1 M HCl solution are added. Immediately, a white solid precipitates off from the suspension. The solid is collected on a Buchner funnel, washed with water and ethanol, and then it is dried in the oven at 50°C (caution: the product has a stinky smell). A light pink solid is obtained after the drying step (25,6 g, 98% yield).

1H (DMSO, 500 MHz): δ 13.87 (b, 1H), 7.98-7.99 (m, 1H), 7.55-7.57 (m, 1H), 7,23 (d, j = 8.6 Hz)

13C – Not enough soluble

Synthesis of S-(6-bromobenzo[d]thiazol-2-yl)-N-(tert-butyl)thiohydroxylamine (BrTBBS)

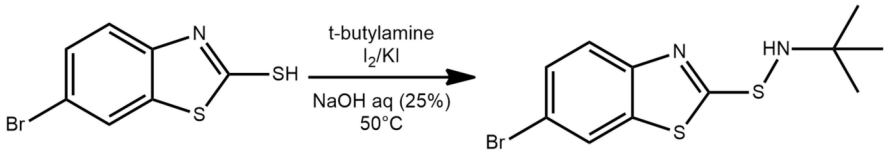

	MW ($gmol^{-1}$)	M (g)	n (mmol)	V (mL)
BrMBT	246.14	10	40.6	-
Tert-butylamine	73.14	29.69	406	20.7
NaOH (25% solution)	40	3.25	81.25	13
Potassium iodide	166	10.13	60.9	-
Iodine	253.81	10.3	40.6	-
Water	-	-	-	400

BrMBT is suspended in 100 mL of water in a 1000 mL one-necked round-bottomed flask. NaOH solution is added drop-wise to the stirred suspension. The suspended material dissolves, obtaining a brown solution. Then, tert-butylamine is added to the solution and the reaction mixture is heated up to 50°C.

Meanwhile, iodine and potassium iodide are –partially – dissolved in 300 mL of water using ultrasonication. The oxidizing solution is loaded in a

dropping funnel and added dropwise to the reaction mixture. Whenever a drop fall in the reaction mixture, the solution changes locally color from brown to white. While the addition goes on, the brown solution turns into a white suspension. After that the oxidizing mixture has been added, the suspension is stirred for 1 hour, then the suspended solid is collected on a Buchner funnel. The product is obtained by continuous extraction with a soxhlet apparatus using methylene chloride as solvent (~200 mL). Once extracted, the solvent is removed under reduced pressure, affording a crystalline white solid that is taken up with ethanol and collected on a buchner funnel and dried in the oven at 50°C (4.42 g, 34,3% yield).

1H (CD2Cl2, 400 MHz): δ 7.96-7.97 (m, 1H), 7.64-7.66 (m, 1H), 7.50-7.53 (m, 1H), 3,58 (br, 1H), 1.31 (s, 9H)

13C (CD2Cl2, 100.7 MHz): δ 182.1, 154.3, 136.8, 129.0, 123.5, 122.5, 116.6, 55.5, 28.7

Synthetic attempt for tert-butyl benzo[d]thiazol-2-ylthio(tert-butyl)carbamate

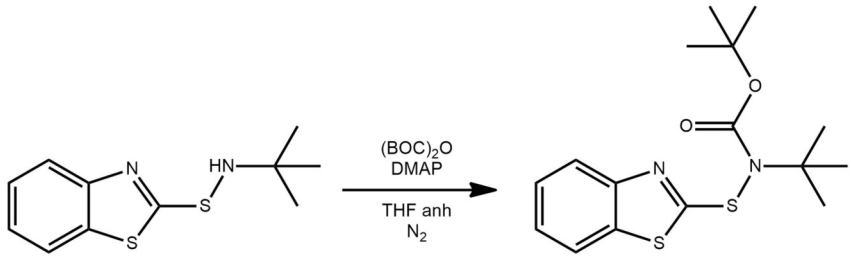

	MW ($gmol^{-1}$)	M (mg)	n (mmol)	V (mL)
N-tert-butyl-benzothiazole 2-sulfenamide (TBBS)	238.37	500	2.1	-
BOC anhydride	218.25	950	4.2	-
DMAP	122.17	260	2.1	-
THF	-	-	-	10

TBBS and BOC-anhydride are added to a 50 mL two-necked round-bottomed flask under inert atmosphere (nitrogen). Anhydrous THF is added with a syringe. A yellow solution is obtained. The reaction mixture is stirred at room temperatures. The reaction is monitored with TLC plate analysis (methylene chloride as eluent).

After four days the reaction color changed to orange. The solvent is evaporated and the residual solid is triturated with ethanol. A solid precipitates off, but most of the material remain dissolved. The solvent is evaporated again and the residual solid is purified via column chromatography on silica. Three different fractions are separated, but from the NMR analysis no one of those fractions contains the desired product.

Appendix C – Diffusion test in rubber samples

As we mentioned in the previous chapters, we tested the efficiency of the EC capsules as diffusional barrier. To do so, we encapsulated a fluorescent molecule – a quinacridone derivative - in EC, in order to have the possibility to track its diffusional path in the rubber sample. Quinacridone (QA) is a pigment, and it is not soluble by definition; in fact, quinacridone crystallize in a plethora of crystal structure due to the possibility to form simultaneously hydrogen bond networks and π-stacks[80]. However, quinacridone's solubility can be greatly enhanced by functionalization of the nitrogen atom on the ring, making impossible the formation of a H-bond network.

As we discussed previously, the technique of the latent pigment can be effectively applied also to quinacridone; the t-BOC derivative (QA-BOC) is highly soluble and can be processed in solution, while a thermal treatment allows the conversion back to the pristine pigment. Our group showed how this technique could be helpful to improve the performance of quinacridone in luminescent solar concentrators[77]. Briefly, luminescent solar concentrators are, in its most general form, a plastic slab with a fluorophore dispersed in. The fluorophore absorbs incident light and re-emits the light inside the slab; due to the design of the slab, it acts as a waveguide, guiding the emitted light at the borders of the slab, where it can be, for example, harvested by solar cells. Since the slabs are prepared by cast polymerization of methyl methacrylate (MMA), the fluorophore must be soluble in MMA. Alkylated quinacridone

derivatives are soluble in MMA, but they are not stable in terms of photodegradation, while pristine quinacridone is remarkably stable. The latent pigment technique allowed us to synthesize a soluble, highly fluorescent quinacridone derivative; this derivative has been homogeneously dispersed in MMA and, once the slab has been obtained, the pristine pigment has been regenerated by a thermal treatment at 110°C. From TGA data, the thermal decomposition of the t-BOC moiety is located around 175°C, but the process starts –even if slower – at lower temperatures, and can go to completion. The important thing to notice is that the regenerated pigment is still fluorescent; this is due to the fact that, when the cleavage of the t-BOC moiety happens, they cannot form the stable H-bond network for a matter of dilution into the slab. If the thermal cleavage of QA-BOC happens in solution, however, a magenta suspension is obtained, meaning that the quinacridone molecules aggregates strongly[81].

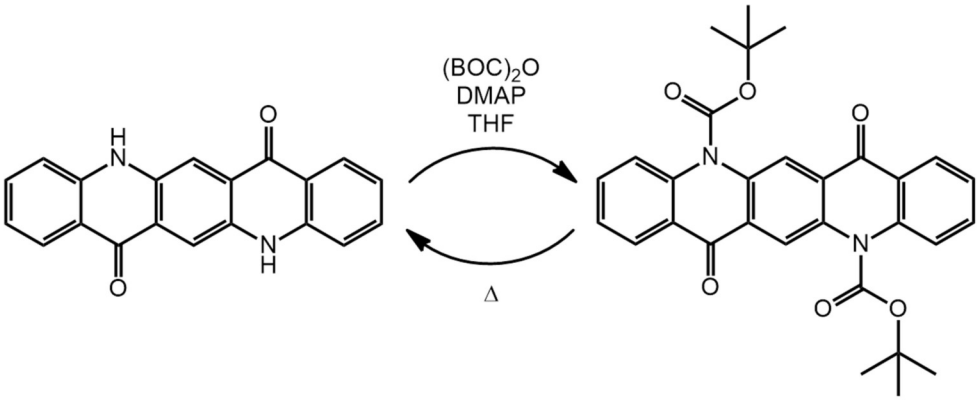

We can, therefore, make the following observations:

- QA-BOC is extremely fluorescent – even at the solid state – and soluble;
- QA, on the other hand, is non fluorescent and insoluble;
- If QA is regenerated from QA-BOC in solution, aggregation takes place. The regenerated QA is non fluorescent;
- If QA is regenerated from QA-BOC in a diluted condition, aggregation is prevented. The regenerated QA is fluorescent.

It must be noticed that in the PMMA slab a great contribution against aggregation is given by the crosslink of the slab itself.

We decided to use the previously reported observation to design our experiment. QA-BOC has been synthesized according to literature procedures. QA-BOC is encapsulated in EC following the optimized procedure developed for TBBS; the obtained capsules have a QA-BOC load of 4%.

Then, two rectangular pieces of BR are cut in half. A few milligrams of the encapsulated QA-BOC is put in between of the two halves. Similarly, the same thing is done with pristine QA-BOC powder. The two halves are stick together using a few drops of toluene on the exterior part of the samples. In both the two samples the solid-state fluorescence of QA-BOC is clearly visible using a Wood's lamp (figure 70).

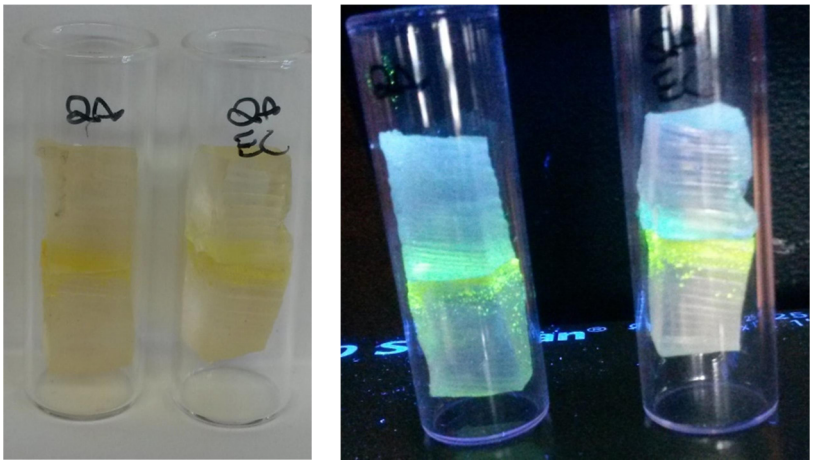

Figure 70 - Photo of the rubber samples containing pristine quinacridone (QA) and encapsulated quinacridone (QA-EC) under ambient illumination (left) and under a Wood's lamp (right).

Then, the two samples are placed in a glass vial (to maintain their shape and vertical orientation) and then the samples are placed in the oven at 120°C for two hours. After this treatment, the two samples look very different:

- The sample containing the pristine QA-BOC powder exhibit a broad diffusive profile along the sample. In proximity of the reservoir, the pigment is regenerated (according to the color change). However, QA fluorescence can be observed moving towards the end of the diffusion path (figure 71).

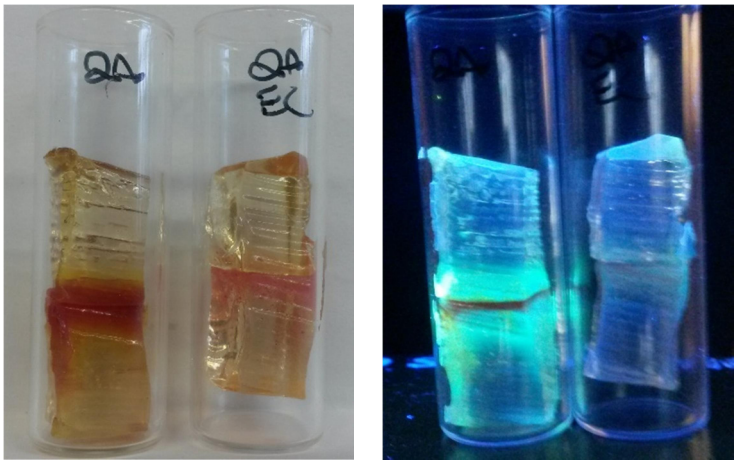

Figure 71 - Photo of the rubber samples containing pristine quinacridone (QA) and encapsulated quinacridone (QA-EC) after the thermal treatment (two hours at 120°C) under ambient illumination (left) and under a Wood's lamp (right)

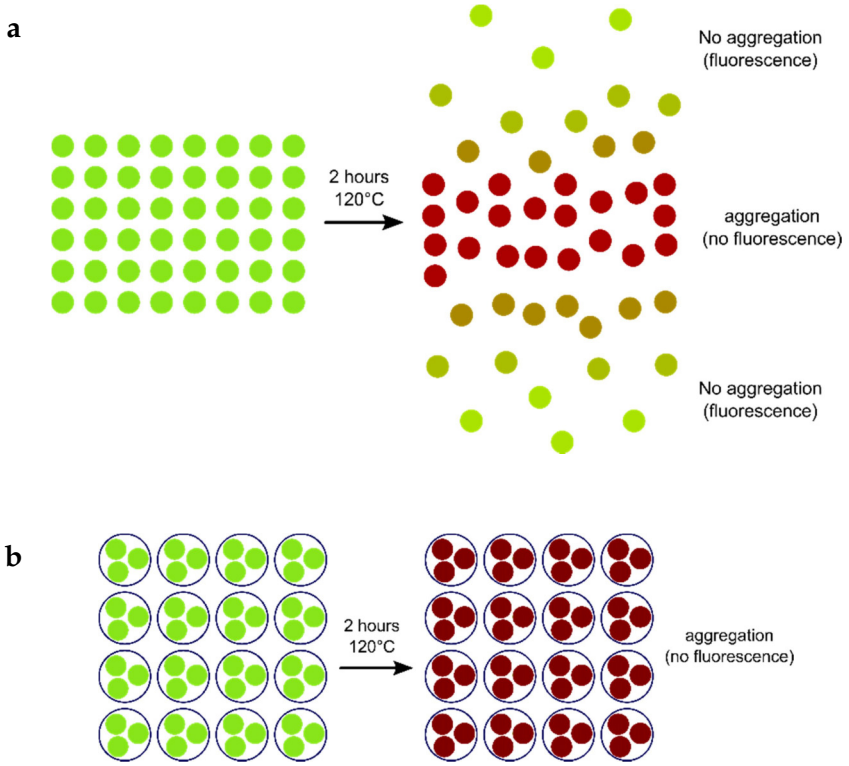

Figure 72 - Proposed explanation for the difference in the diffusion profile: (a) pristine QA can diffuse and aggregates only where the concentration is high. Diluted QA molecules do not aggregate, maintaining their fluorescence. (b) QA cannot diffuse and all the molecules aggregates (no residual fluorescence).

- The sample containing encapsulated QA-BOC shows no diffusion at all. QA is concentrated in the middle of the sample, and no residual fluorescence can be observed.

Pristine QA-BOC is free to diffuse into the rubber sample, and so it does. In the middle of the sample, the concentration is higher, and the pigment – once regenerated – is able to aggregate; however, moving along the diffusion profile, QA-BOC concentration is lower, and dilution prevents the H-bond network formation. This explains the residual fluorescence that can be observed under the Wood's lamp. On the other hand, encapsulated QA-BOC's diffusion is hindered because of the capsule wall presence. When the pigment regeneration occurs, the H-bond network can, therefore, easily form. No residual fluorescence is observed, meaning that all of QA-BOC reverted back to pristine QA in a "concentrated" environment. Figure 72 summarizes the proposed explanation.

Therefore, we interpreted these two observation – the difference in the diffusion profile and the absence of residual fluorescence in the encapsulated sample – as a proof of the efficacy of the capsules as diffusional barriers. Of course, we make this statement having in mind that this is not the system that will be used in our experiments: QA and TBBS will have different diffusion/partition coefficient, and, most important, the melting point of the two species are completely different. But this goes to say that the capsule structure is efficient, so the reason for their inefficient behavior in rubber blends is located elsewhere (i.e. in the structure collapse after TBBS melting).

Bibliography

[1] A. Y. Coran, in *Sci. Technol. Rubber (Fourth Ed.* (Eds.: J.E. Mark, B. Erman, C.M. Roland), Academic Press, Boston, **2013**, pp. 337–381.

[2] L. Bateman, A. T. McPherson, *Science (80-.).* **1964**, *143*, 1429.

[3] G. E. Decker, R. W. Wise, D. Guerry, *Rubber Chem. Technol.* **1963**, *36*, 451–458.

[4] N. J. Morrison, M. Porter, *Rubber Chem. Technol.* **1984**, *57*, 63–85.

[5] G. Oenslager, *Ind. Eng. Chem.* **1933**, *25*, 232–237.

[6] M. L. Weiss, *Vulcanization Accelerator*, **1922**, US1411231A.

[7] G. Bruni, E. Romani, *Giorn. chim. ind. ed. appli* **1921**, *3*, 351.

[8] Z. Ewald, O. Ludwig, B. Max, *Vulcanization Accelerator*, **1934**, US1942790.

[9] P. N. Son, *Rubber Chem. Technol.* **1973**, *46*, 999–1006.

[10] G. Heideman, J. W. M. Noordermeer, R. N. Datta, B. van Baarle, *Rubber Chem. Technol.* **2005**, *78*, 245–257.

[11] H. Umland, *Vulcanization Activator Method*, **1994**, US5302315A.

[12] J. Kruželák, S. Richard, H. Ivan, *Chem. Pap.* **2016**, *70*, 1533.

[13] P. Ghosh, S. Katare, P. Patkar, J. M. Caruthers, V. Venkatasubramanian, *Rubber Chem. Technol.* **2003**, *76*, 592–693.

[14] R. H. Campbell, R. W. Wise, *Rubber Chem. Technol.* **1964**, *37*, 635–649.

[15] P. N. Son, K. E. Andrews, A. T. Schooley, *Rubber Chem. Technol.* **1972**, *45*, 1513–1531.

[16] M. H. S. Gradwell, W. J. McGill, *J. Appl. Polym. Sci.* **1994**, *51*, 169–176.

[17] a. V. Chapman, a. J. Tinker, *KGK-Kautschuk und Gummi Kunststoffe* **2003**, *56*, 533–544.

[18] J. B. Gardiner, *Rubber Chem. Technol.* **1968**, *41*, 1312–1328.

[19] J. B. Gardiner, *Rubber Chem. Technol.* **1970**, *43*, 370–399.

[20] J. B. Gardiner, *Rubber Chem. Technol.* **1969**, *42*, 1058–1078.

[21] F.-X. Guillaumond, *Rubber Chem. Technol.* **1976**, *49*, 105–111.

[22] M. Mishra, *Handbook of Encapsulation and Controlled Release*, CRC Press, **2015**.

[23] B. K. Kim, S. J. Hwang, J. B. Park, H. J. Park, *J. Microencapsul.* **2002**, *19*, 811–822.

[24] B. K. Green, L. Schleicher, *Oil-Containing Microscopic Capsules and Method of Making Them*, **1957**, US2800457.

[25] C. Andres, *Food Process.* **1977**, *38*, 44–56.

[26] M. N. Singh, K. S. Y. Hemant, M. Ram, H. G. Shivakumar, *Res. Pharm. Sci.* **2010**, *5*, 65–77.

[27] H. R. Kruyt, *Colloid Science*, Elsevier Pub. Co., **1952**.

[28] M. Jelvehgari, M. Maghsoodi, H. Nemati, *Res. Pharm. Sci.* **2010**, *5*, 29–39.

[29] U. A. Shinde, M. S. Nagarsenker, *Indian J. Pharm. Sci.* **2009**, *71*, 313–317.

[30] C. Thies, *J. Colloid Interface Sci.* **1973**, *44*, 133–141.

[31] E. L. Wittbecker, P. W. Morgan, *J. Polym. Sci. Part A Polym. Chem.* **1959**, *40*, 289–297.

[32] L. Janssen, K. Te Nijenhuis, *J. Memb. Sci.* **1992**, *65*, 69–75.

[33] S. K. Yadav, K. C. Khilar, A. K. Suresh, *AIChE J.* **1996**, *42*, 2616–2626.

[34] F. Salaün, G. Bedek, E. Devaux, D. Dupont, L. Gengembre, *J. Memb. Sci.* **2011**, *370*, 23–33.

[35] E. Mathiowitz, M. D. Cohen, *J. Memb. Sci.* **1989**, *40*, 1–26.

[36] E. A. Stefanescu, C. Stefanescu, G. S. Huvard, M. A. McHugh, *Polym.*

Prepr. **2009**, *50*, 506.

[37] E. Mathiowitz, M. D. Cohen, *J. Memb. Sci.* **1989**, *40*, 27–41.

[38] P. J. Mulqueen, A. Waller, I. M. Shirley, M. Chavant, *Formulation*, **2007**, WO2007072046.

[39] K. Dietrich, H. Herma, R. Nastke, E. Bonatz, W. Teige, *Acta Polym.* **1989**, *40*, 243–251.

[40] Z. H. Zhen, *Adv. Mater. Res.* **2011**, *236*, 1169–1173.

[41] H. Chang, T. Lu, Q. Xu, Q. Sun, G. Han, *Zhongguo Suliao* **2010**, *24*, 72–75.

[42] H. Guo, H. Li, H. Fan, *Gongneng Cailiao* **2006**, *37*, 559.

[43] H. Y. Lee, S. J. Lee, I. W. Cheong, J. H. Kim, *J. Microencapsul.* **2002**, *19*, 559–569.

[44] R. Arshady, *Microspheres Microcapsules & Liposomes: Preparation & Chemical Applications*, Citus Books, **1999**.

[45] IARC, *Monogr. Eval. Carcinog. Risks to Humans* **2006**, *88*.

[46] J. Smets, J. Odhavji DIhora, A. Pintens, S. J. Guinebretiere, A. K. Druckrey, P. D. Sands, N. Yan, *Benefit Agent Containing Delivery Particle*, **2012**, US2012071392.

[47] R. Bodmerier, H. Chen, *J. Pharm. Pharmacol.* **1988**, *40*, 754–757.

[48] X. Guo, R. Bodmeier, *STP pharma Sci.* **1997**, *7*, 521–528.

[49] S. Benita, J. P. Benoit, F. Puisieux, C. Thies, *J. Pharm. Sci.* **1984**, *73*, 1721–1724.

[50] Y.-Y. Yang, T.-S. Chung, N. P. Ng, *Biomaterials* **2001**, *22*, 231–241.

[51] R. Jeyanthi, R. C. Mehta, B. C. Thanoo, P. P. DeLuca, *J. Microencapsul.* **1997**, *14*, 163–174.

[52] N. J. Zuidam, E. Shimoni, *Encapsulation Technol. Act. Food Ingredients Food*

Process. **2010**, 3–30.

[53] M. Hemati, R. Cherif, K. Saleh, V. Pont, *Powder Technol.* **2003**, *130*, 18–34.

[54] C. A. Finch, R. Bodmeier, *Ullmann's Encycl. Ind. Chem.* **2000**, 11842–11857.

[55] M. Errasquin, *Crosslinking Agents Encapsulated in Polymers and Methods of Manufacturing the Same*, **2005**, US20050004319.

[56] M. Jobmann, G. Rafler, M. Hensel, *Microencapsulated Rubber Additives and Method for Production Thereof*, **2008**, US20080227888.

[57] L.-K. Ju, U. Anozie, *Method of Encapsulation and Immobilization*, **2013**, WO2013003722.

[58] A. Boermia, B. Van Baarle, *Rubber World* **2006**, 20–24.

[59] R. Guo, a. G. Talma, R. N. Datta, W. K. Dierkes, J. W. M. Noordermeer, *Eur. Polym. J.* **2008**, *44*, 3890–3893.

[60] R. C. R. Nunes, E. B. Mano, *Polym. Compos.* **1995**, *16*, 421–423.

[61] A. F. Martins, L. L. Y Visconte, R. C. R Nunes, R. de Janeiro, **2002**, 637–641.

[62] H. Kasai, H. Oikawa, S. Okada, H. Nakanishi, *Bull. Chem. Soc. Jpn.* **1998**, *71*, 2597–2601.

[63] H. Auweter, H. Haberkorn, W. Heckmann, D. Horn, E. Lüddecke, J. Rieger, H. Weiss, *Angew. Chem. Int. Ed. Engl.* **1999**, *38*, 2188–2191.

[64] R. Arshady, *Polym. Eng. Sci.* **1990**, *30*, 915–924.

[65] P. Parida, S. C. Mishra, S. Sahoo, A. Behera, B. P. Nayak, *J. Pharm. Anal.* **2016**, *6*, 341–344.

[66] F. Li, X. Wang, D. Wu, *Energy Convers. Manag.* **2015**, *106*, 873–885.

[67] T. Feczkó, O. Varga, M. Kovács, T. Vidóczy, B. Voncina, *J. Photochem. Photobiol. A Chem.* **2011**, *222*, 293–298.

[68] F.-L. Jin, X. Li, S.-J. Park, *J. Ind. Eng. Chem.* **2015**, *29*, 1–11.

[69] S. Desgouilles, C. Vauthier, D. Bazile, J. Vacus, J. L. Grossiord, M. Veillard, P. Couvreur, *Langmuir* **2003**, *19*, 9504–9510.

[70] B. B. Lakshmi, C. J. Patrissi, C. R. Martin, *Chem. Mater.* **1997**, *9*, 2544–2550.

[71] L. L. Hench, J. K. West, *Chem. Rev.* **1990**, *90*, 33–72.

[72] C. R. Silva, C. Airoldi, *J. Colloid Interface Sci.* **1997**, *195*, 381–387.

[73] H. P. S. Abdul Khalil, A. H. Bhat, A. F. Ireana Yusra, *Carbohydr. Polym.* **2012**, *87*, 963–979.

[74] E. A. Englund, H. N. Gopi, D. H. Appella, *Org. Lett.* **2004**, *6*, 213–215.

[75] J. S. Zambounis, Z. Hao, A. Iqbal, *Nature* **1997**, *388*, 131.

[76] E. D. Głowacki, M. Irimia-Vladu, M. Kaltenbrunner, J. Gsiorowski, M. S. White, U. Monkowius, G. Romanazzi, G. P. Suranna, P. Mastrorilli, T. Sekitani, et al., *Adv. Mater.* **2013**, *25*, 1563–1569.

[77] S. Mattiello, A. Sanzone, P. Brazzo, M. Sassi, L. Beverina, *European J. Org. Chem.* **2015**, *2015*, 5723–5729.

[78] L. Zhu, M. Zhang, M. Dai, *J. Heterocycl. Chem.* **2005**, *42*, 727–730.

[79] J. J. D'Amico, M. W. Harman, R. H. Cooper, *J. Am. Chem. Soc.* **1957**, *79*, 5270–5276.

[80] E. F. Paulus, F. J. J. Leusen, M. U. Schmidt, *CrystEngComm* **2007**, *9*, 131–143.

[81] M. Sytnyk, E. D. Głowacki, S. Yakunin, G. Voss, W. Schöfberger, D. Kriegner, J. Stangl, R. Trotta, C. Gollner, S. Tollabimazraehno, et al., *J. Am. Chem. Soc.* **2014**, *136*, 16522–16532.